Robust uncertainty quantification of tsunami ionospheric holes for the 2011 Tohoku-Oki earthquake using satellite data.

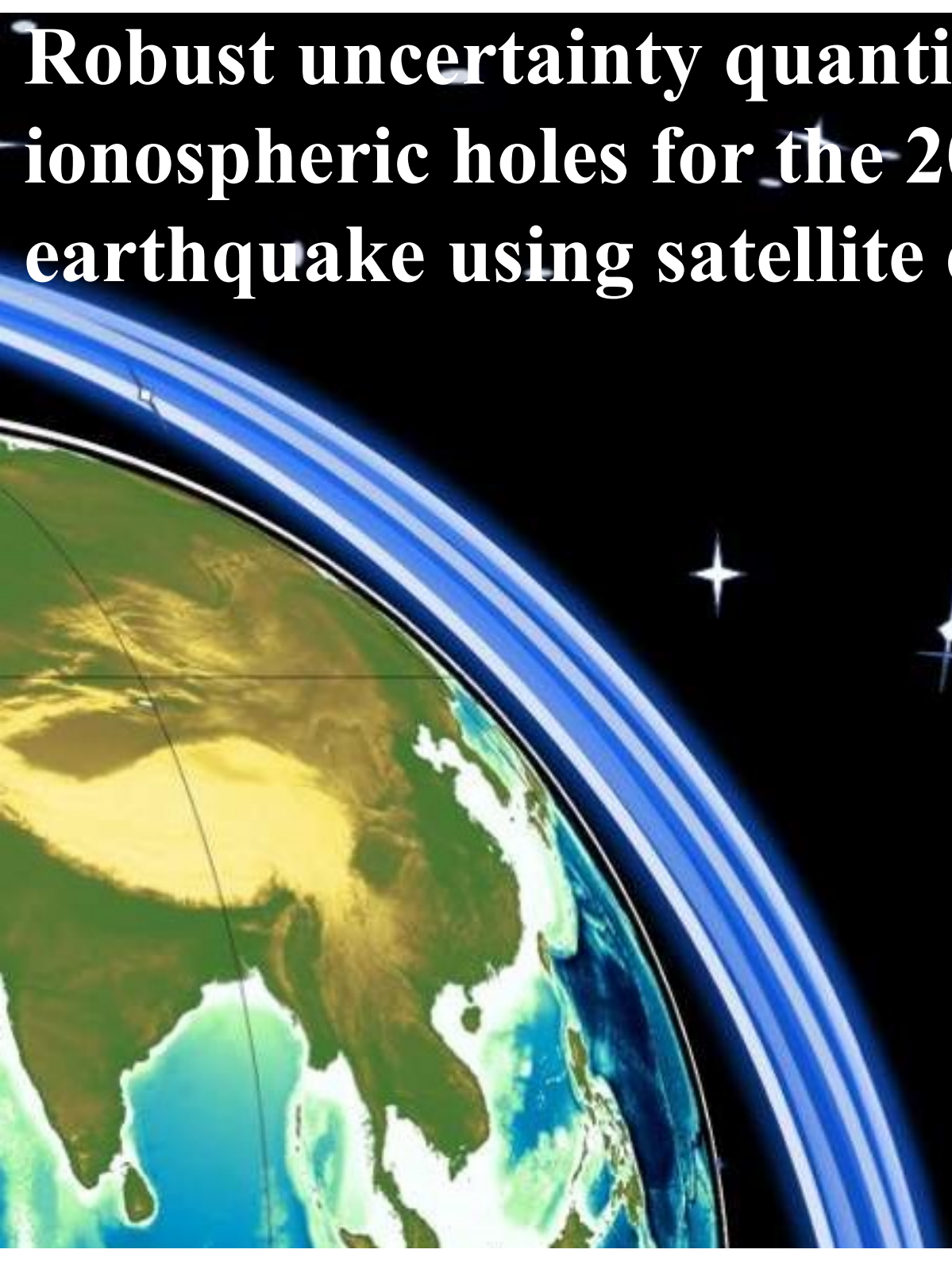

Ryuichi KANAI

University College London

Alan Turing Institute

[Collaborated researchers]

Prof. Alan Smith

University College London

Prof. Serge Guillas

University College London

Prof. Masashi Kamogawa

University of Shizuoka

Prof. Toshiyasu Nagao

Tokai University

Home
Latest news
UCL in the media
Services for media
Student news
Staff news
Tell us your story
Contact us

Space-based system using GPS satellites could warn of incoming tsunamis

28 April 2022

A new method for detecting tsunamis using existing GPS satellites orbiting Earth could serve as an effective warning system for countries worldwide, according to a new study by an international team led by UCL researchers.

SPACE-BASED SYSTEM USING GPS SATELLITES COULD WARN OF INCOMING TSUNAMIS

RESEARCH BRIEFS 28 April 2022 Source(s): University College London

TechCrunch

GPS signals could detect tsunamis better and faster than seismic sensors

Stefanie Waldek

May 5, 2022 · 3 min read

GPS networks are already a crucial part of everyday life around the world, but an international team of scientists has found a new, potentially life-saving use for them: tsunami warnings.

Collaboration

UCL

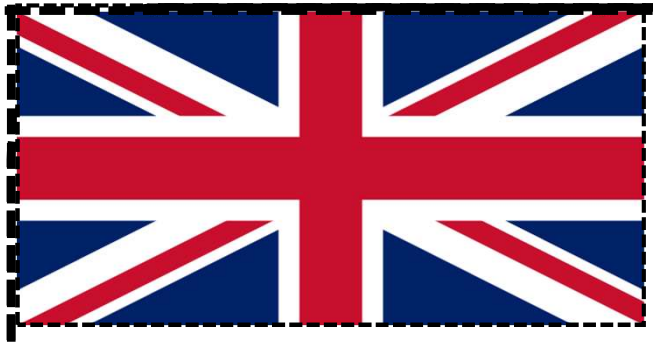

Space Science

UCL's Mullard Space Science Laboratory

Statistics

UCL's Statistical Science department

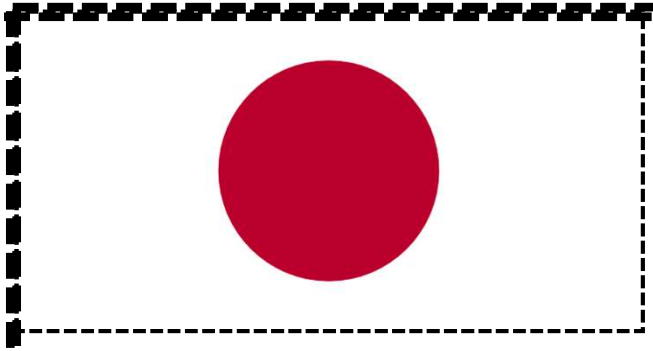

Seismology

Tokai University

Electrodynamics

University of Shizuoka

Space-based analysis

Rough sketch

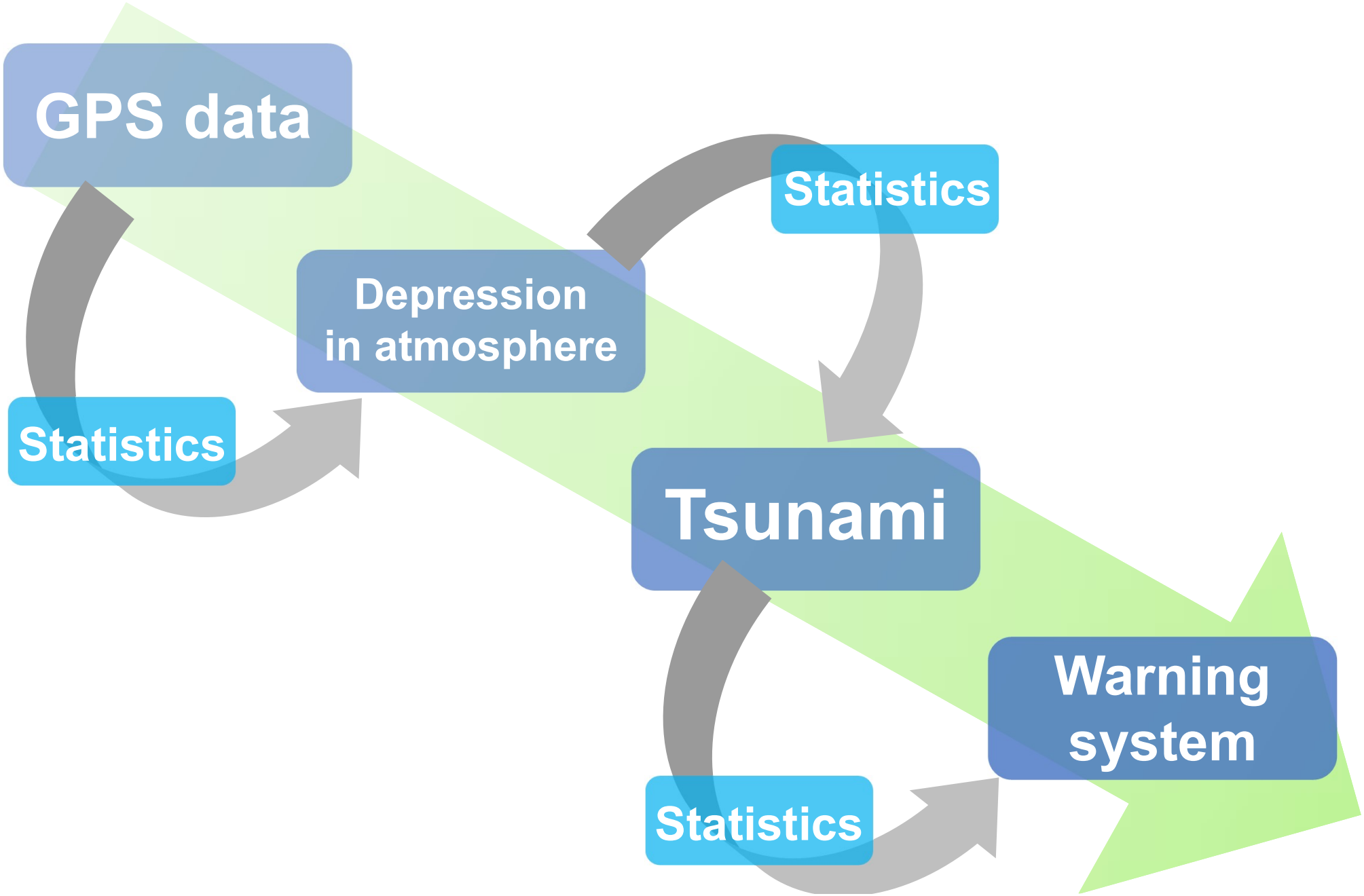

Contents

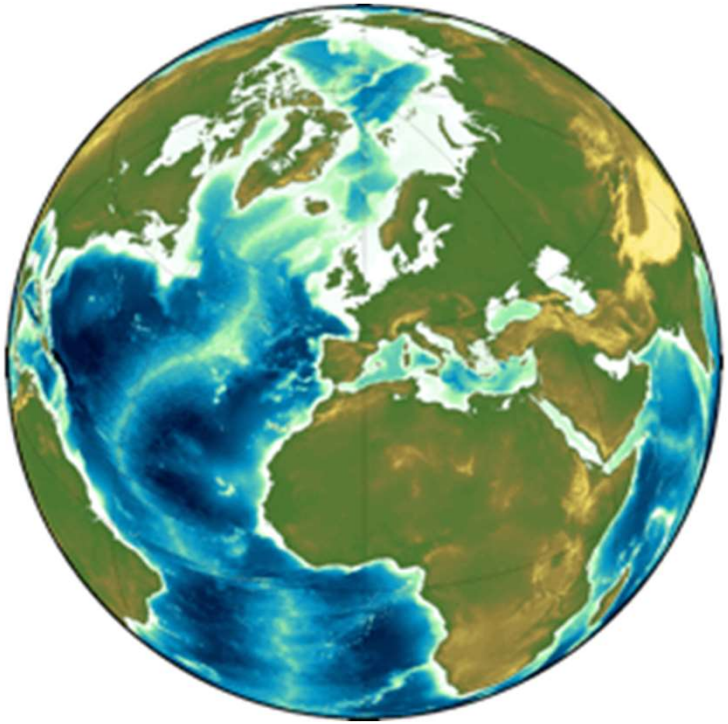

Background

UCL

11th March 2011

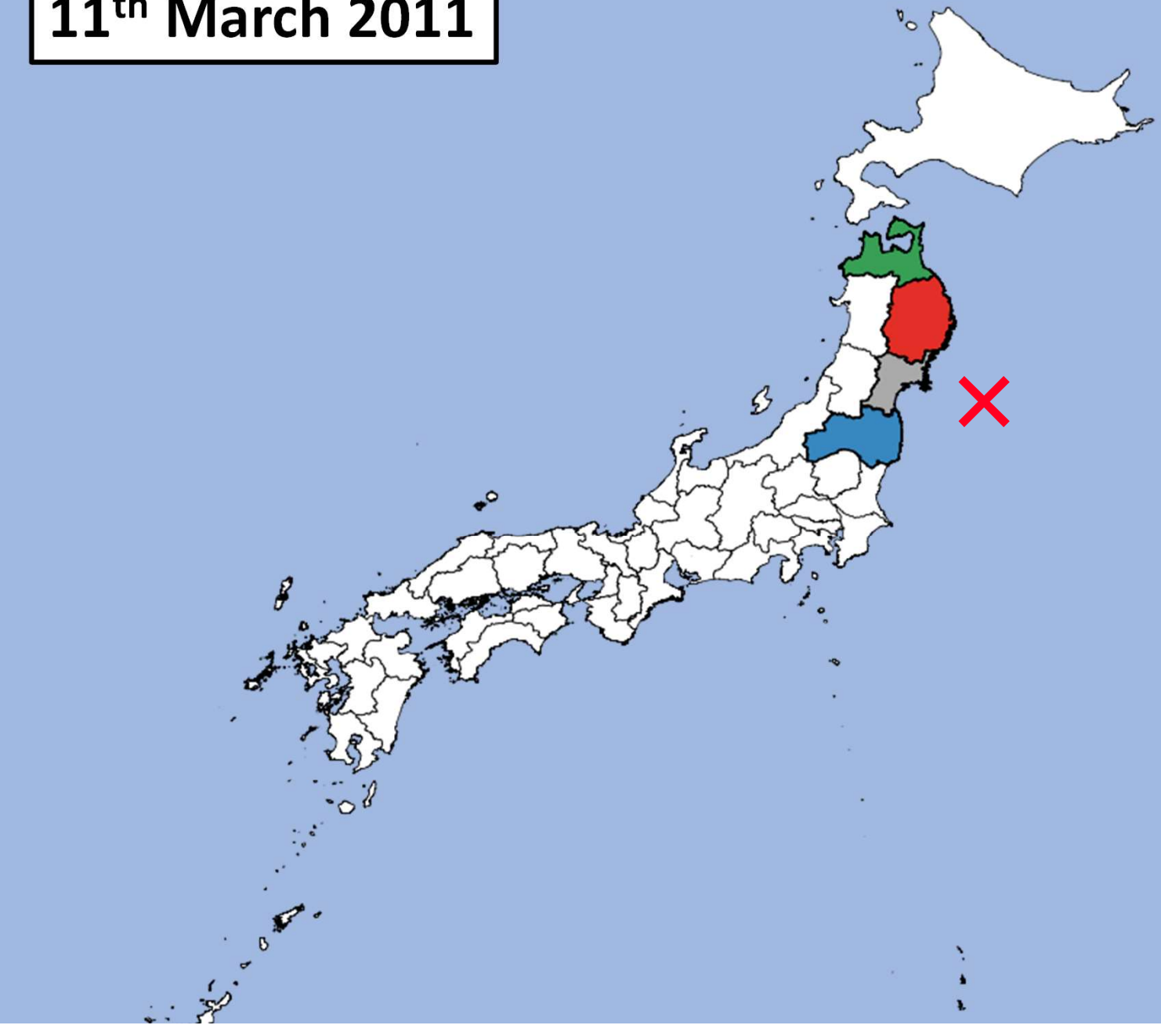

[Time]
05:46:24 (UTC)

[Location]
38.297°N 142.373°E

[Depth]
29.0 km

[Magnitude]
9.1

Background

UCL

11th March 2011

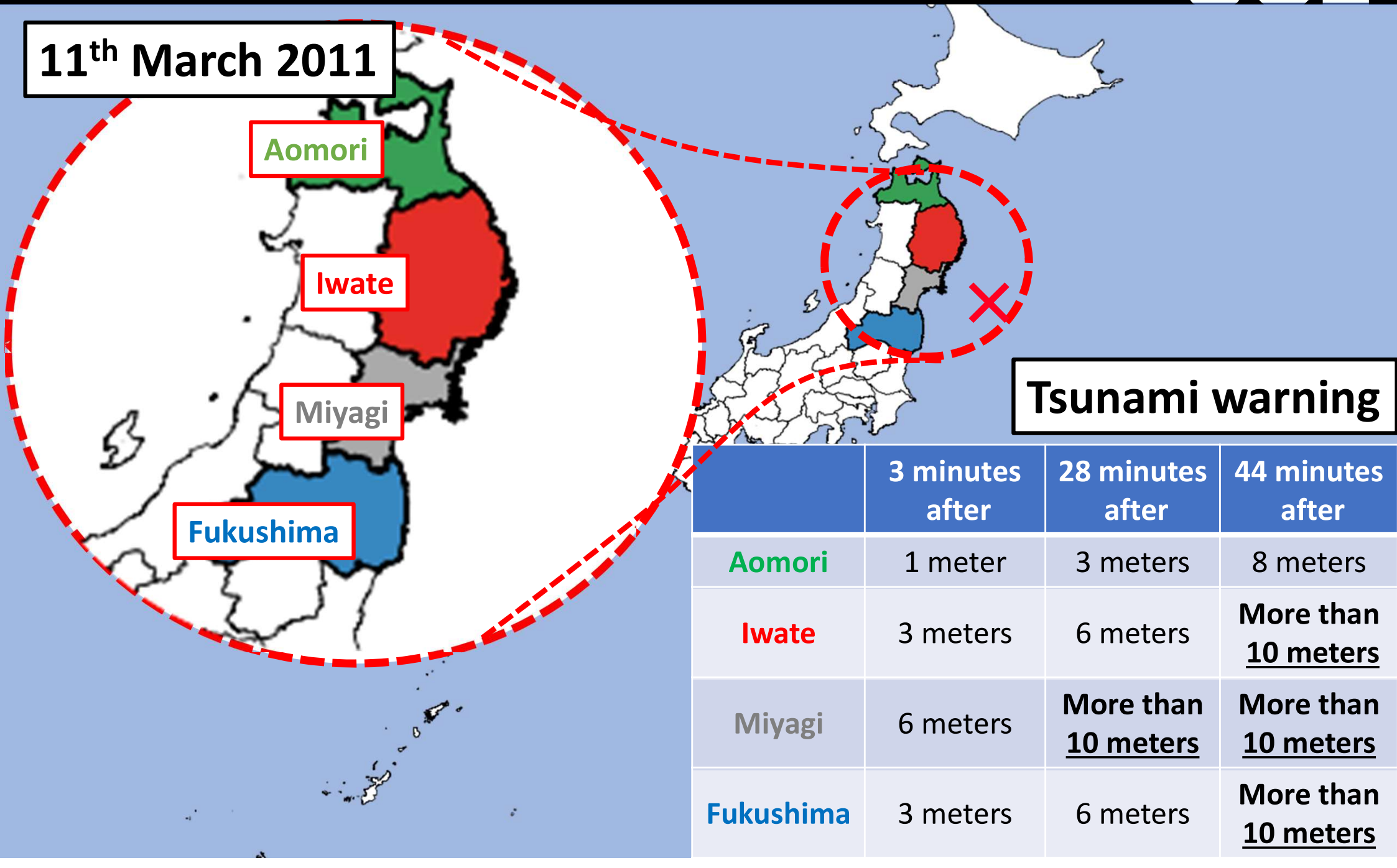

Tsunami warning

	3 minutes after	28 minutes after	44 minutes after
Aomori	1 meter	3 meters	8 meters
Iwate	3 meters	6 meters	**More than 10 meters**
Miyagi	6 meters	**More than 10 meters**	**More than 10 meters**
Fukushima	3 meters	6 meters	**More than 10 meters**

Background

How to overcome?

Traditional Seismology

→ **Magnitude cannot be estimated.**

Distribute buoys densely in the ocean

→ **Impossible due to budget constraints. No ship can sail.**

Distribute instruments on the seafloor

→ **Impossible to know where earthquakes occur in advance.**

A possible solution

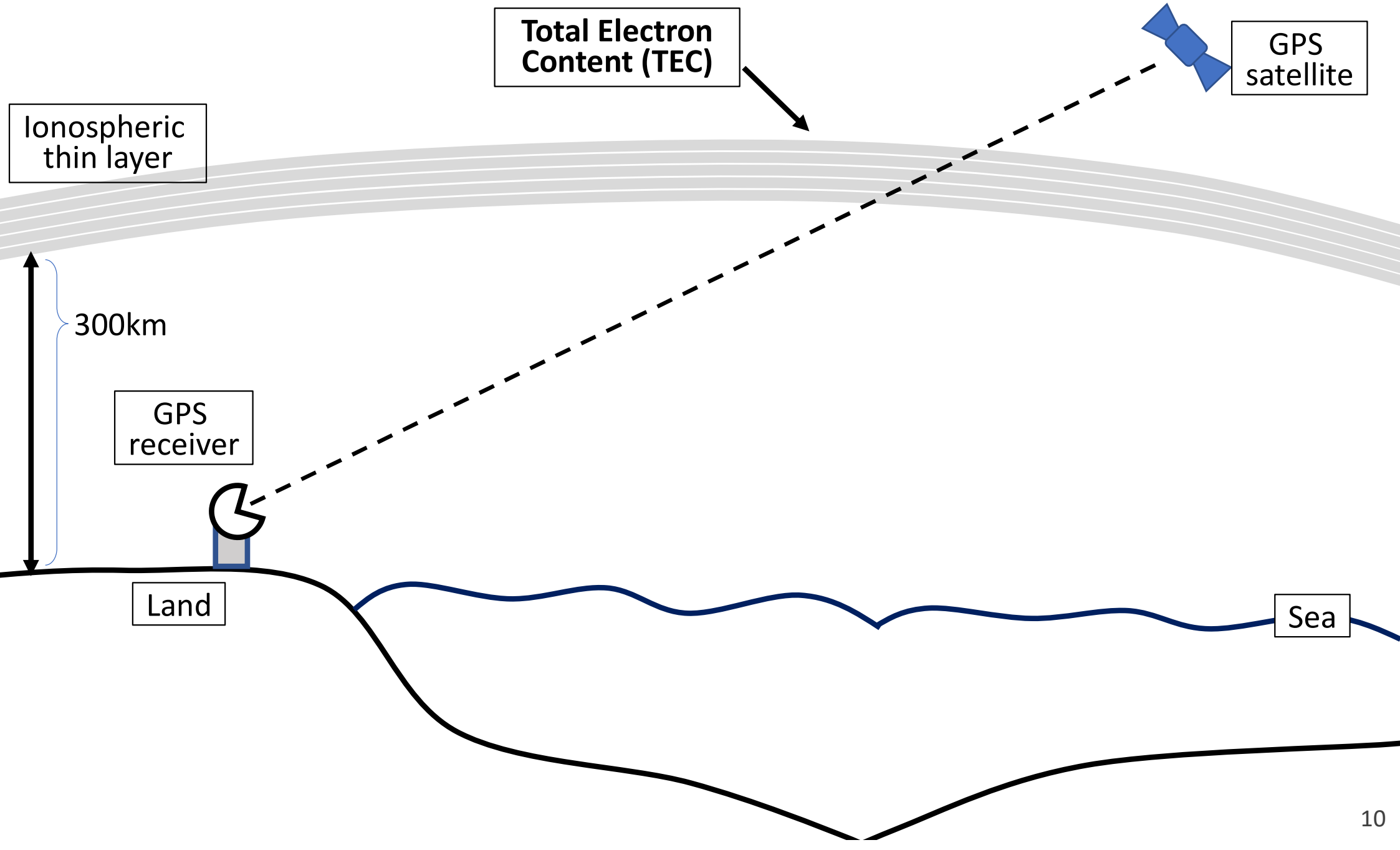

A possible solution

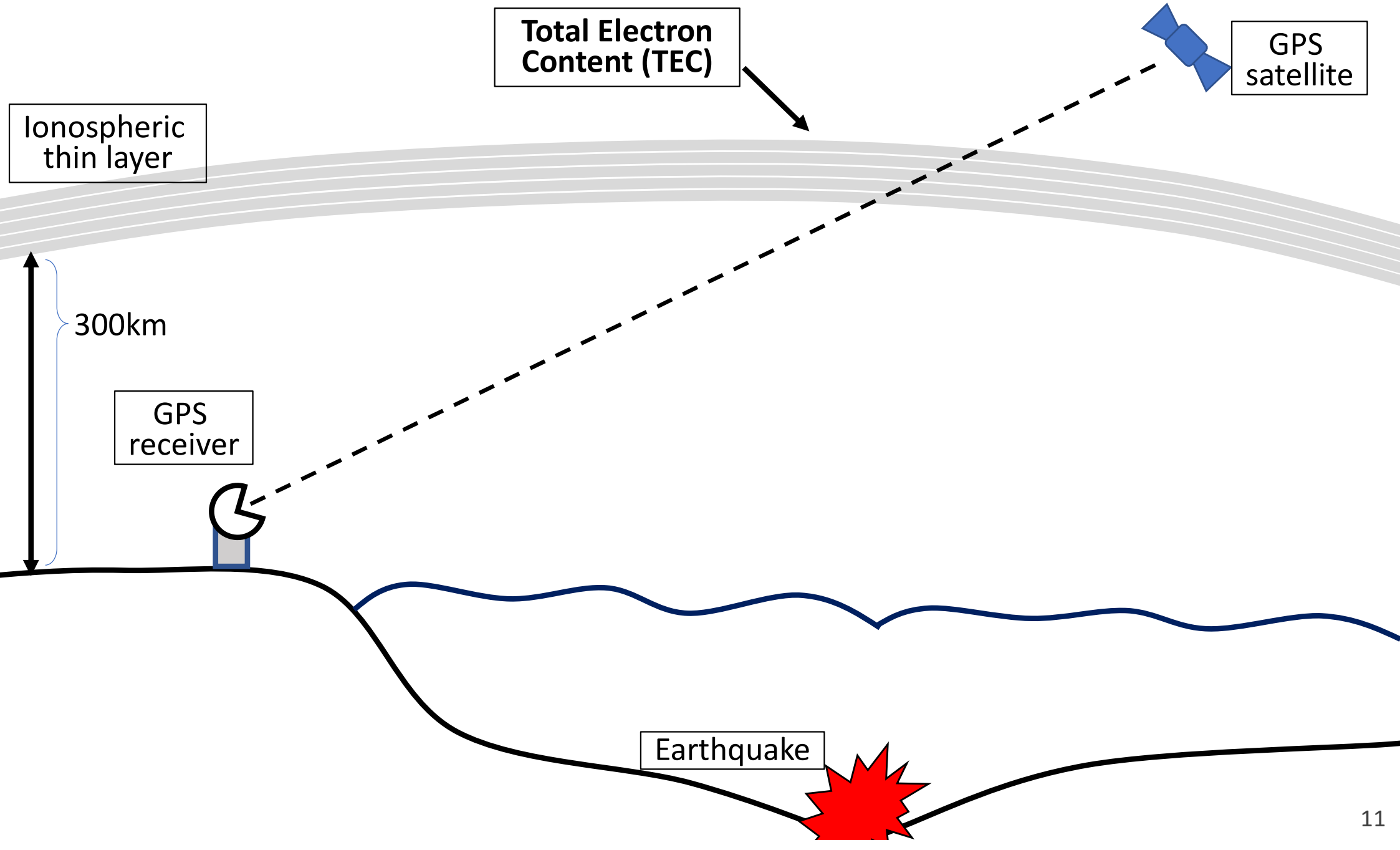

A possible solution

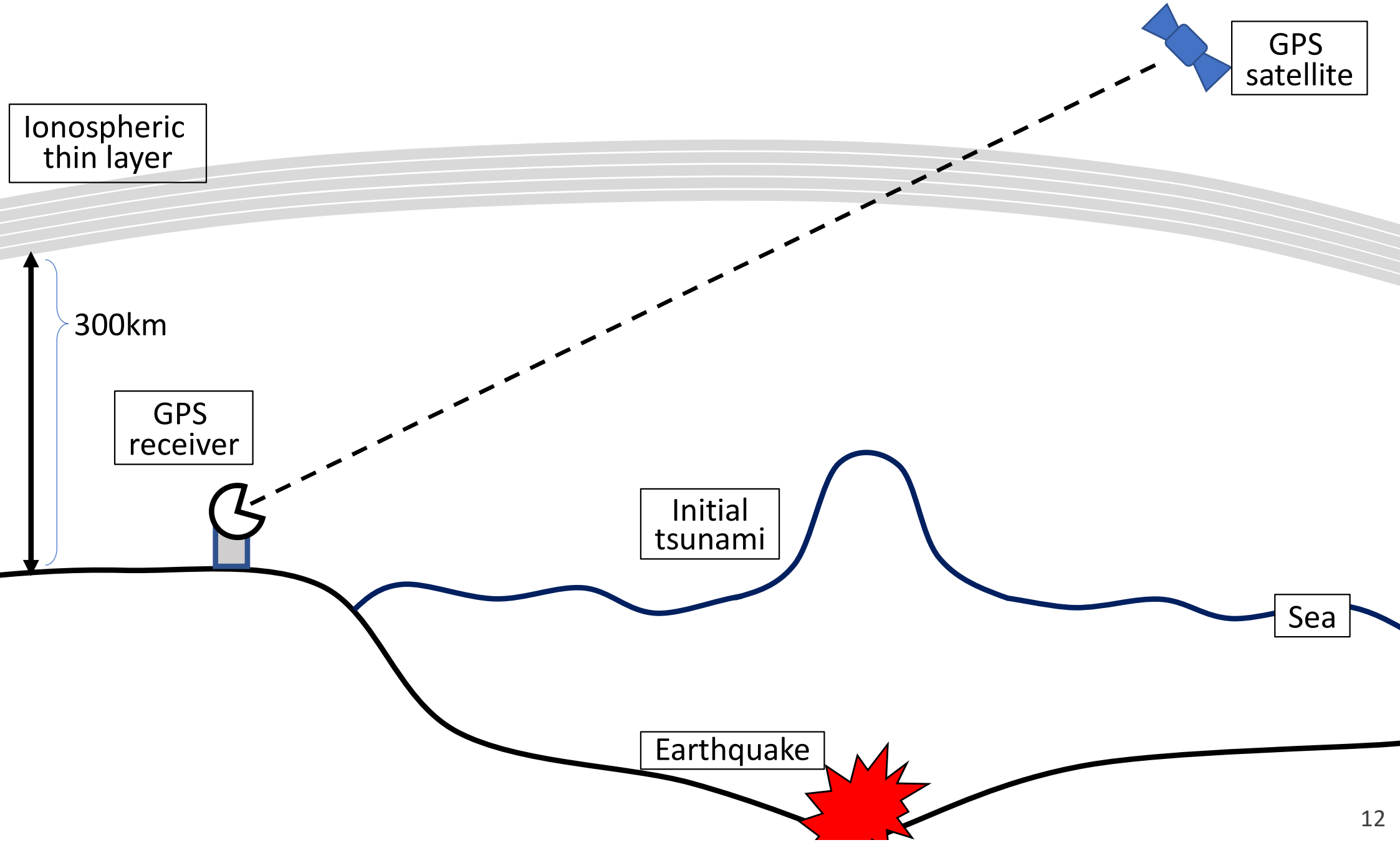

A possible solution

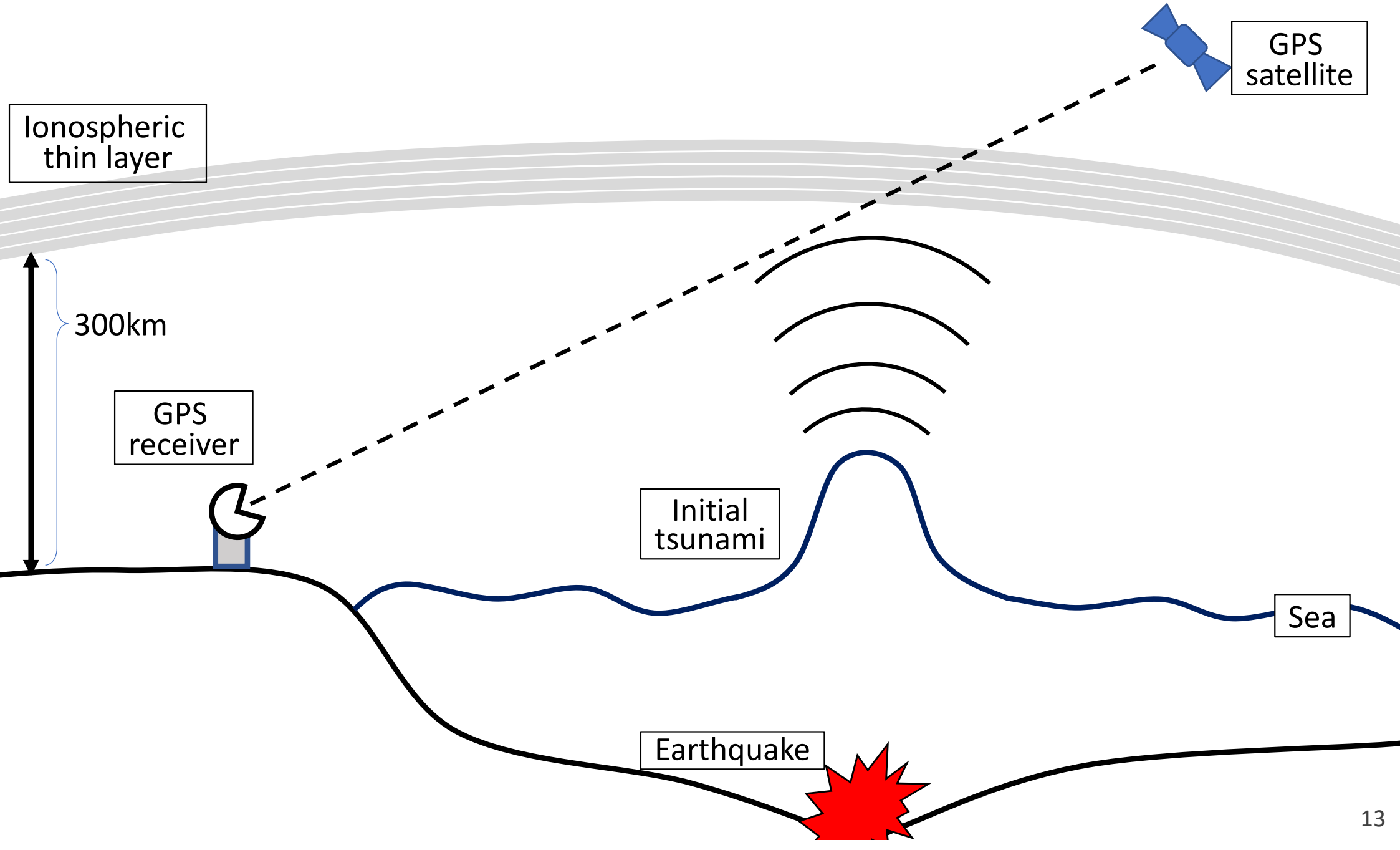

A possible solution

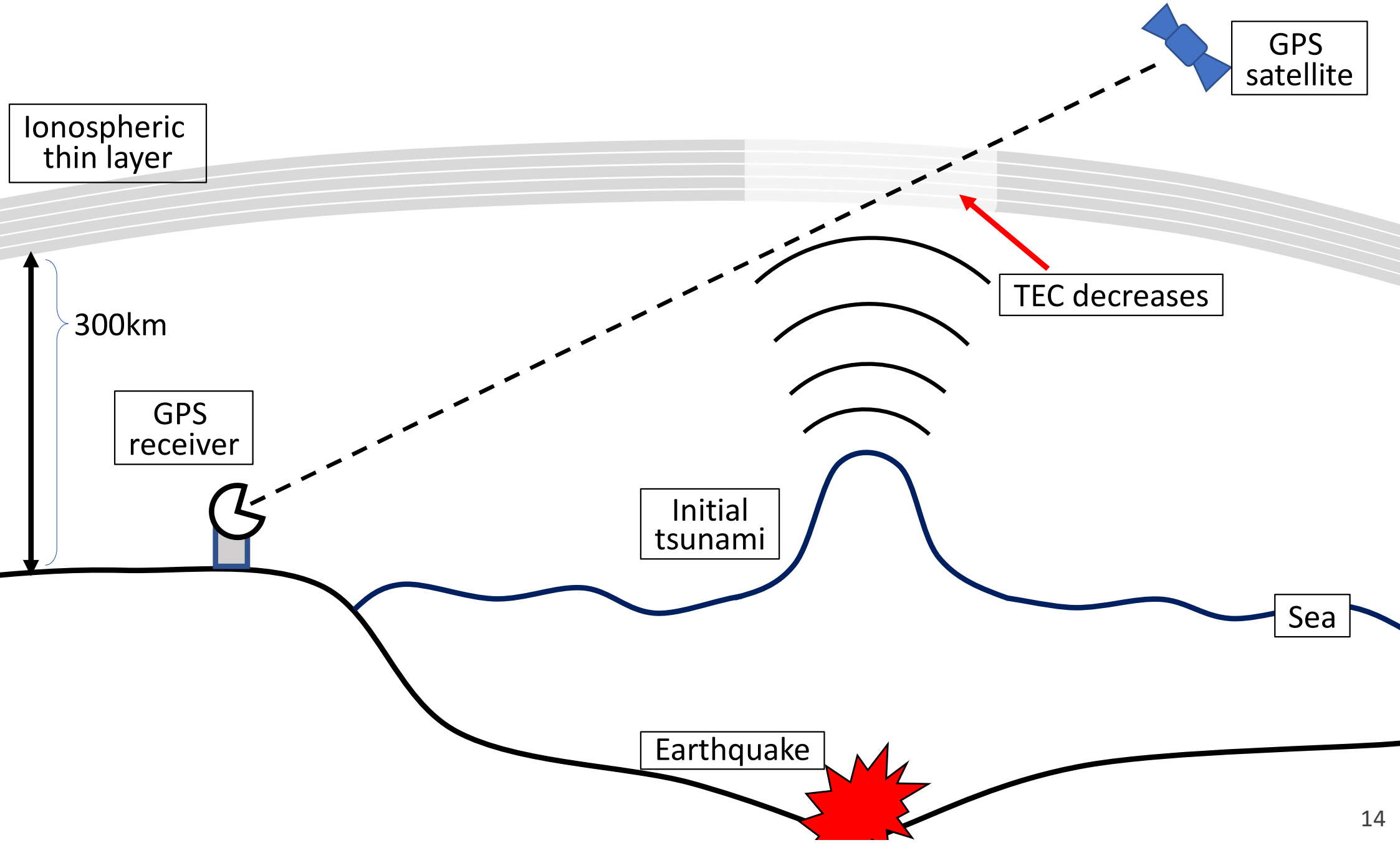

A possible solution

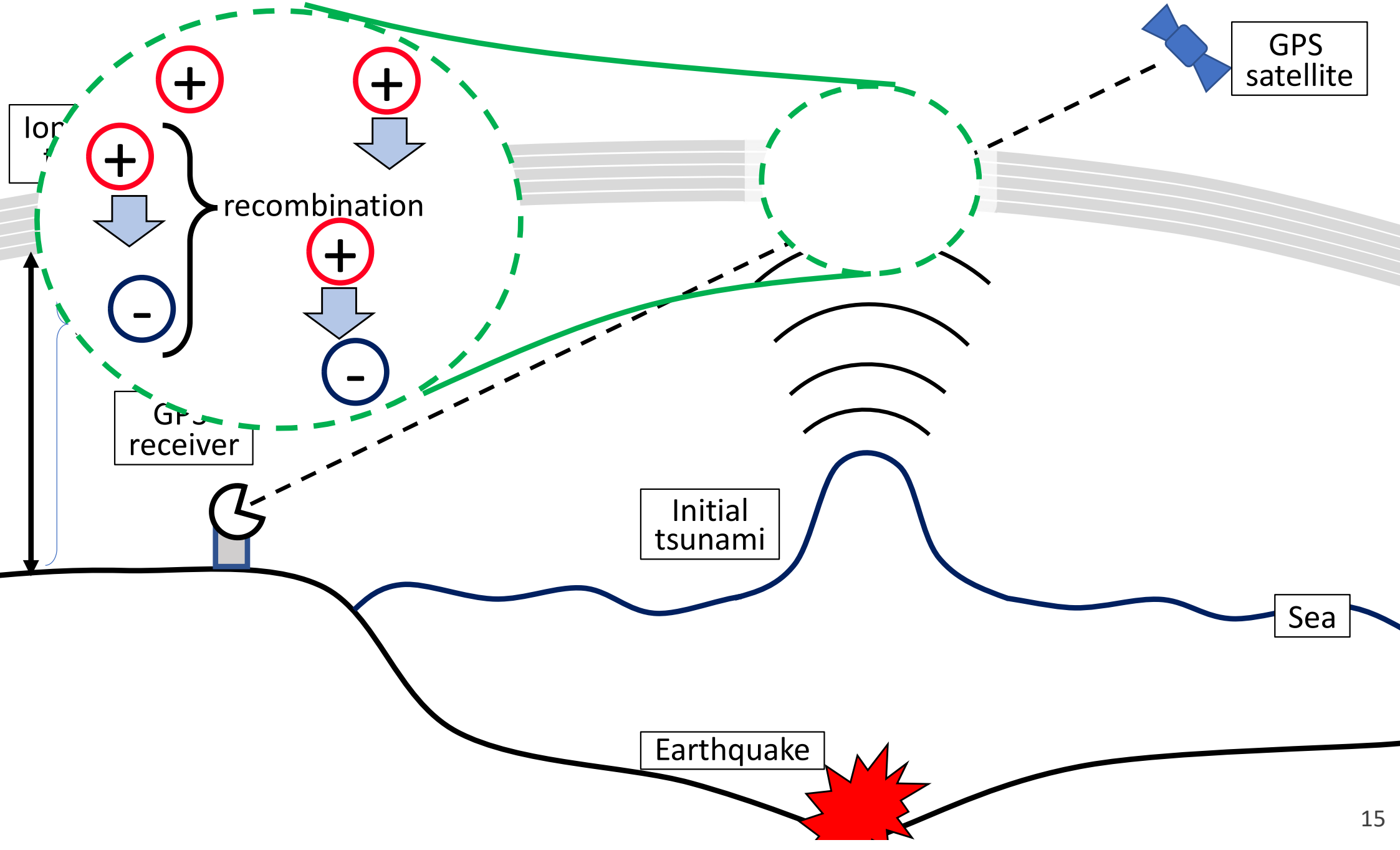

A possible solution

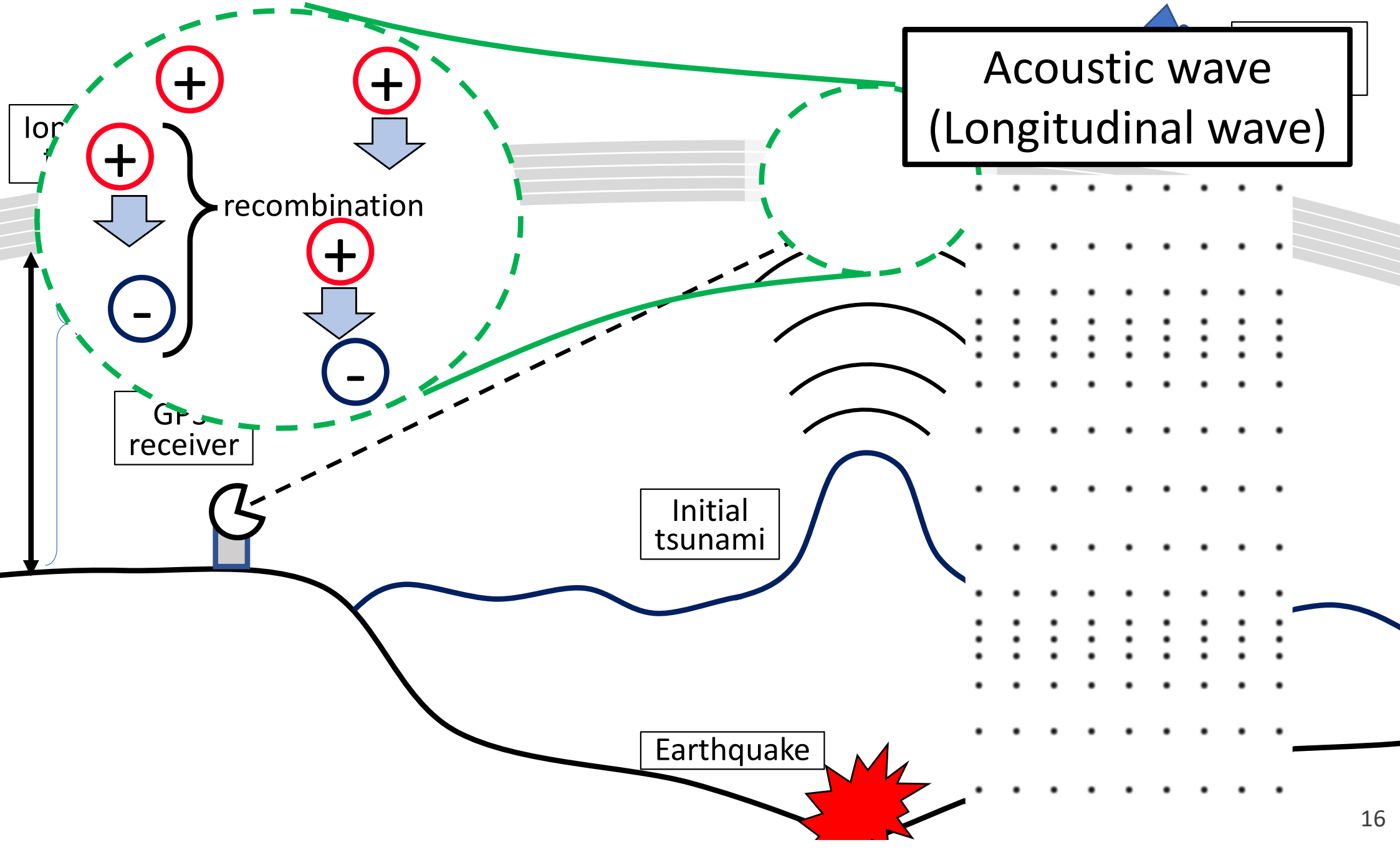

A possible solution

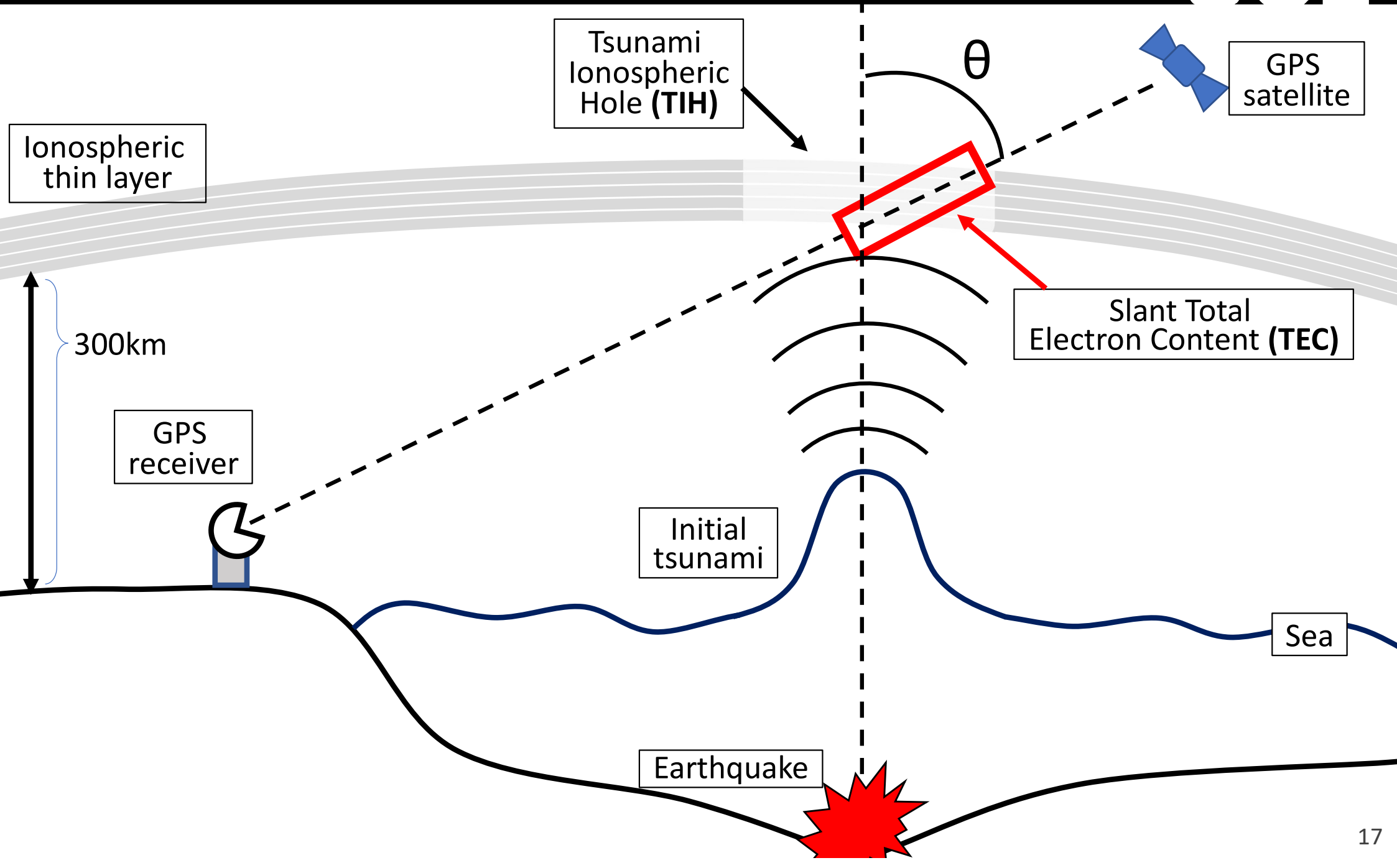

A possible solution

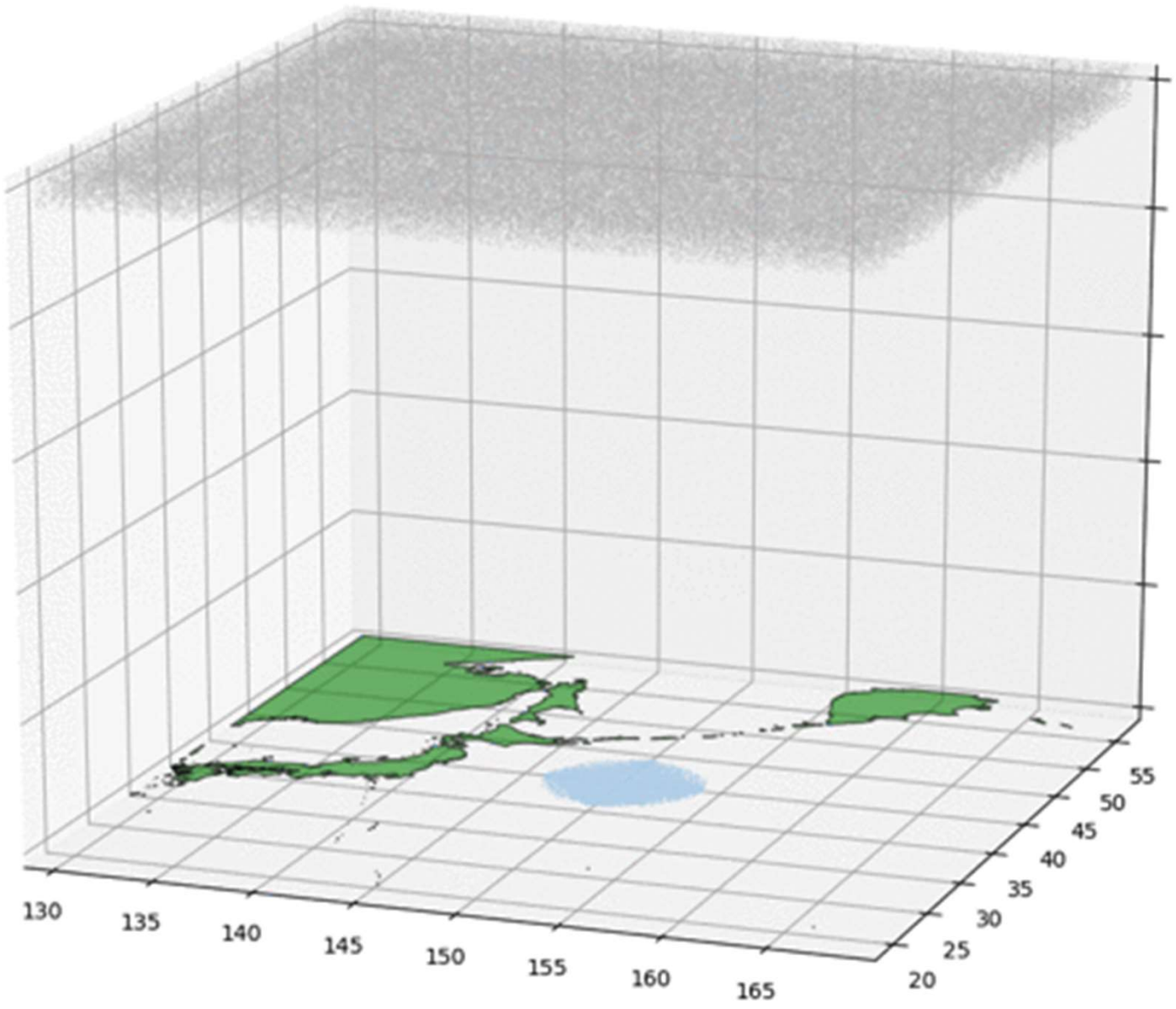

A possible solution

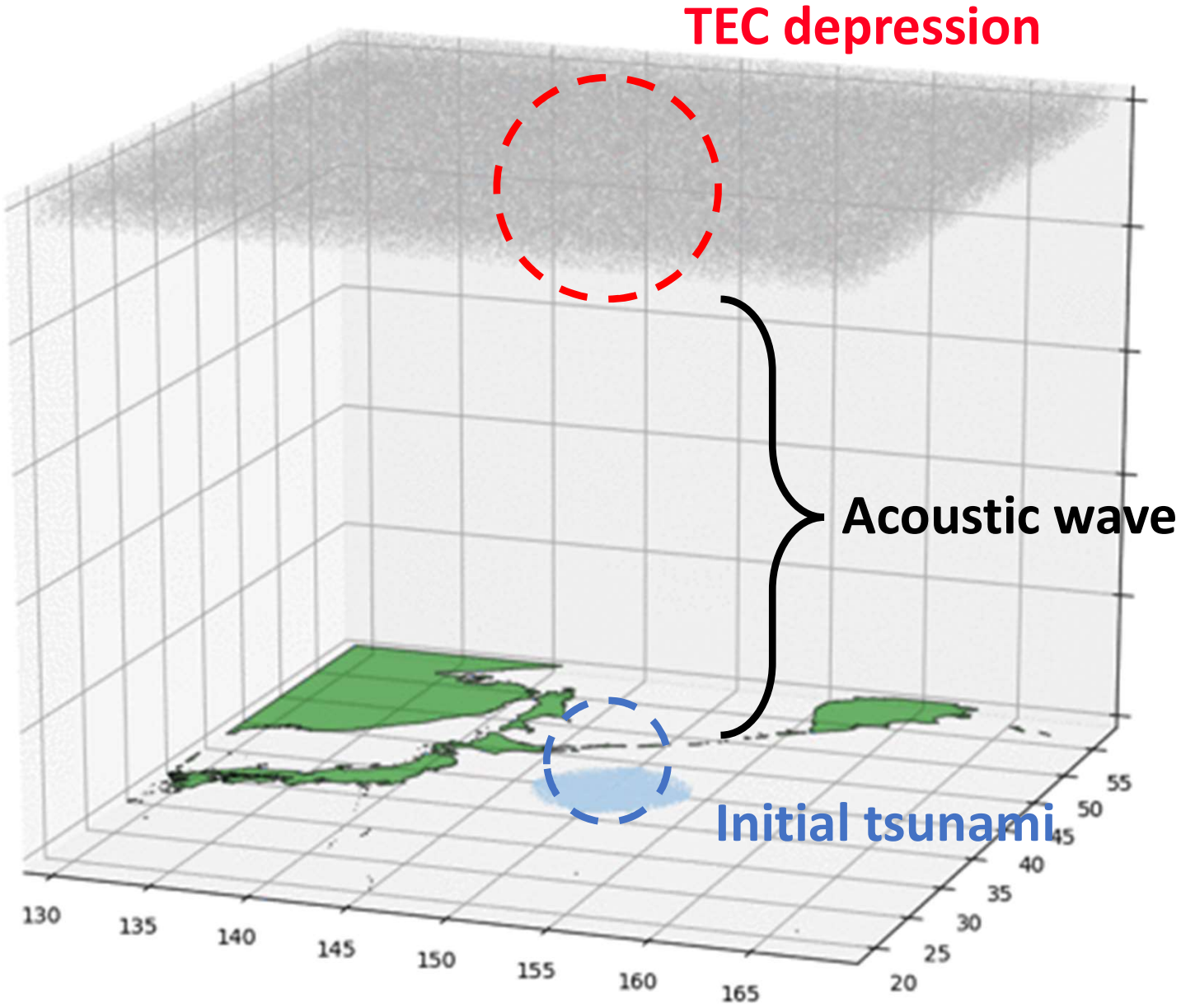

GPS data

Statistics

Contents

Our approach

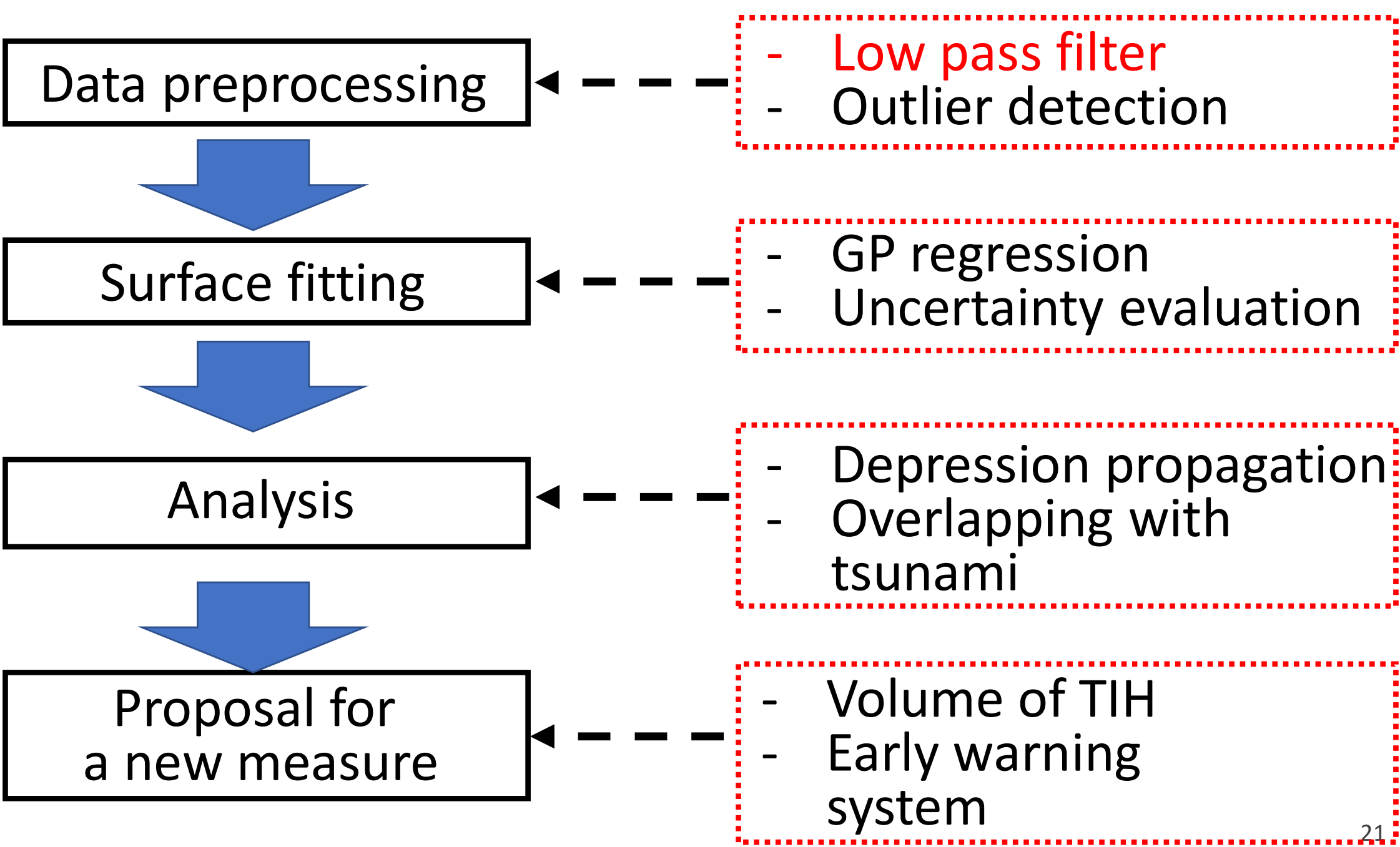

[Redisplaying] Detected data

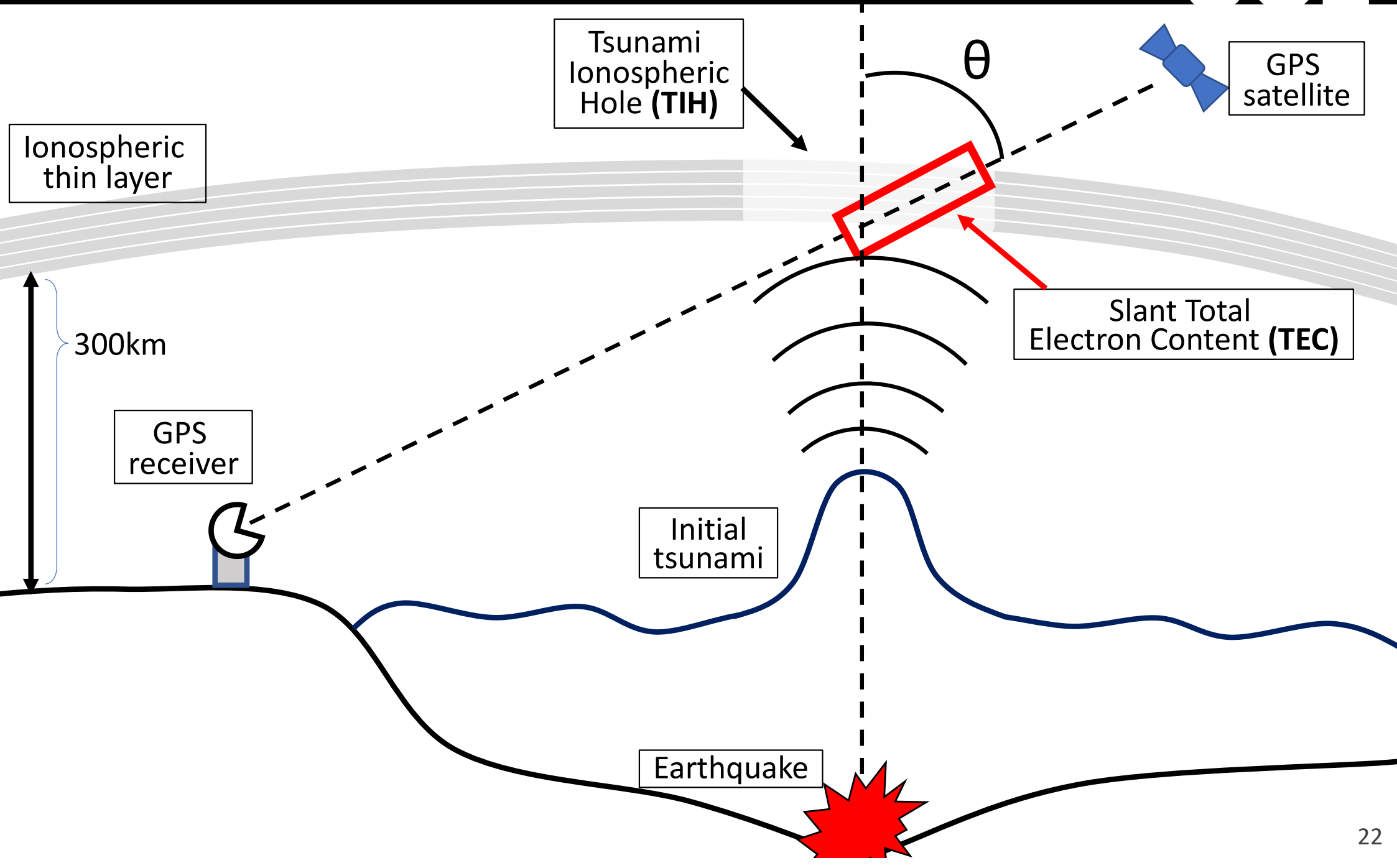

Detected data

Receiver 564

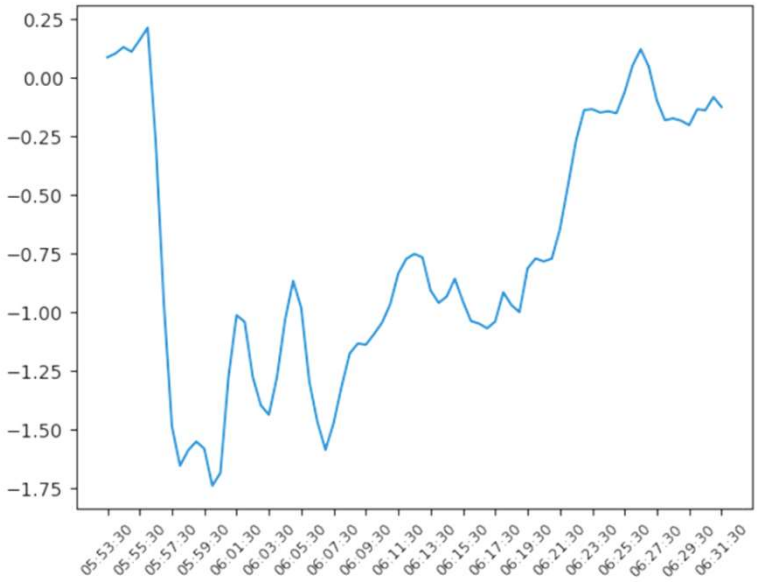

Receiver 565

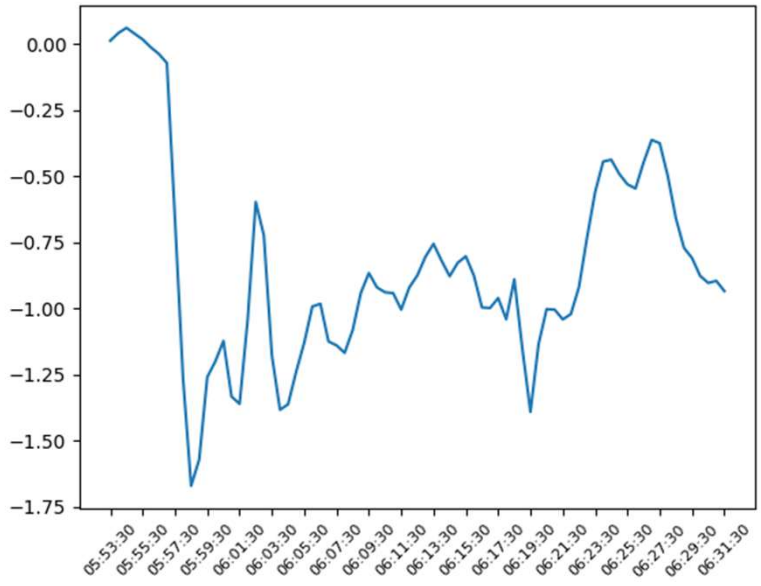

Receiver 610

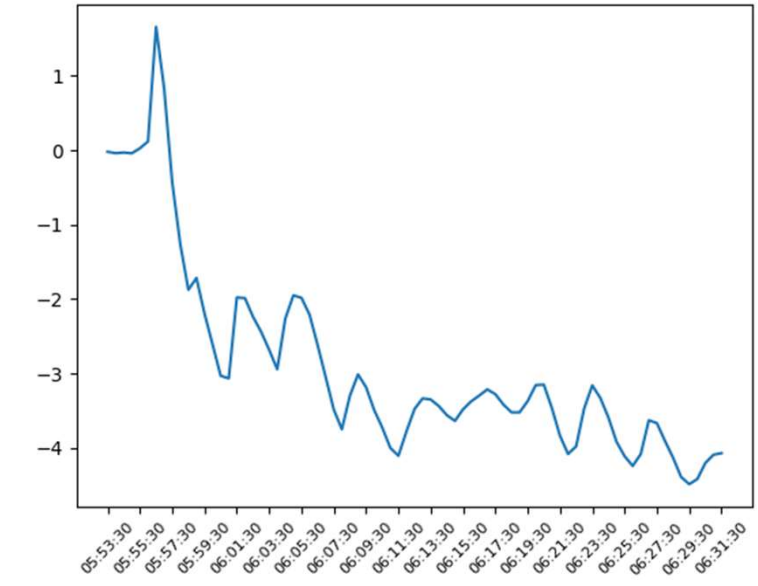

Receiver 3025

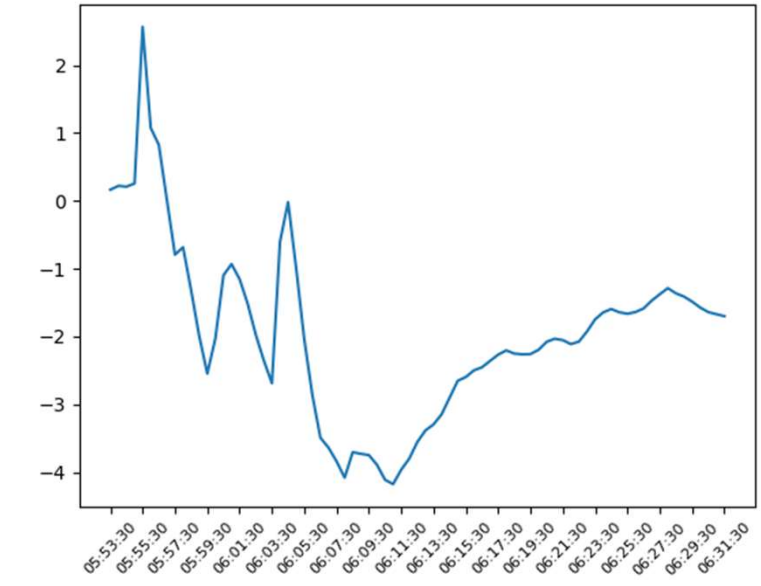

Satellite 26

This satellite is the one which is located near the epicenter. All the graphs displayed here are electron density depression data captured by the satellite 26.

The data can be purchased by the Japanese government.

Detected data

Fourie Transform

The Fourier Transform transforms a function f into a function $\hat{f}$ that describes the frequencies contained in f. In other words, the Fourier Transform is a frequency domain representation of f.

$$\hat{f}(\xi) := \int_{-\infty}^{\infty} f(x) e^{-2\pi i x \xi} \, dx$$

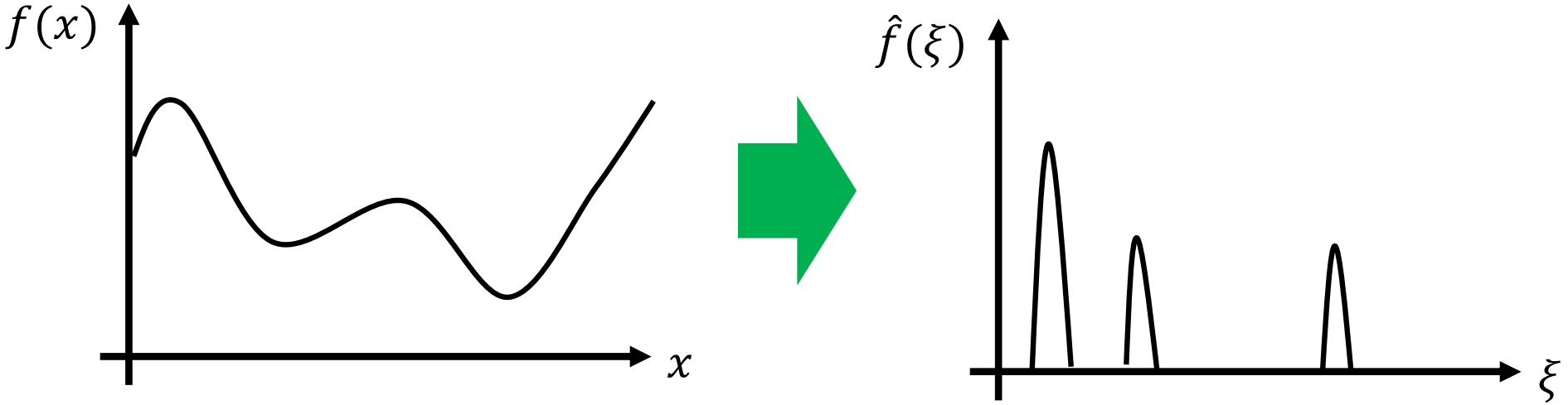

Detected data

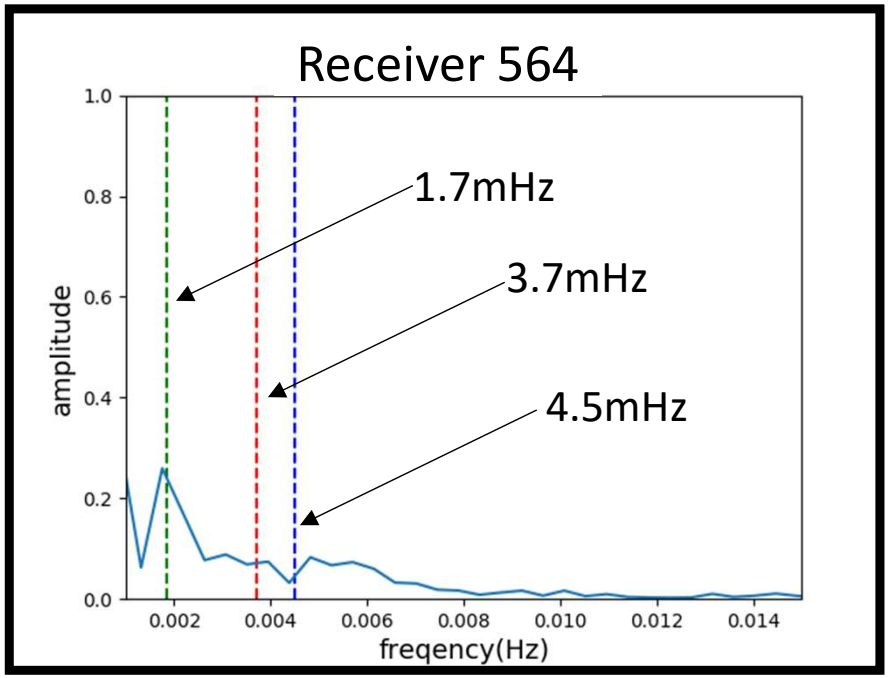

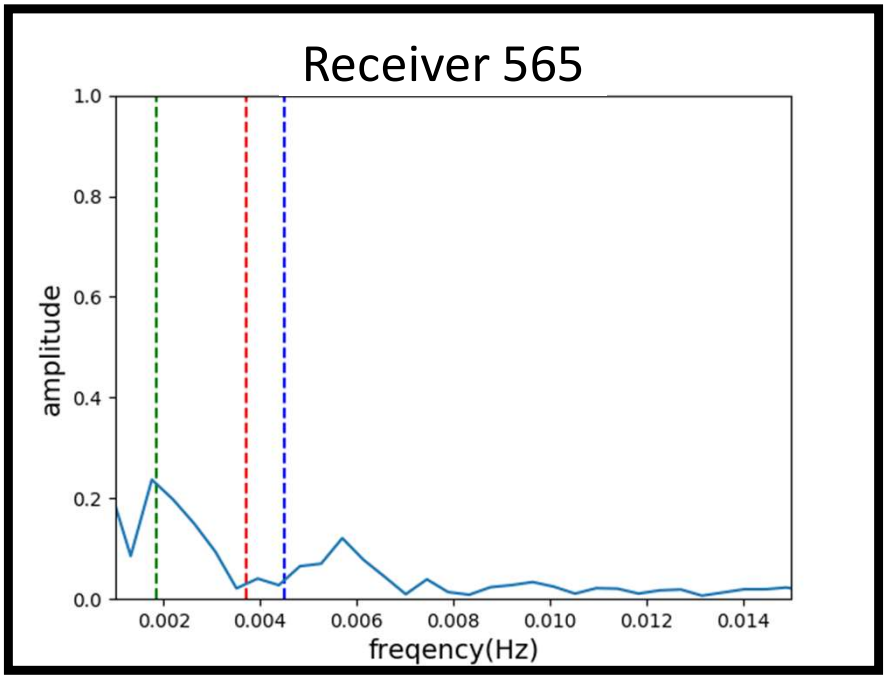

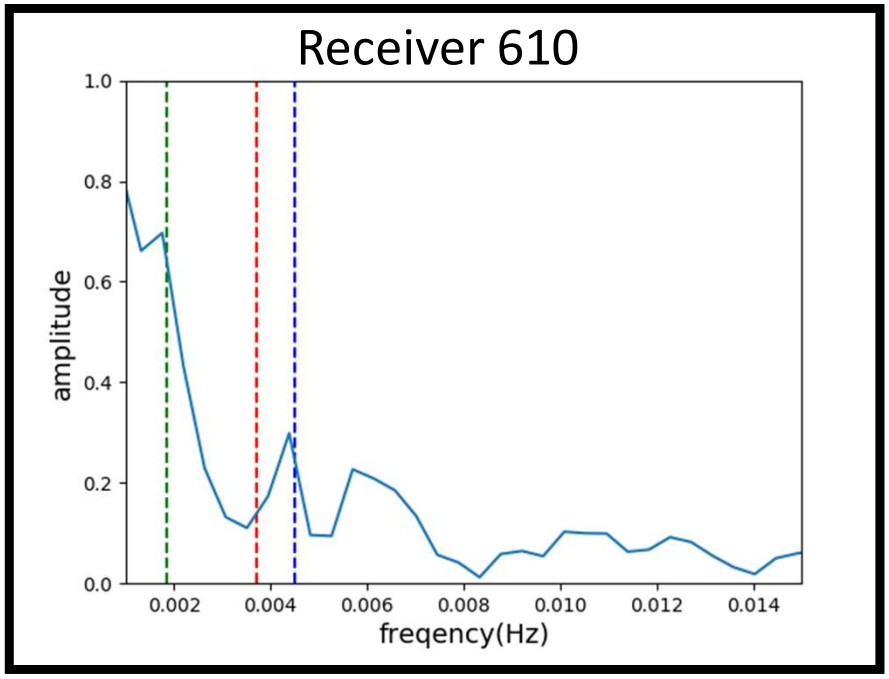

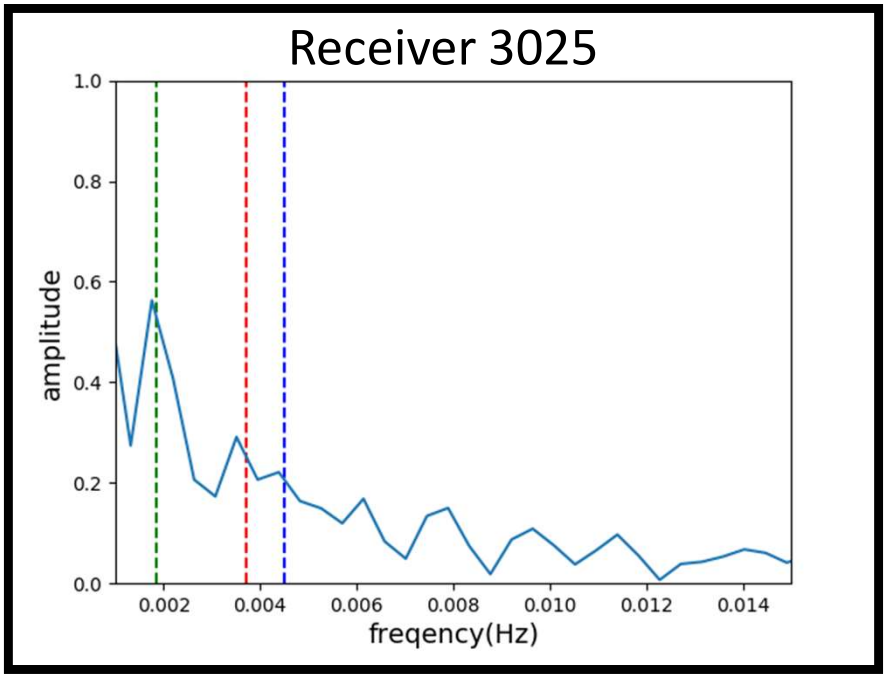

Satellite 26

This satellite is the one which is located near the epicenter. All the graphs displayed here are electron density depression data captured by the satellite 26.

The data can be purchased by the Japanese government.

Detected data

UCL

Receiver 564

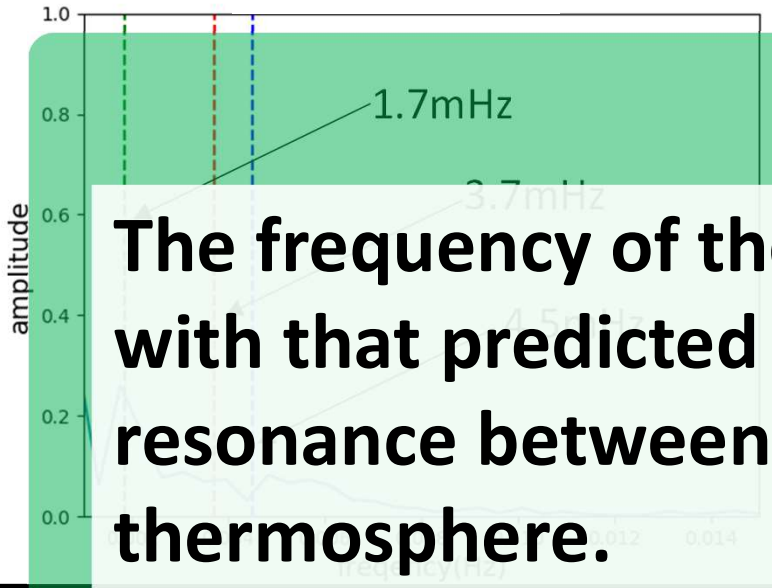

Receiver 565

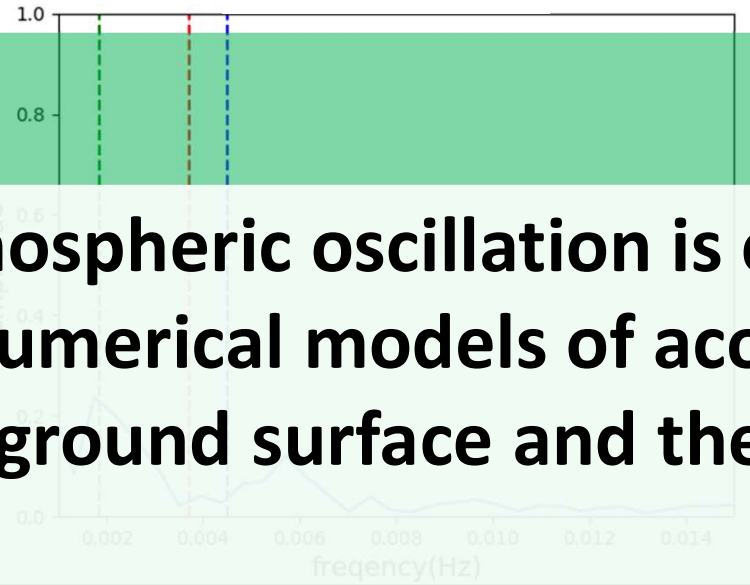

Receiver 610

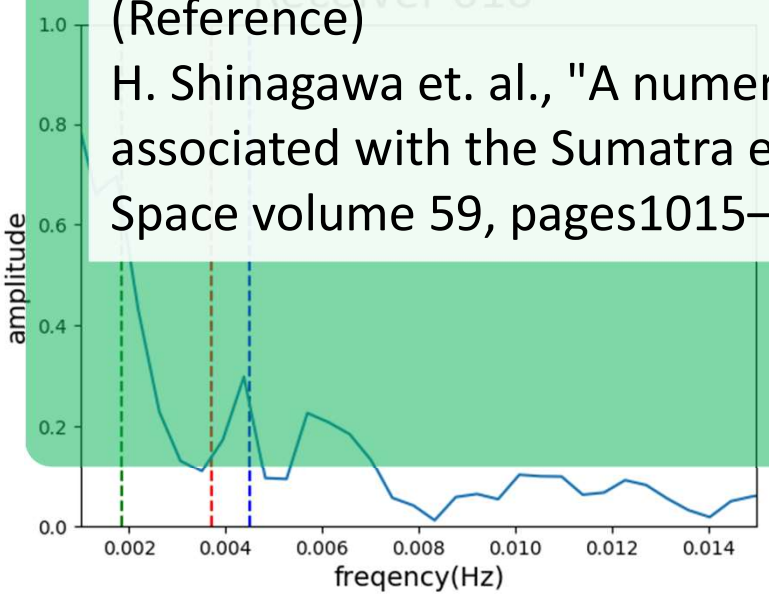

Receiver 3025

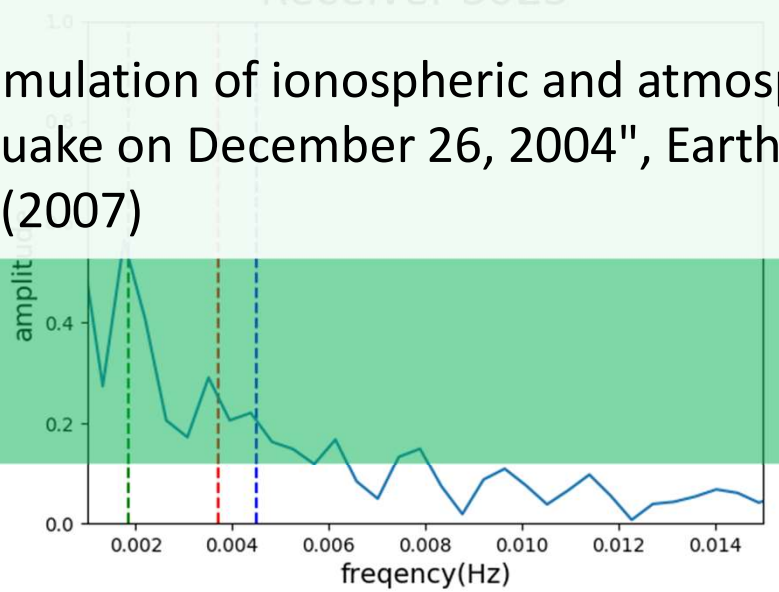

The frequency of the ionospheric oscillation is consistent with that predicted by numerical models of acoustic resonance between the ground surface and the lower thermosphere.

(Reference)
H. Shinagawa et. al., "A numerical simulation of ionospheric and atmospheric variations associated with the Sumatra earthquake on December 26, 2004", Earth, Planets and Space volume 59, pages1015–1026 (2007)

Satellite 26

This satellite is the one which is located near the epicenter. All the graphs displayed here are electron density depression data captured by the satellite 26.

The data can be purchased by the Japanese government.

Low pass filter

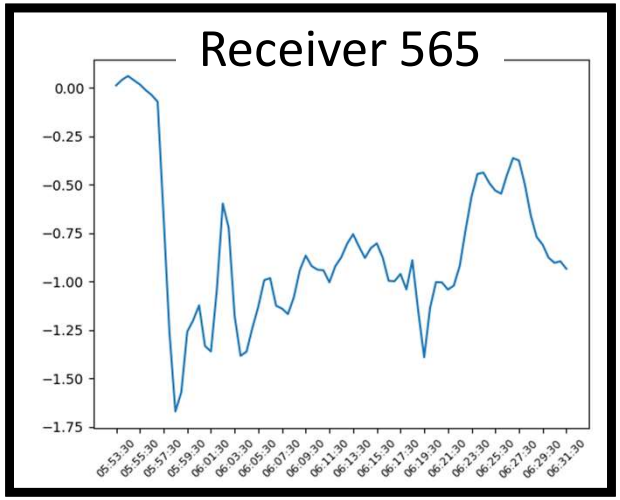

- The data shows the electron density depression.
- Many fluctuations are observed.
- High frequency components should be removed.

Fouire Taransform → ✗ **Not** applicable to Real-time analysis

Linear Regression → ✗ **Not** applicable to Real-time analysis

Backward Moving Average → ✓ **Applicable** to Real-time analysis

Low-pass filtered data

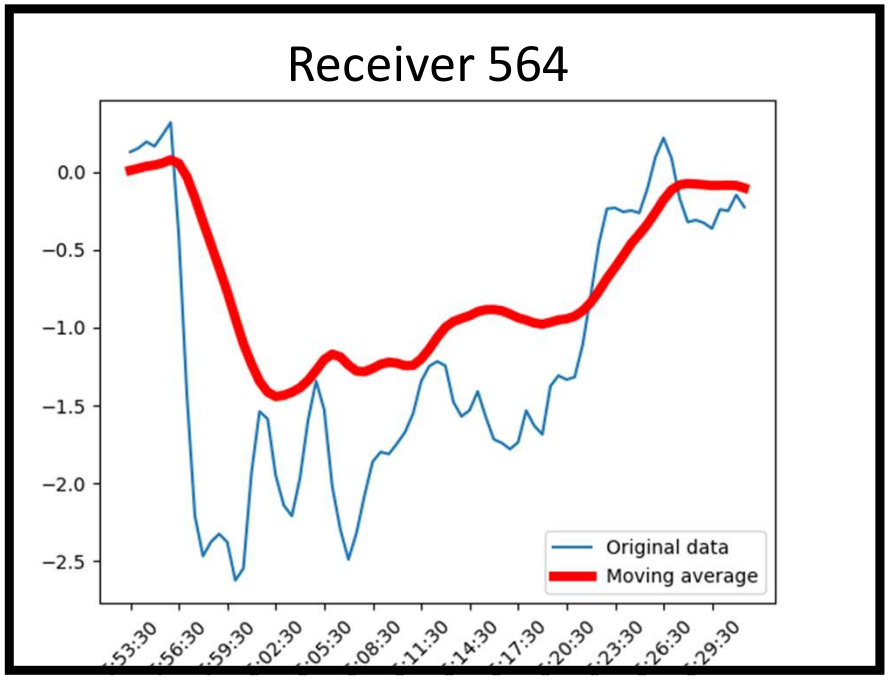

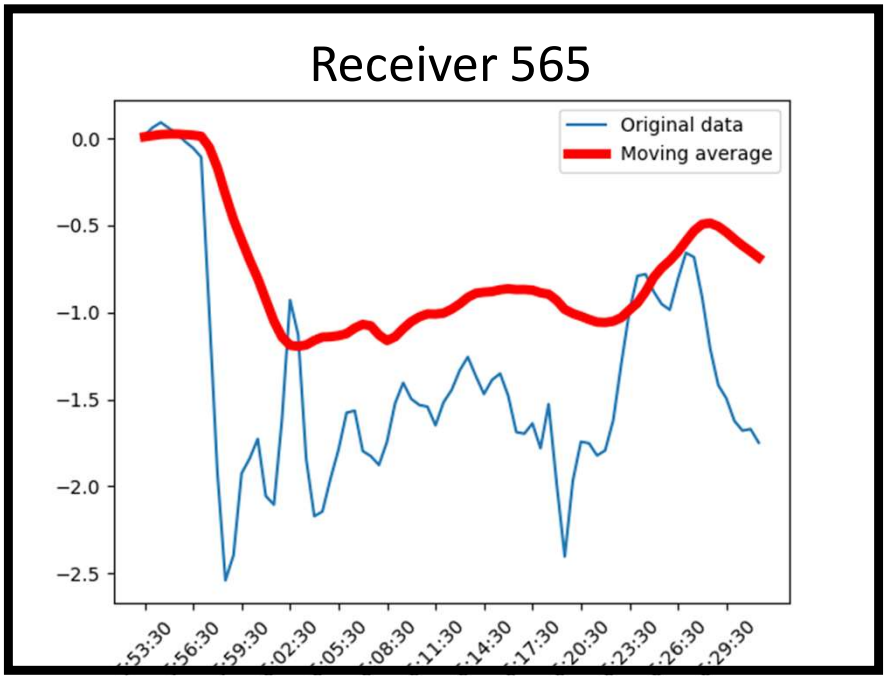

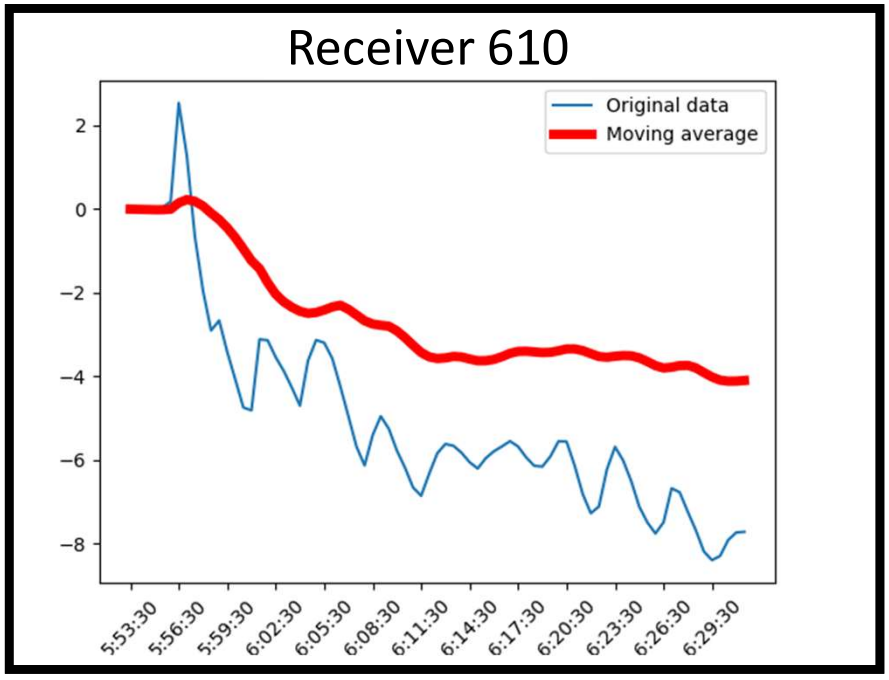

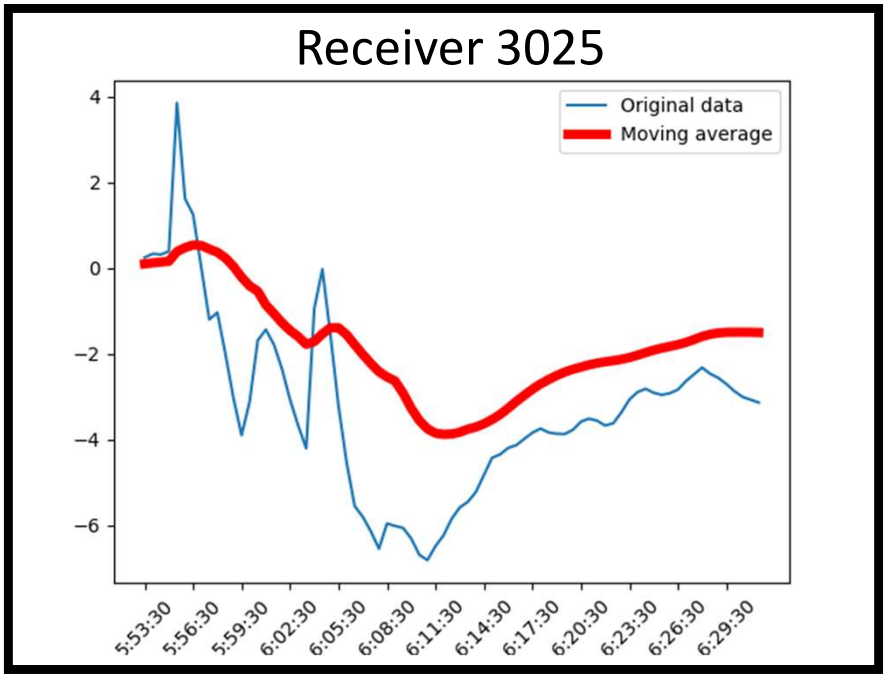

Low-pass filter

Only low frequency modes can be obtained through the low-pass filter based on the backward moving average.

Our approach

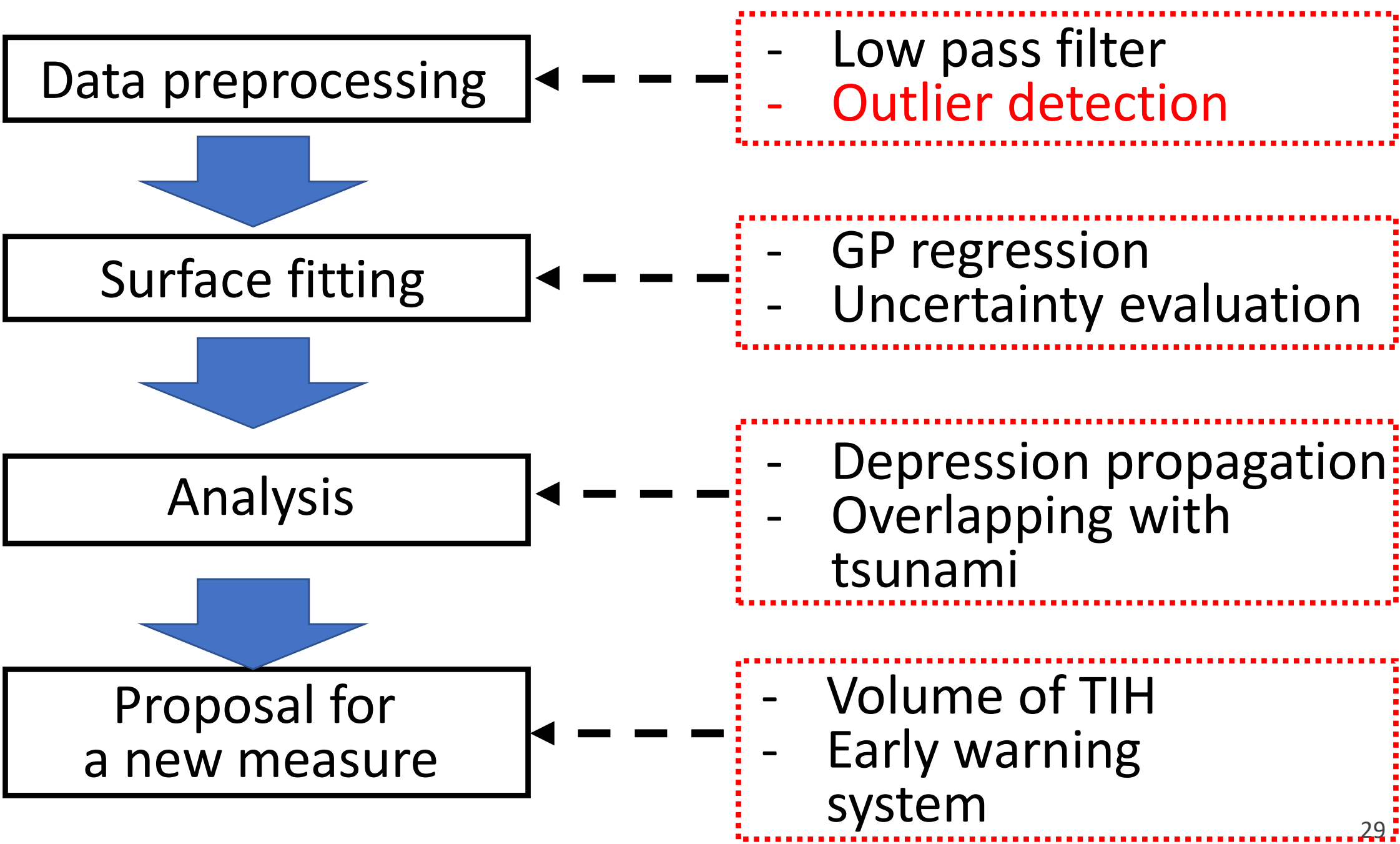

[Redisplaying] Detected data

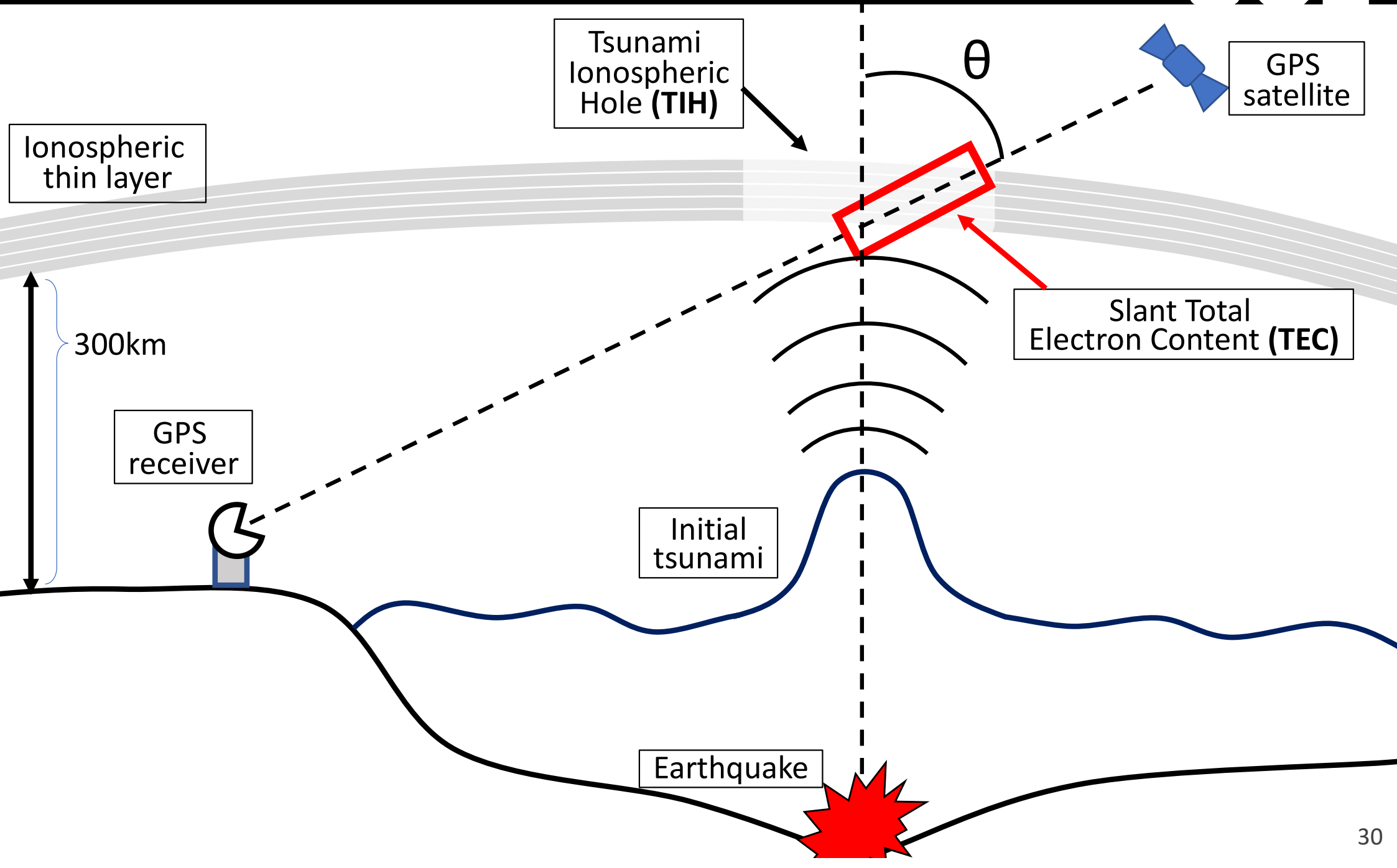

Outliers

3D plot of low-pass filtered data

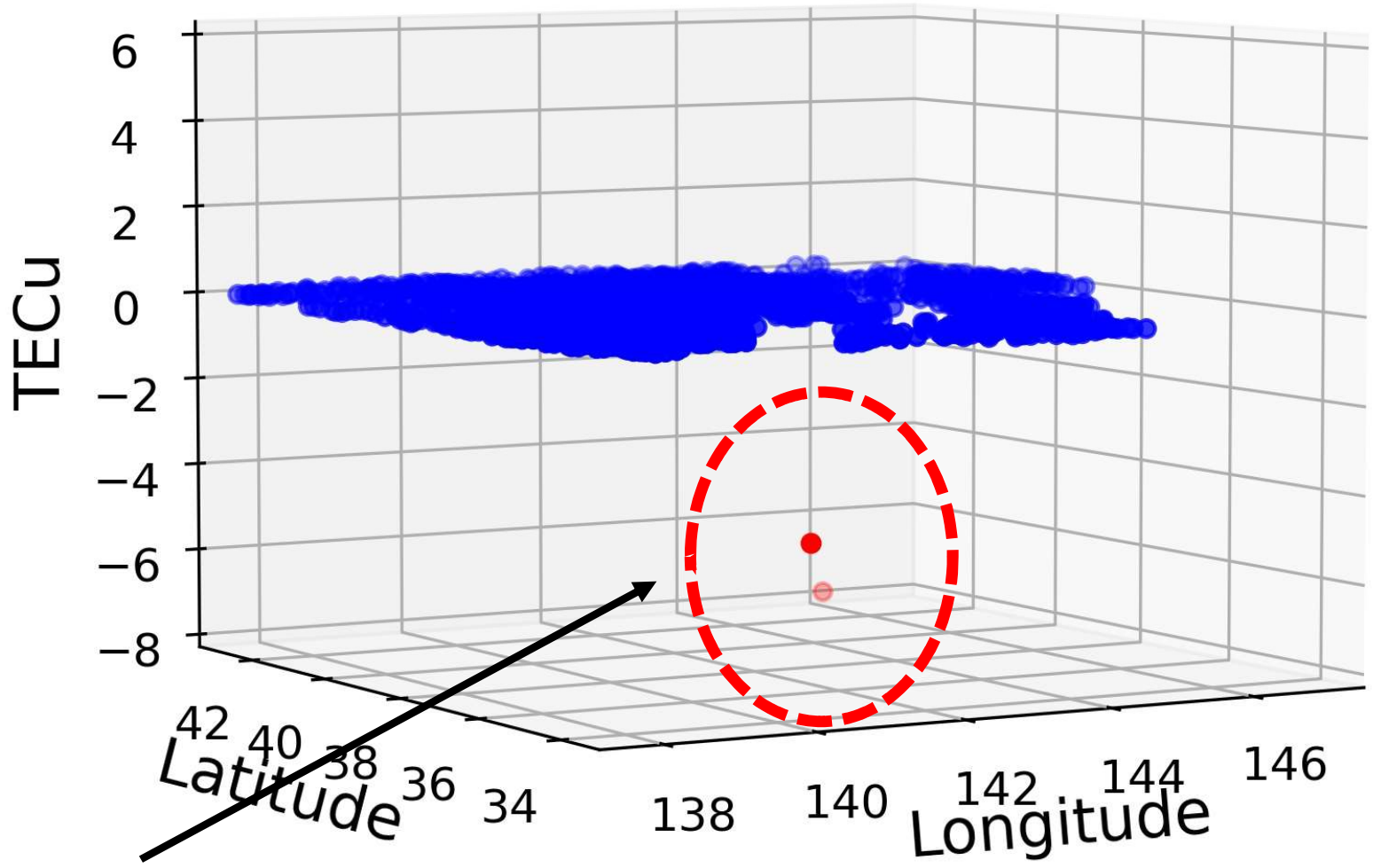

These two data points seem to be outlier

Outlier Detection

UCL

TECu

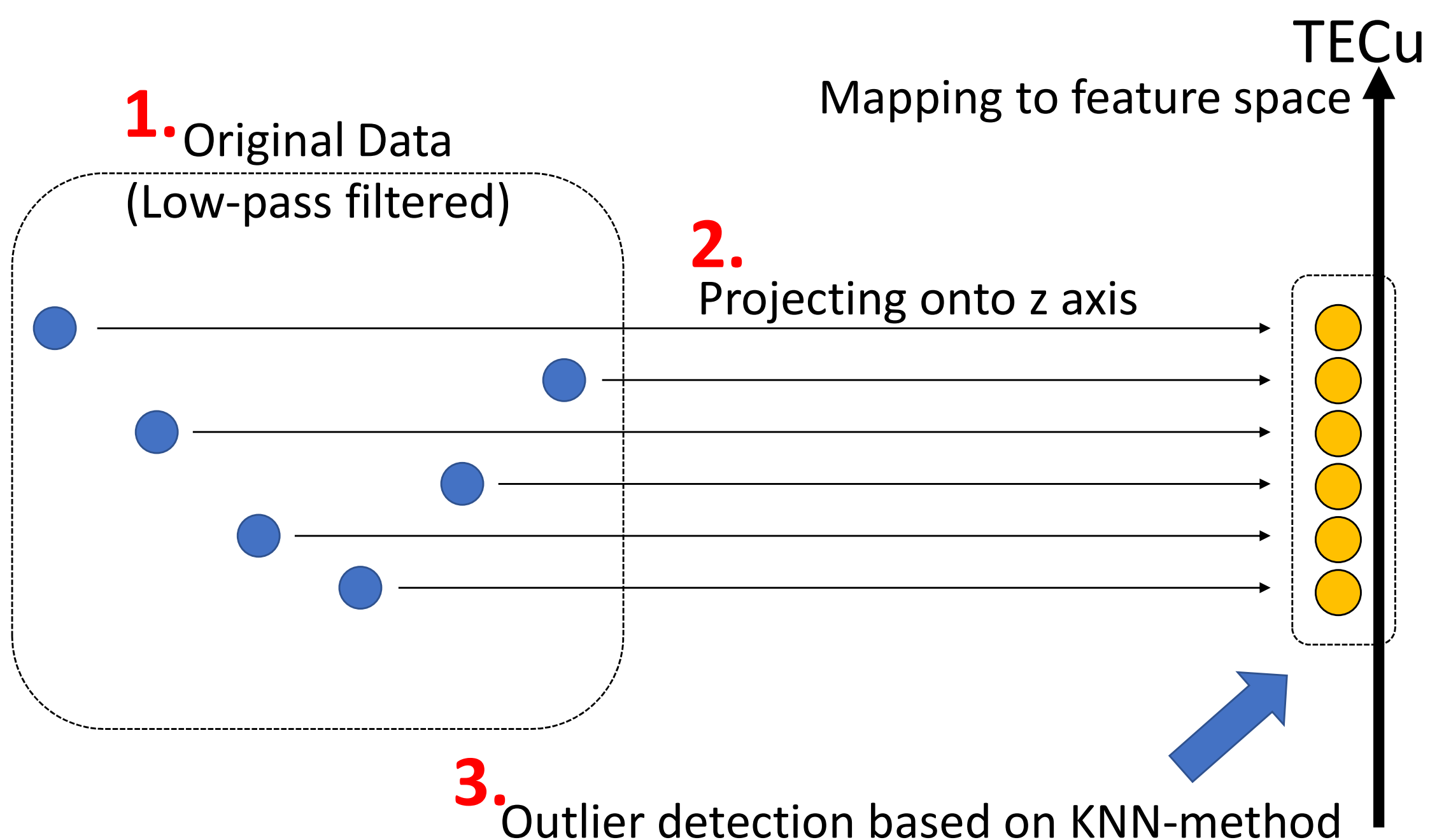

Previous method

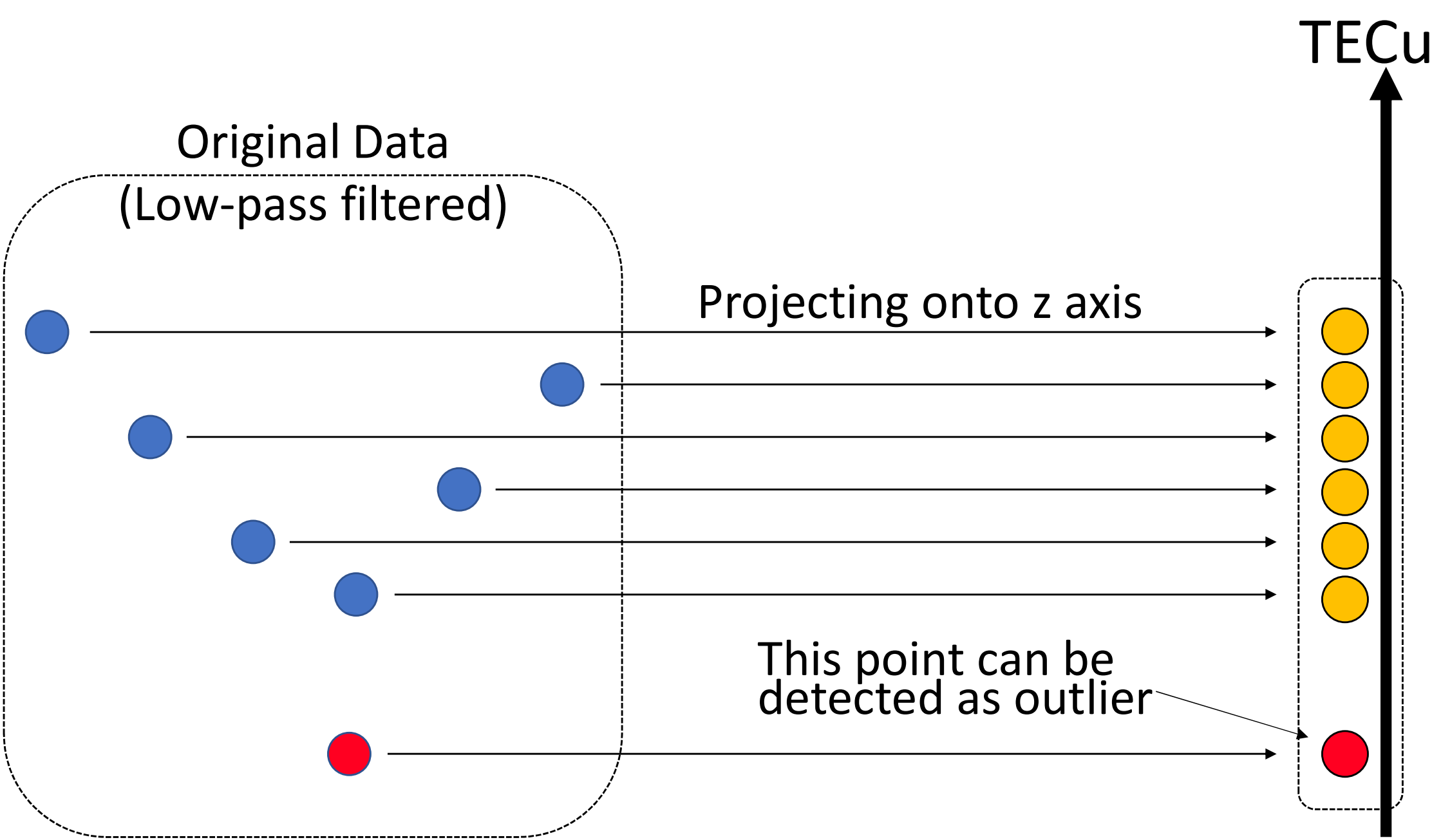

Previous method

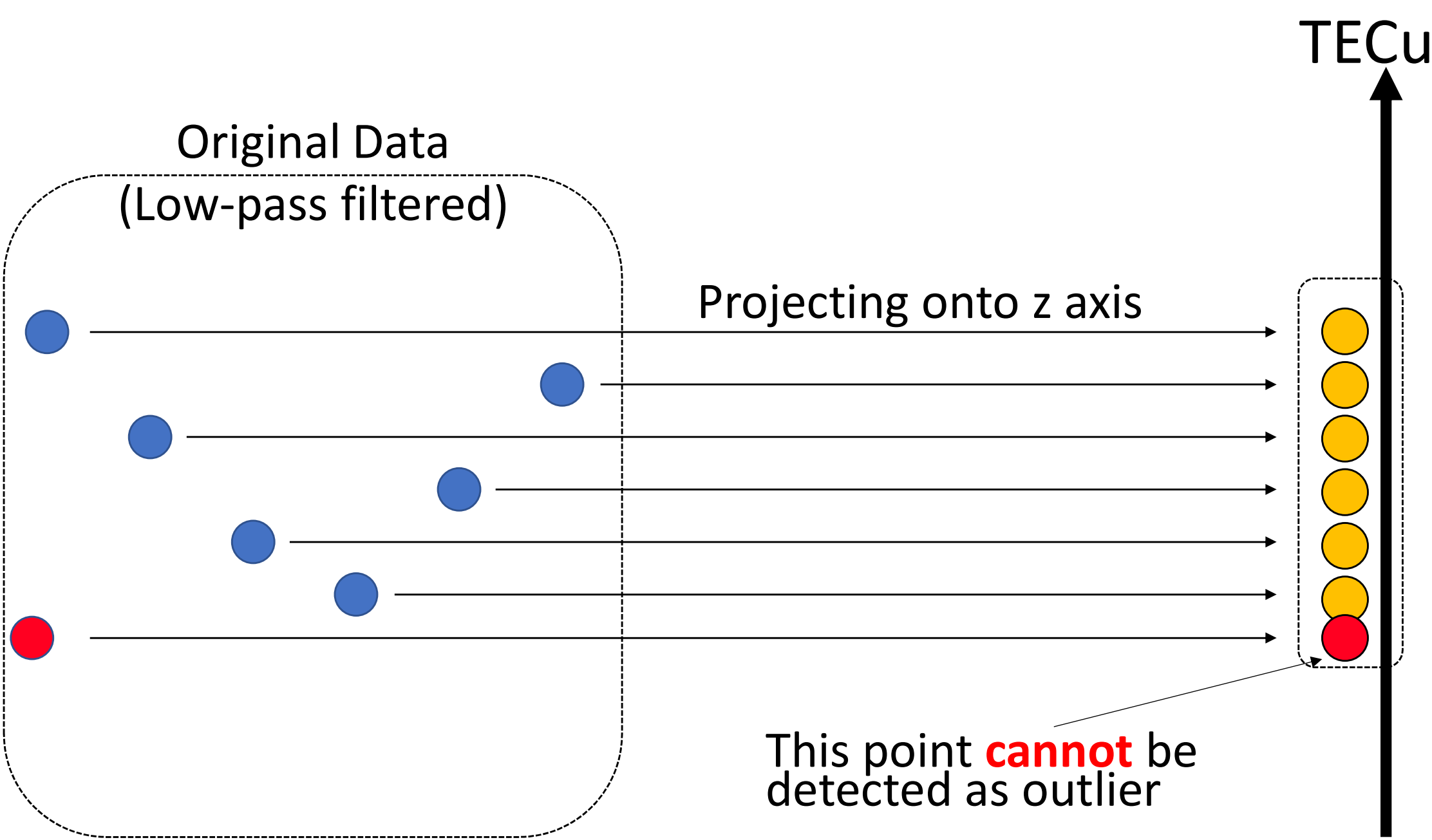

New method

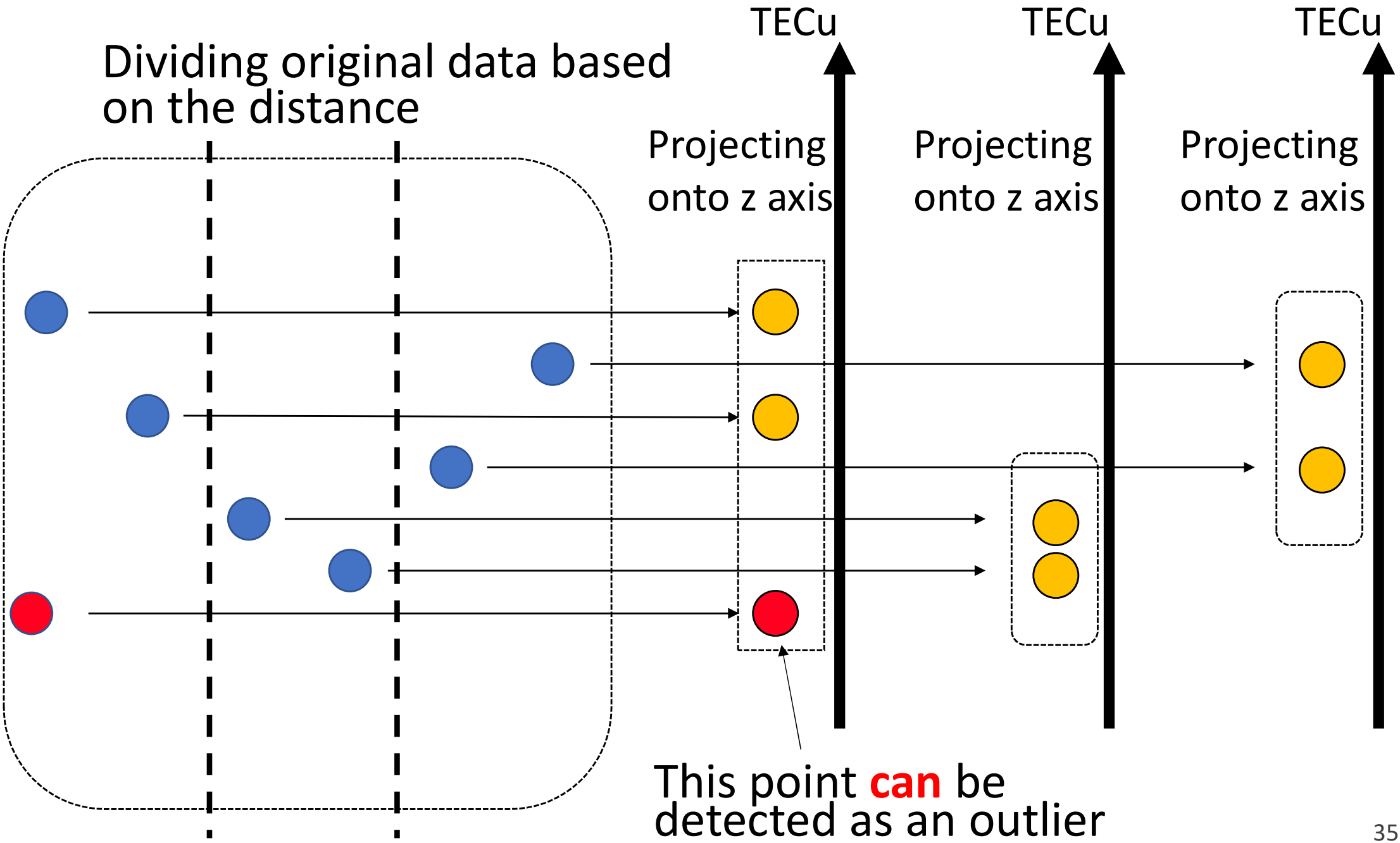
Dividing original data based on the distance
TECu
TECu
TECu
Projecting onto z axis
Projecting onto z axis
Projecting onto z axis
This point can be detected as an outlier

Outlier Detection

Input: Threshold $= 3$,
n: The number of the observation points in the targeting area
for $i = 1, \cdots, n$ **do**
Select a data point S_i from the entire targeting area
Select all data points $\{T\}$ located within 200km radius circle centered on S_i
Count the number, n_i, of $\{T\}$ and set $k_i = \sqrt{n_i}$
for $j = 1, \cdots, n_i$ **do**
Calculate the distance d_j between T_j and S_i
end for
Sort $\{T\}$ based on $\{d\}$ in ascending order
Calculate the TEC difference D_i between S_i and the k_ith nearest point
if $D_i > 3$ **then**
S_i is considered as an outlier
Identify the receiver which detects S_i
end if
end for

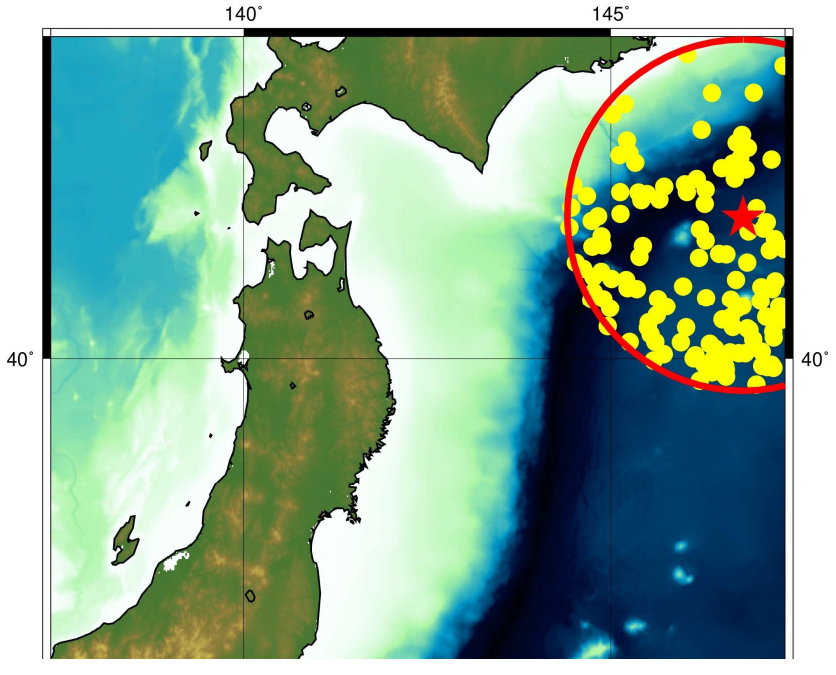

The method can be implemented in real-time

Variogram Cloud (at 6:08:00 UTC)

- ✓ Two outliers are detected by the method.
- ✓ These two points make the variogram cloud strange.

$$y = \frac{|\mathrm{TEC}(x_1) - \mathrm{TEC}(x_2)|^2}{2}$$
$$x = |x_1 - x_2|$$

3D plot

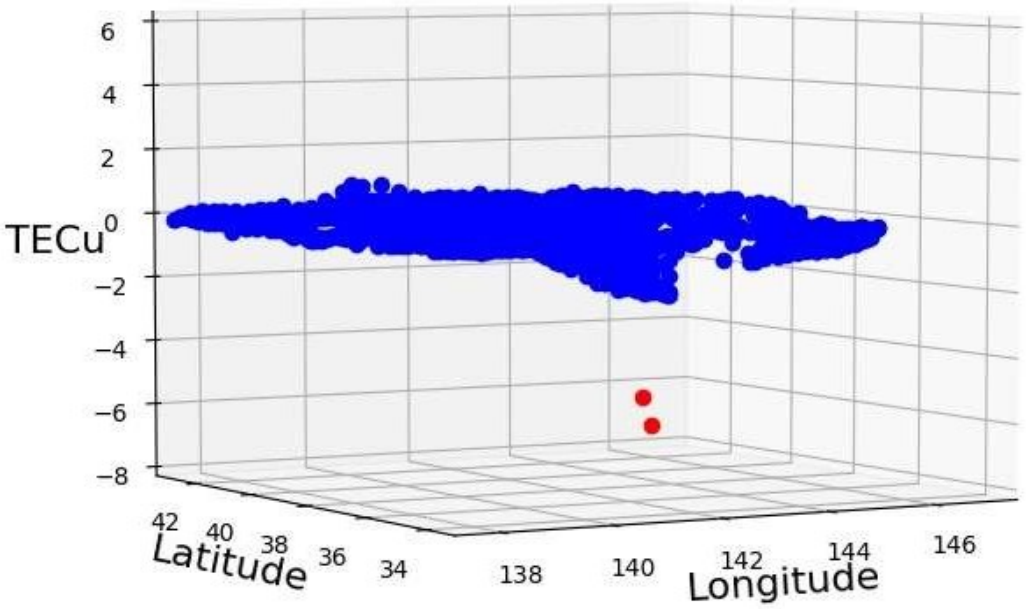

Variogram cloud

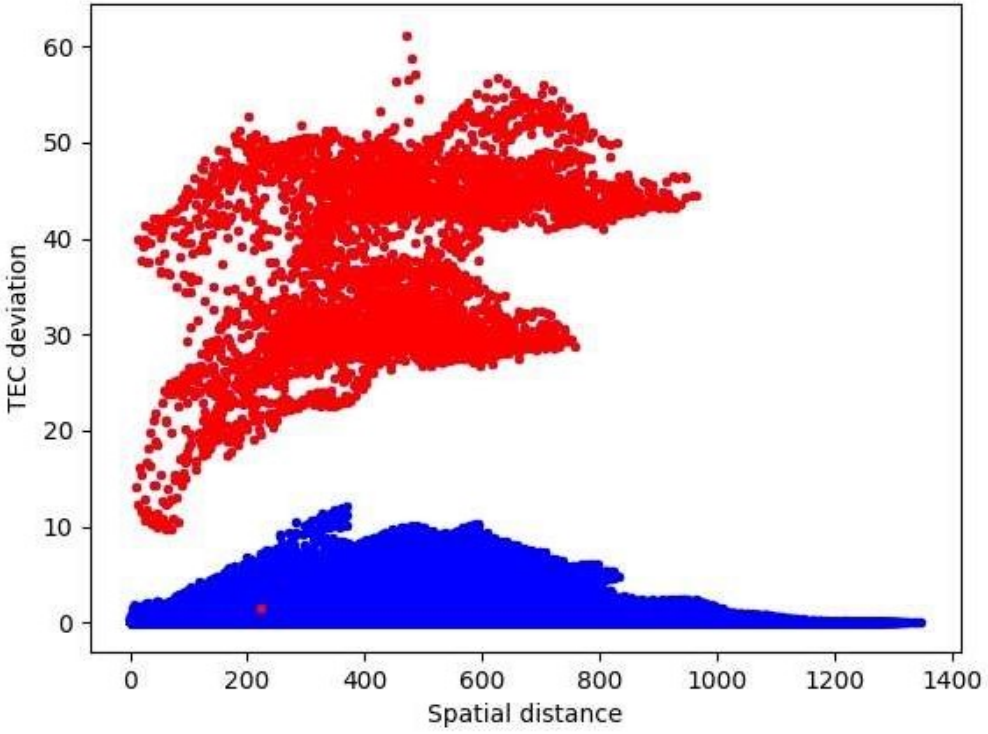

Outliers and Broken Receivers

These two outliers are detected by receiver **175** and **588**

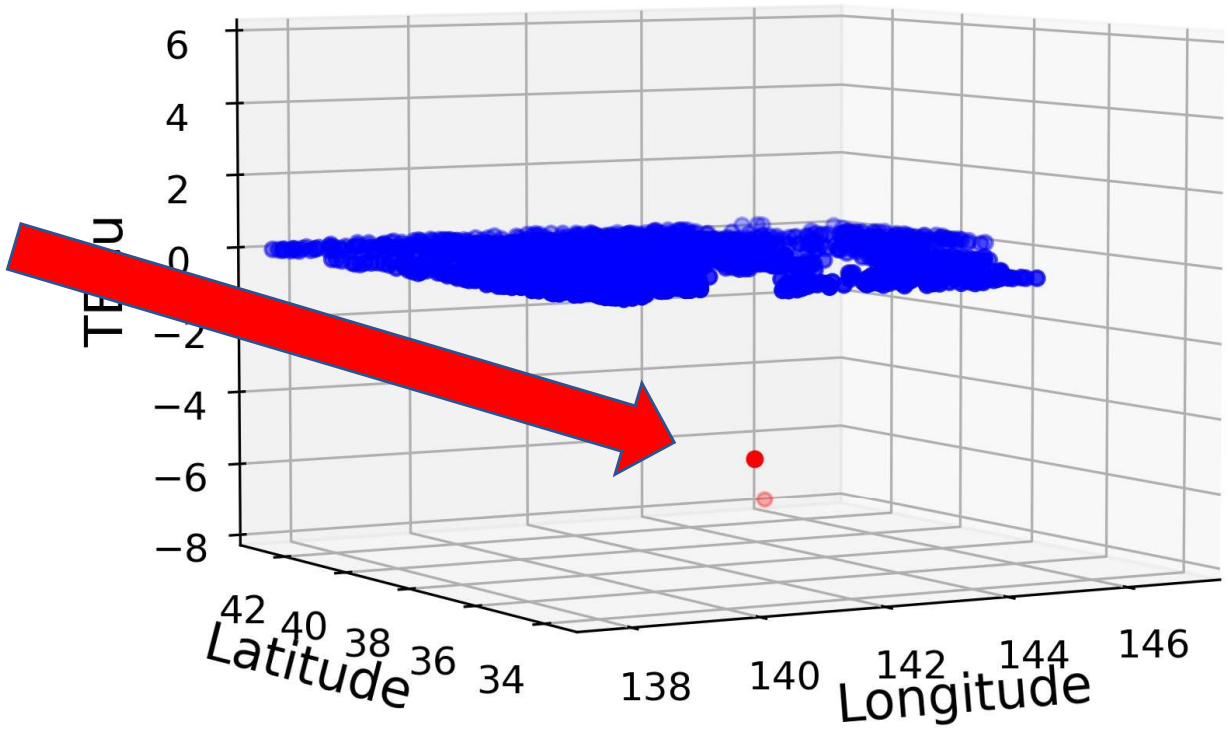

- GPS receiver **175**
- GPS receiver **588**

were broken and repaired by the Japanese government organization.

- Getting distorted can be avoided
- Broken receivers can be identified.

Original Data Captured by Satellites

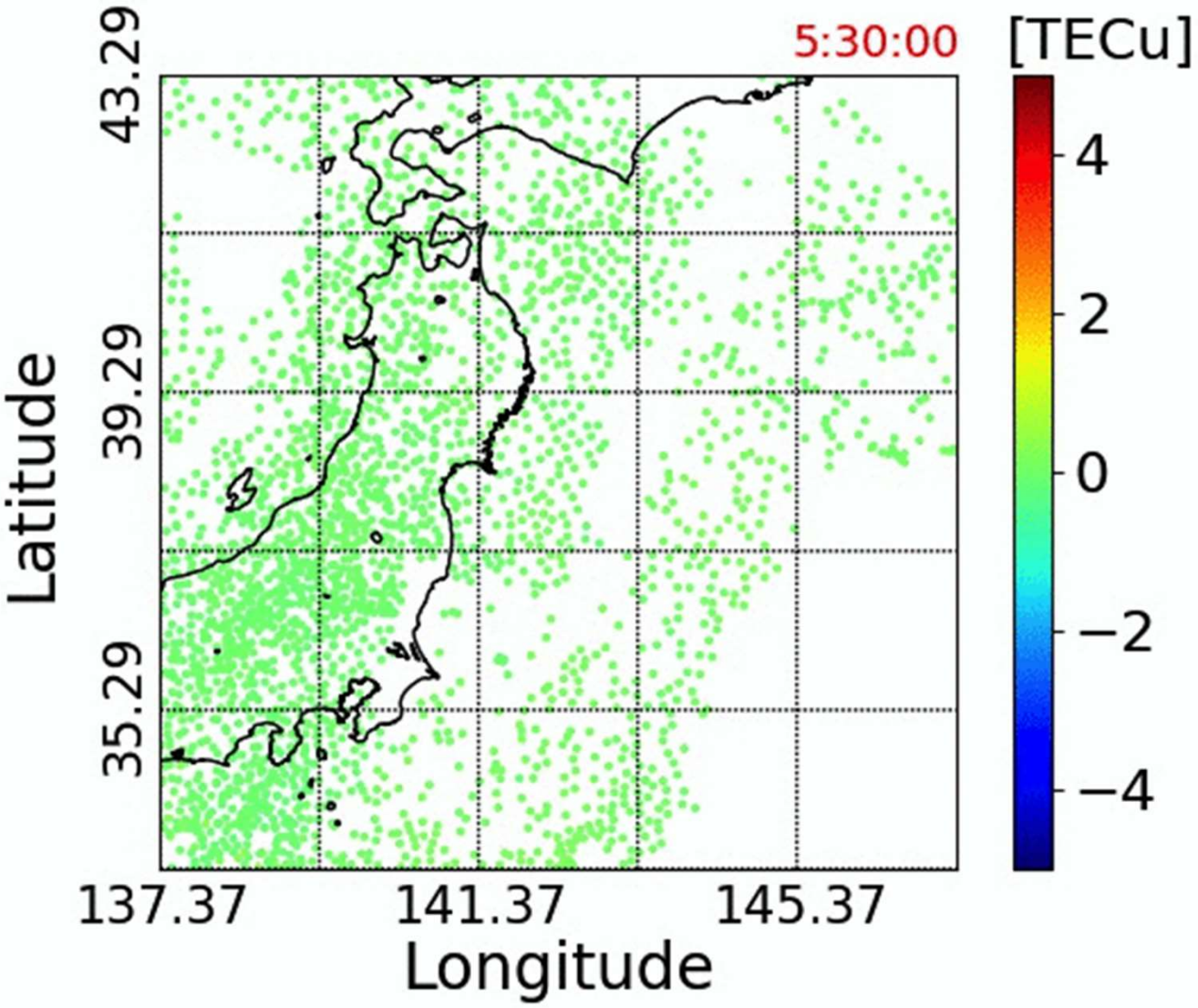

Original data
from 5:30:00 to 6:16:30

The red star mark ★
is the epicenter

The earthquake occurred
at 6:46:30

Problems

UCL

Data points are not uniformly distributed.

The electron density depression is anisotropic.

Detected measurement points are moving.

Network is sparse in some areas (other than Japan) .

Our approach

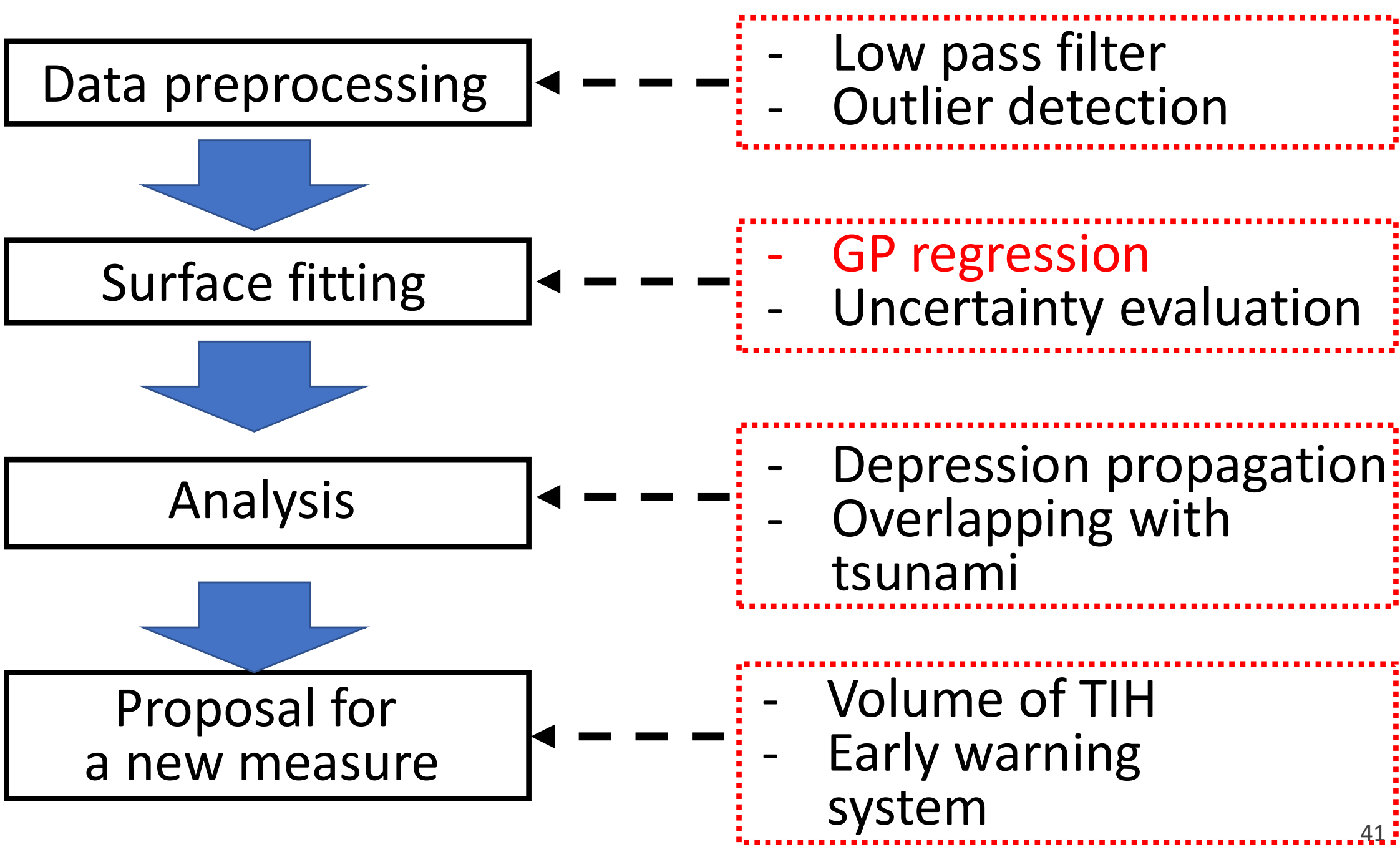

Gaussian Process Regression

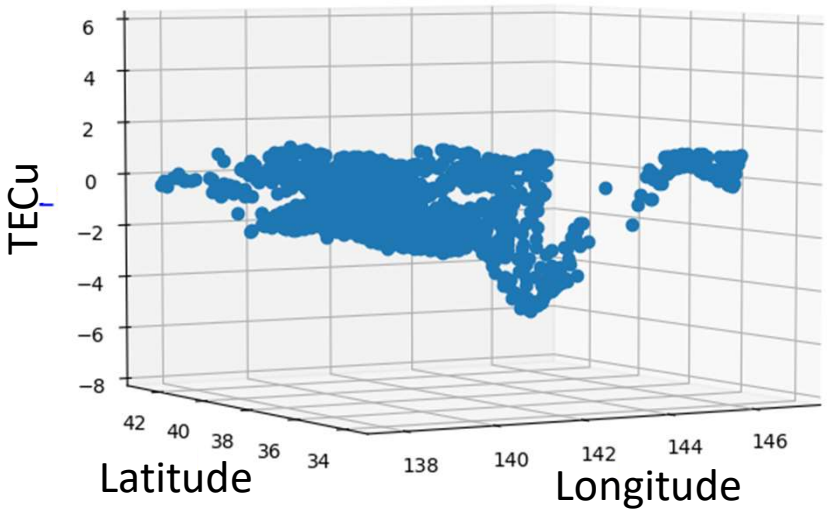

Surface fitting

Matérn Kernel covariance function

$$k_\nu(\boldsymbol{x_p}, \boldsymbol{x_q}) = \frac{2^{1-\nu}}{\Gamma(\nu)} \left(\frac{\sqrt{2\nu} r}{l} \right)^{\nu} K_\nu \left(\frac{\sqrt{2\nu} r}{l} \right), \qquad \text{where } r = |\boldsymbol{x_p} - \boldsymbol{x_q}|$$

$$cov(y_p, y_q) = k_\nu(\boldsymbol{x_p}, \boldsymbol{x_q}) + \sigma^2 \delta_{p,q}$$

The smoothness depends on ν.

Advantages

- ✓ Nonparametric method
- ✓ Evaluation of the uncertainty

Surface Fitting

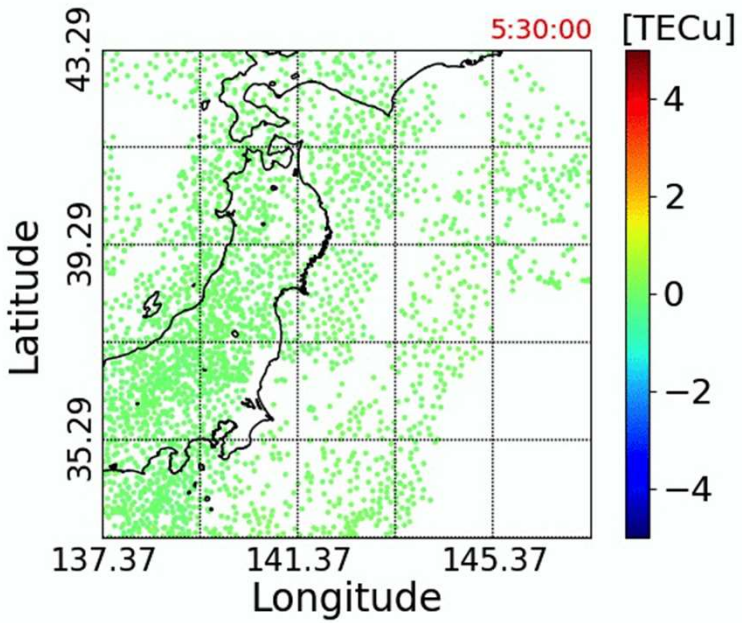

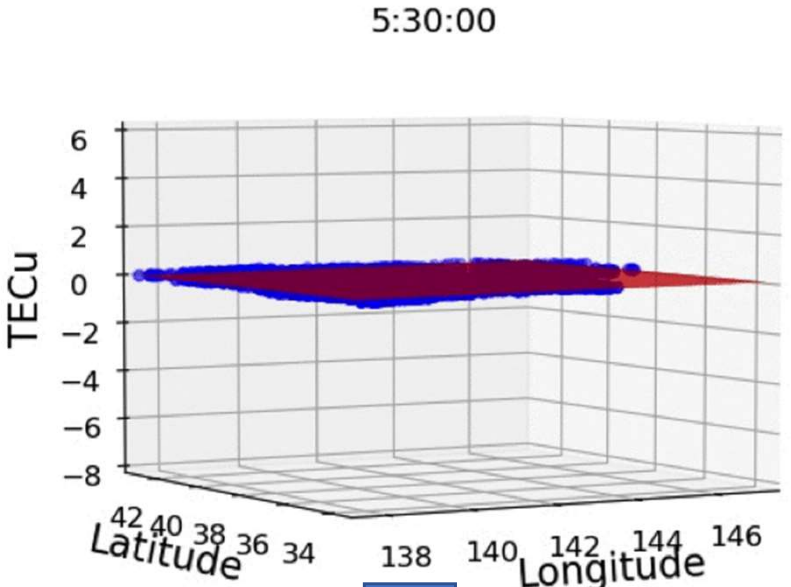

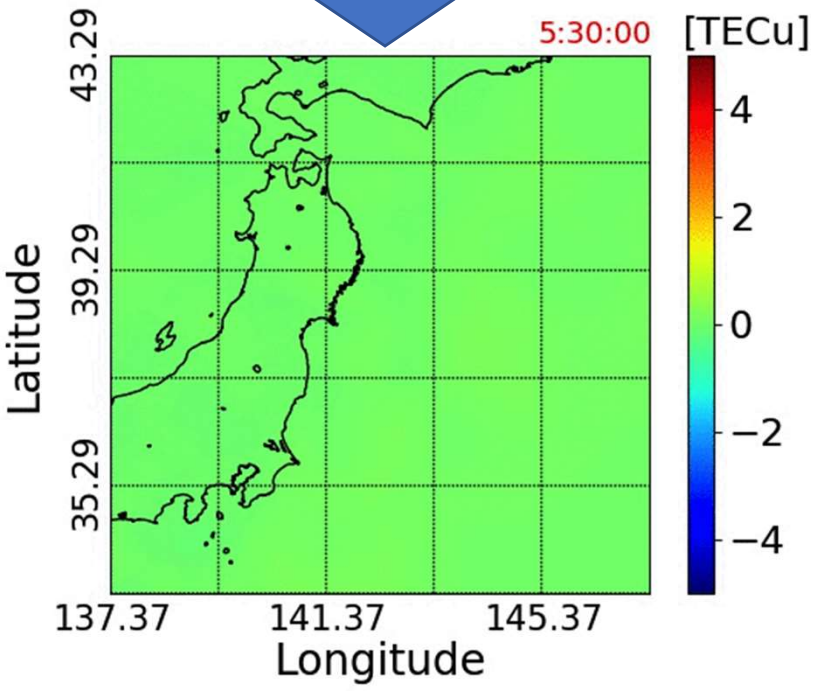

- The TEC depression (TIH) is estimated successfully.
- 2D projection shows that TIH has anisotropy.

Sparse Data

Remove **95%** of GPS receivers.
Apply our method to the sparse data

TIH is estimated successfully

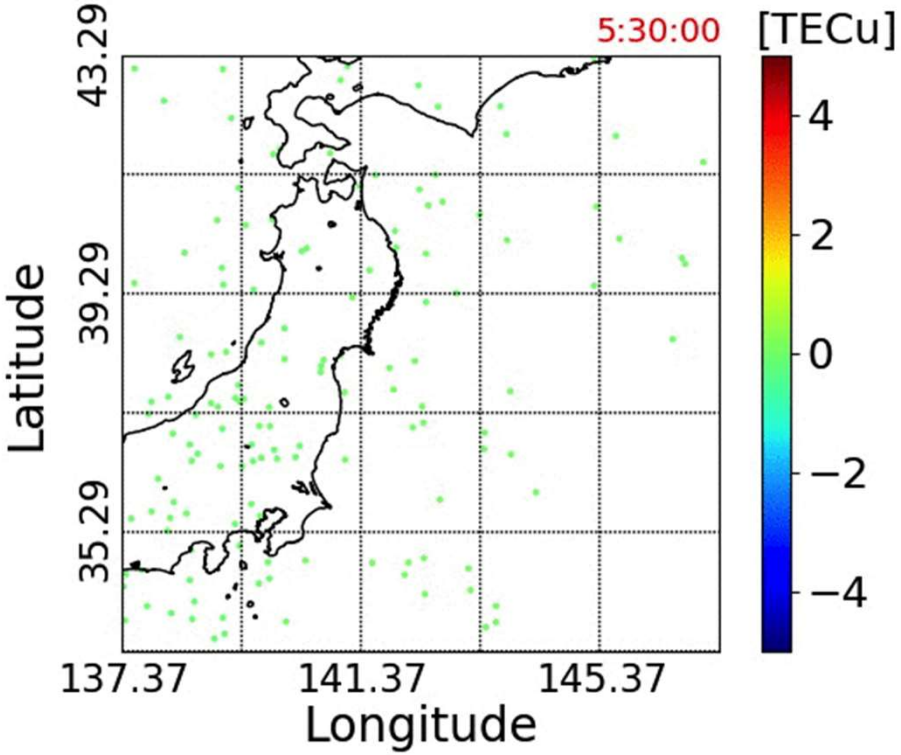

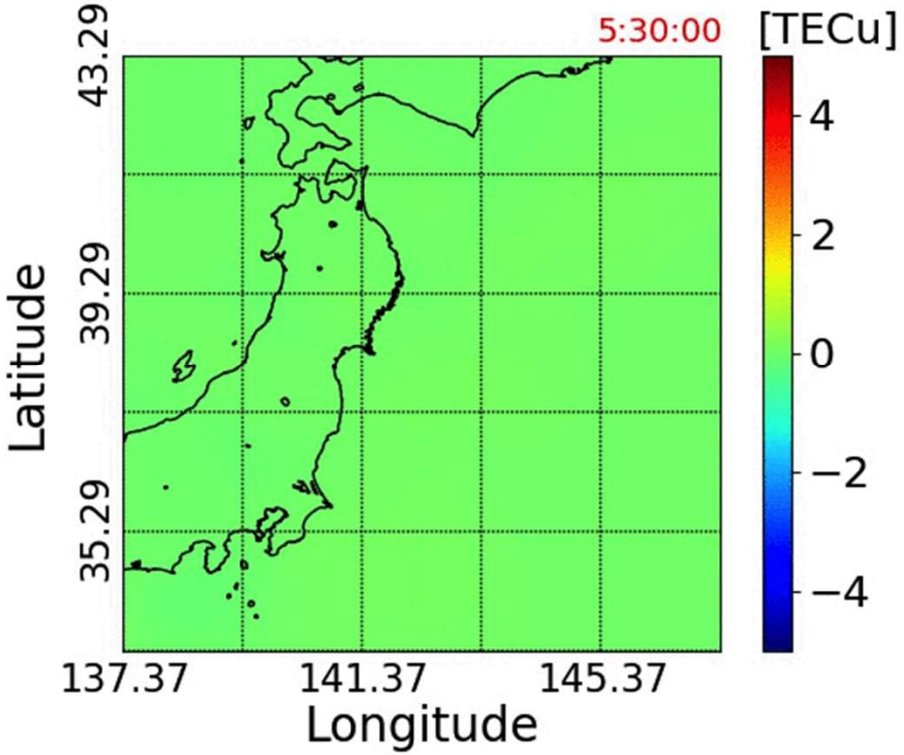

Our method can be applied to data in other countries where GPS receiver network is sparse.

Computation time

Time	5:46:30	6:00:00	6:08:00	6:16:00
Computation time (sec)	411.5	627.6	653.6	736.7

Data is detected by satellite every 30 seconds

Computation time is More than 10 minutes

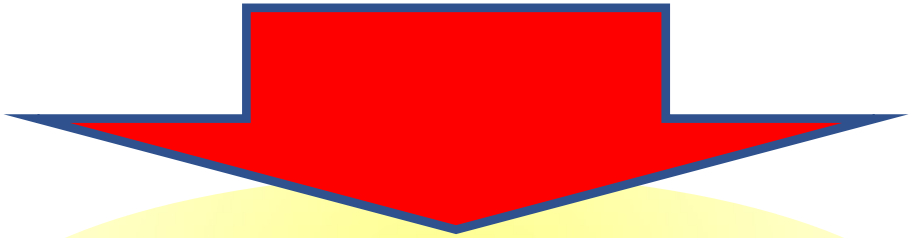

Acceleration is necessary to apply the method in real-time

Computation acceleration

Ordinary Gaussian Process

- Cholesky decomposition

---> Computation burden $O(n^3)$

INLA-SPDE approach

- inference with a GMRF

---> Computation burden $O(n^{3/2})$

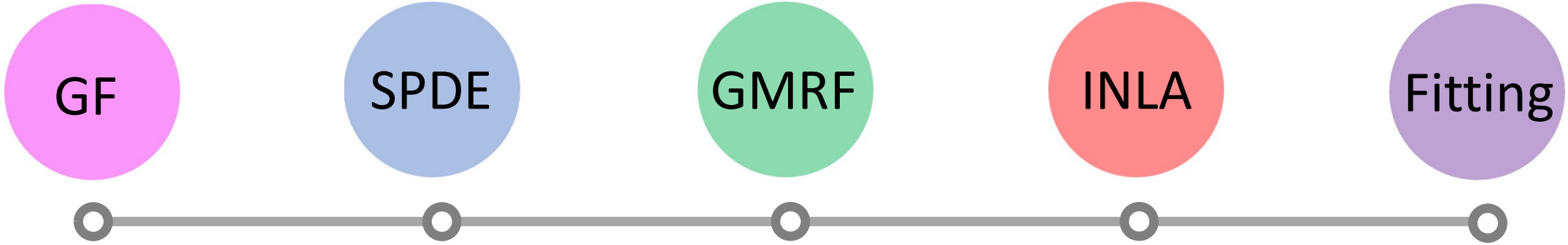

Gaussian Field (GF) with Matérn covariance function represents the Electron density depression.

A certain stochastic partial differential equation (SPDE) can construct Gaussian Markov Random Field (GMRF).

GMRF is defined by sparse matrices that allow for computationally effective numerical methods.

Integrated Nested Laplace Approximation (INLA) algorithm can deal with Bayesian inference for GMRF.

Computation for the surface fitting can be accelerated.

INLA-SPDE approach

Stochastic Partial Differential Equation

$$\frac{\sigma^2}{2^{\nu-1}\Gamma(\nu)}(\kappa\|\mathrm{v}-\mathrm{u}\|)^{\nu}K_{\nu}(\kappa\|\mathrm{v}-\mathrm{u}\|)$$

Matérn covariance function

$K_{\nu}(\cdot)$: modified Bessel function of the second kind

$$(\kappa^2 - \Delta)^{\alpha/2}\mathbf{x}_{GF}(\mathrm{u}) = \mathcal{W}(\mathrm{u}) \quad (1)$$

$\mathrm{u} \in D \subset \mathbb{R}^d$

$\alpha = \nu + d/2$

$\kappa > 0, \nu > 0$

$\Delta = \sum_{i=1}^{n} \frac{\partial^2}{\partial x_i^2}$

$(\kappa^2 - \Delta)^{\alpha/2}\mathbf{x}_{GF}(\mathrm{u}) = \mathcal{W}(\mathrm{u})$ ← solution

$\mathbf{x}_{GF}(\mathrm{u})$

The Gaussian Field (GF) with a Matérn function

This approach, that is the SPDE approach, uses a finite element representation to define the GF with Matérn function as a linear combination of basis functions defined on a triangulation of the domain D.

P. Whittle "On stationary processes in the plane." Biometrika, 41, 434–449 (1954).

INLA-SPDE approach

UCL

The basis function representation

To construct a discrete approximation

$$\mathbf{x}_{GF}(\mathrm{u}) = \sum_{i=1}^{n} \psi_l(u)\omega_l \quad (2)$$

$\psi_l(u)$: basis functions

ω_l : weights

n : the total number of vertices,

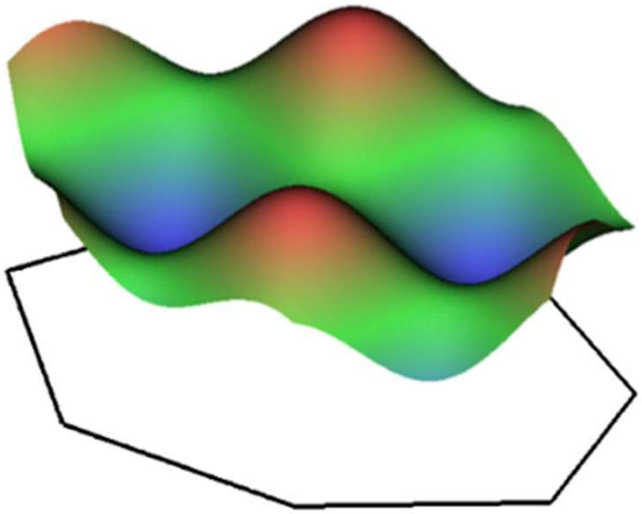

(a) Spatial random field

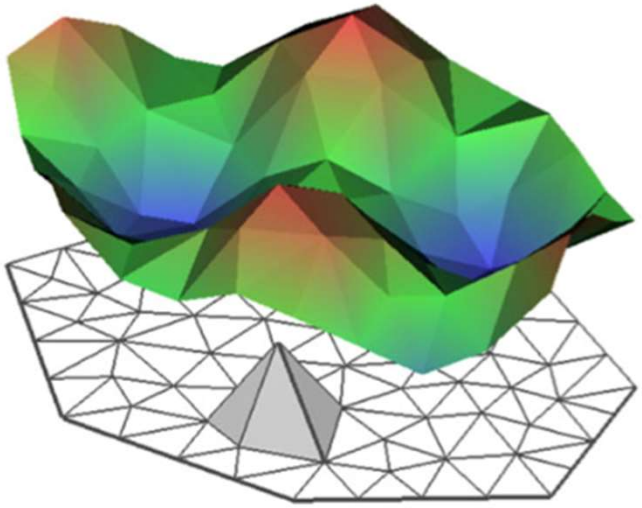

(b) corresponding finite element representation of the spatial random field

- The height of each triangle is given by the weight.
- The values in the interior of the triangle are determined by linear interpolation.

M. Cameletti, F. Lindgren, D. Simpson, H. Rue "Spatio-temporal modeling of particulate matter concentration through the SPDE approach." AStA Adv Stat Anal 97:109–131 (2013)

INLA-SPDE approach

UCL

Gaussian Markov Random Fields (GMRF)

A spatial process that models the spatial dependence of data observed on areal units, such as regular grid, lattice structure or geographic regions and has Markovian property (See the next slide sheet).

- An n-dimensional GMRF with mean μ and symmetric and positive definite precision matrix Q, is expressed as

$$\mathbf{x}_{GMRF} \sim \mathcal{N}(\mu, \mathrm{Q}^{-1})$$

- The density of $\mathbf{x}_{GMRF}$ is

$$\pi(\mathbf{x}_{GMRF}) = (2\pi)^{-n/2}|\mathrm{Q}|^{1/2} \exp\left[-\frac{1}{2}(\mathbf{x}_{GMRF} - \mu)^T \mathrm{Q}(\mathbf{x}_{GMRF} - \mu)\right]$$

H. Rue and S. Martino "Approximate Bayesian inference for latent Gaussian models by using integrated nested Laplace approximations" J. R. Statist. Soc. B 71, Part2, 319–392 (2009)

INLA-SPDE approach

Markovian property

The Markovian property is related to the definition of a neighbourhood structure, in that the full conditional distribution of $\mathbf{x}_i$ ($i = 1, \ldots, n$) depends only on a few of the components of $\mathbf{x}$.

The conditional distribution of $\mathbf{x}_i$

$$\boldsymbol{\pi}(x_i|\mathbf{x}_{-i}) = \boldsymbol{\pi}(x_i|\mathbf{x}_{\boldsymbol{\delta}_i})$$

The notation $\mathbf{x}_{-i}$ denotes all elements in $\mathbf{x}$ except for x_i

This conditional independence relation can be written as

$$x_i \perp \mathbf{x}_{-\{i,\boldsymbol{\delta}_i\}} | \mathbf{x}_{\boldsymbol{\delta}_i}$$

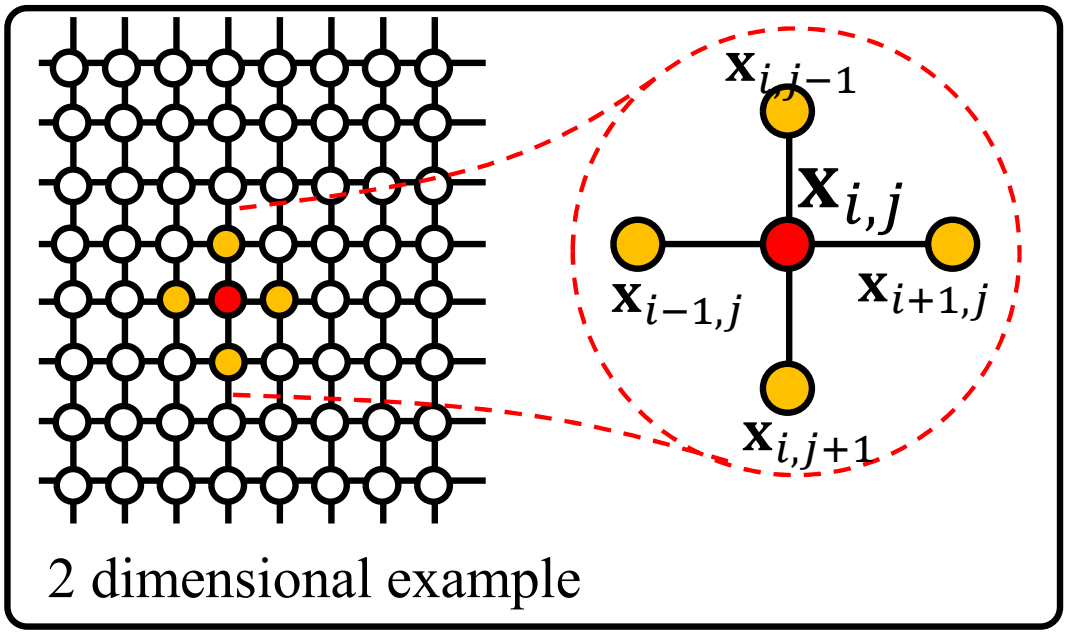

The key point is that this conditional independence property is strictly related to the precision matrix $\mathbf{Q}$.

M. Cameletti, F. Lindgren, D. Simpson, H. Rue "Spatio-temporal modeling of particulate matter concentration through the SPDE approach." AStA Adv Stat Anal 97:109–131 (2013)

INLA-SPDE approach

UCL

the precision matrix $\mathbf{Q}$.

Sparsity $\quad j \notin \{i, \delta_i\} \Leftrightarrow \mathbf{Q}_{i,j} = \mathbf{0}$

The nonzero pattern of $\mathbf{Q}$ is given by the neighbourhood structure of the process.

In other words, $\mathbf{Q}_{i,j} \neq \mathbf{0}$ $\boldsymbol{if}$ $j \in \{i, \delta_i\}$

Ordinary matrix factorization for a dense matrix

$\mathcal{O}(n^3)$

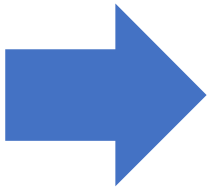

Temporal GMRF with the sparse matrix

$\mathcal{O}(n)$

Spatial GMRF with the sparse matrix

$\boldsymbol{\mathcal{O}(n^{3/2})}$

Spatio-temporal GMRF with the sparse matrix $\mathcal{O}(n^2)$

F. Lindgren and H. Rue "An explicit link between Gaussian fields and Gaussian Markov random fields: the stochastic partial differential equation approach." J. R. Statist. Soc. B 73, Part4, 423–498 (2011).

INLA-SPDE approach

Stochastic Partial Differential Equation

$$(\kappa^2 - \Delta)^{\alpha/2}\mathbf{x}_{GF}(\mathrm{u}) = \mathcal{W}(\mathrm{u}) \quad (1) \qquad \mathbf{x}_{GF}(\mathrm{u}) = \sum_{i=1}^{n} \psi_l(u)\omega_l \quad (2)$$

A stochastic weak solution to the SPDE is given by requiring that

$$\left[\left\langle \varphi_i, (\kappa^2 - \Delta)^{\alpha/2}\mathbf{x}_{GF}\right\rangle\right]_{i=1,\dots,n} \overset{D}{=} \left[\langle \varphi_i, \mathcal{W}\rangle\right]_{i=1,\dots,n}$$

$$\left[\left\langle \varphi_i, (\kappa^2 - \Delta)^{\alpha/2}\psi_l\right\rangle\right]_{i,l}\boldsymbol{\omega} \overset{D}{=} \left[\left\langle \varphi_j, \mathcal{W}\right\rangle\right]_{j=1,\dots,n}$$

$\overset{D}{=}$ denotes equality in distribution.

for each set of **test functions** φ

When $\alpha = 2$, $\varphi = \psi$

$$\left[\left\langle \psi_i, (\kappa^2 - \Delta)\ \psi_l\right\rangle\right]_{i,l}\boldsymbol{\omega} \overset{D}{=} \left[\left\langle \psi_j, \mathcal{W}\right\rangle\right]_{j=1,\dots,n}$$

$$(\kappa^2 \underbrace{[\langle \psi_i, \psi_l\rangle]}_{C} + \underbrace{[\langle \psi_i, -\Delta\psi_l\rangle]}_{G})\boldsymbol{\omega} \overset{D}{=} \underbrace{[\langle \psi_j, \mathcal{W}\rangle]}_{\mathcal{N}(0,C)}$$

F. Lindgren and H. Rue "An explicit link between Gaussian fields and Gaussian Markov random fields: the stochastic partial differential equation approach." J. R. Statist. Soc. B 73, Part4, 423–498 (2011).

INLA-SPDE approach

Stochastic Partial Differential Equation $(\kappa^2 - \Delta)^{\alpha/2}\mathbf{x}_{GF}(\mathrm{u}) = \mathcal{W}(\mathrm{u})$ (1)

A stochastic weak solution to the SPDE is given by

$$\mathbf{x}_{GF}(\mathrm{u}) = \sum_{i=1}^{n} \psi_l(u)\omega_l \quad (2)$$

, where $(\kappa^2 C + G)\boldsymbol{\omega} \sim \mathcal{N}(0, C)$

The precision of the weight, $\boldsymbol{\omega}$, is $(\kappa^2 C + G)^T C^{-1}(\kappa^2 C + G)$

As you know, C and G are sparse, but C^{-1} is not.

To obtain sparse precision matrix we replace theC^{-1} matrix with a diagonal matrix $\tilde{C}^{-1}$ with elements

$$\tilde{C}_{i,i} = \int \psi_i(s)ds$$

The solution has the Markovian property

D. Simpson, F. Lindgren, H. and Rue, "In order to make spatial statistics computationally feasible, we need to forget about the covariance function." Environmetrics 23.1 65-74 (2012)
M. Cameletti, F. Lindgren, D. Simpson, H. Rue "Spatio-temporal modeling of particulate matter concentration through the SPDE approach." AStA Adv Stat Anal 97:109–131 (2013)

INLA-SPDE approach

UCL

Bayesian inference

It is possible to make use of the Integrated Nested Laplace Approximation (INLA) algorithm. It produces almost immediately accurate approximations to posterior distributions

$$\boldsymbol{\pi}(\mathrm{x}|\mathrm{y}) \propto \boldsymbol{\pi}(\mathrm{y}|\mathrm{x})\boldsymbol{\pi}(\mathrm{x})$$

$$\boldsymbol{\pi}(\mathrm{x}, \theta|\, \mathrm{y}) \propto \boldsymbol{\pi}(\theta)\boldsymbol{\pi}(\mathrm{x}|\theta)\boldsymbol{\pi}(\mathrm{x}) \prod \boldsymbol{\pi}(\mathrm{y}_i|\mathrm{x}_i, \theta)$$

$$\tilde{\boldsymbol{\pi}}_{LA}(\mathrm{x}_i|\theta, \mathrm{y}) \propto \left. \frac{\boldsymbol{\pi}(\mathrm{x}, \theta, \mathrm{y})}{\tilde{\boldsymbol{\pi}}_{GC}(\mathrm{x}_{-i}|\mathrm{x}_i, \theta, \mathrm{y})} \right|_{\mathrm{x}_{-i} = \mathrm{x}^*_{-i}(\mathrm{x}_i, \theta)}$$

$\tilde{\boldsymbol{\pi}}_{GC}(\mathrm{x}_{-i}|\mathrm{x}_i, \theta, \mathrm{y})$ is a Gaussian approximation to $\mathrm{x}_{-i}|\mathrm{x}_i, \theta, \mathrm{y}$ around its mode $\mathrm{x}^*_{-i}(\mathrm{x}_i, \theta)$

x is assumed to be a Gaussian Markov random field

$\mathrm{Q}(\theta)$ is variance-covariance matrix

observations y_i are independent of each other

Discretization with triangulation

The number of mesh: 4525

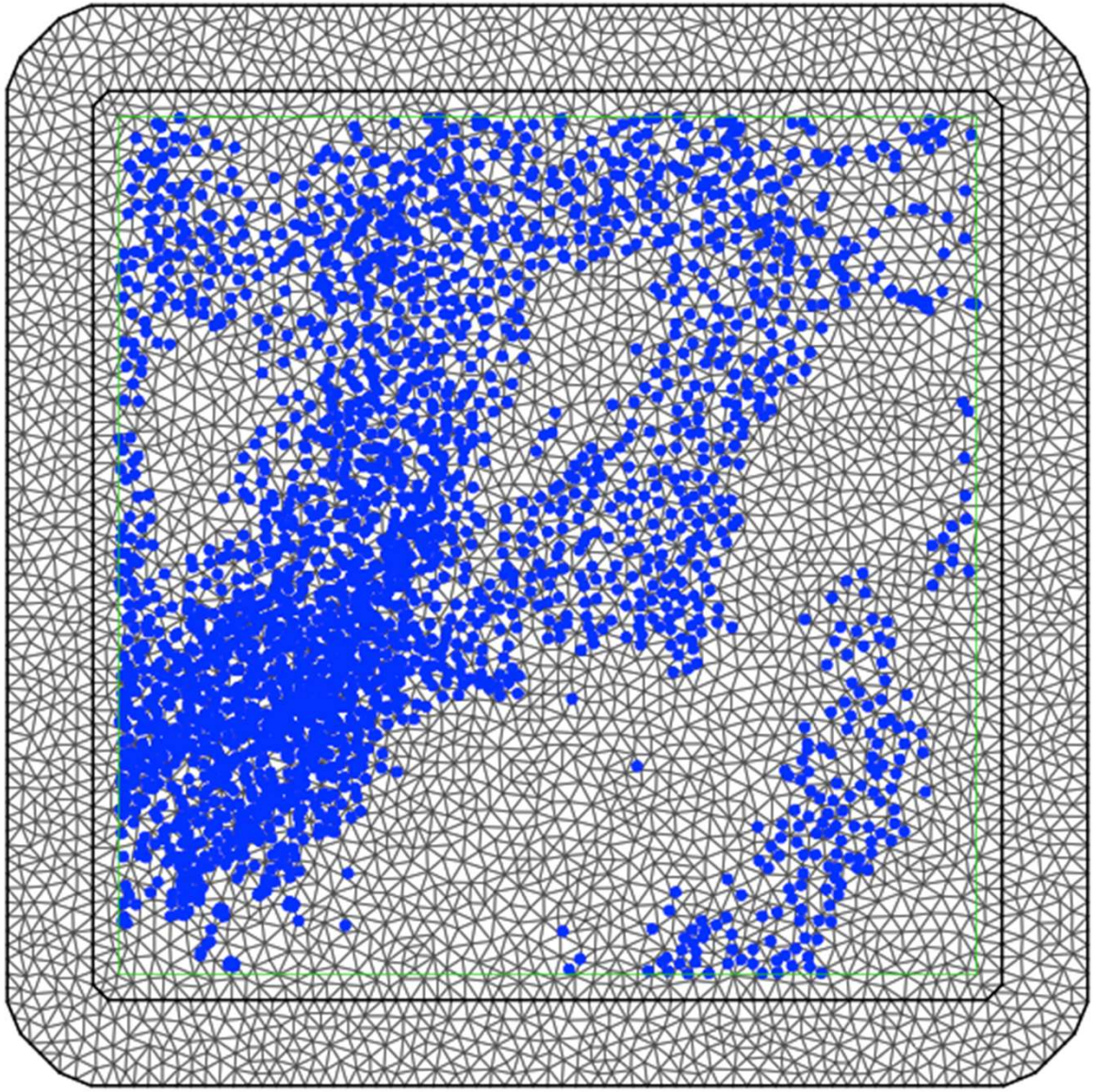

Need to find

1. the number mesh elements which allows faster computation and appropriate fitting.
2. the number threads to parallelise for faster computation.

Acceleration

The number of mesh elements

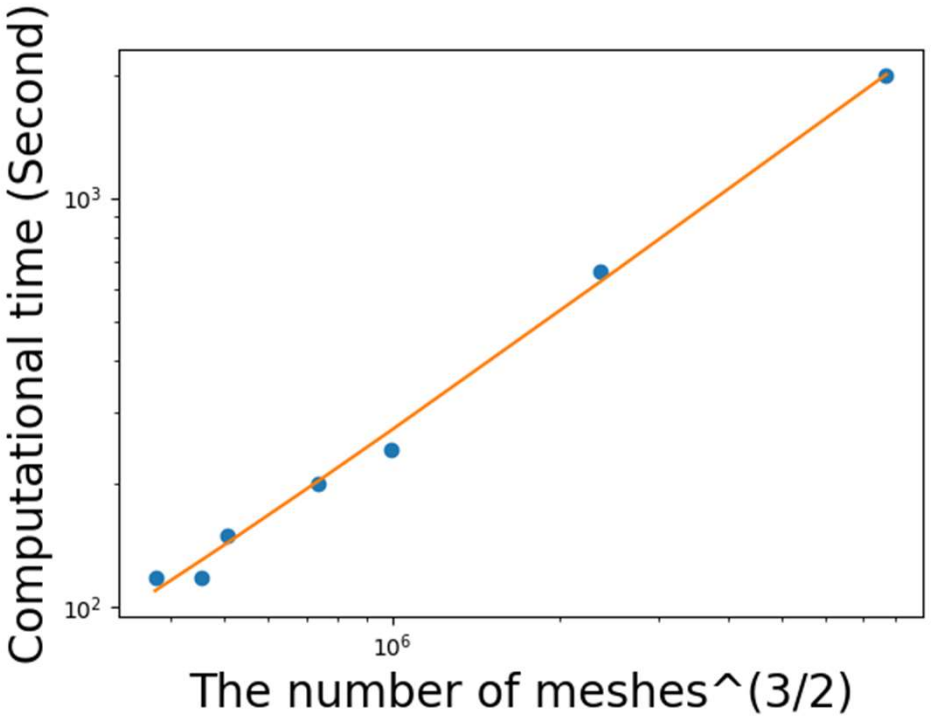

If the number of mesh elements is smaller than around 4500, the surface fitting fails. Also, the computation burden is $\mathcal{O}(n^{3/2})$.

The number of threads

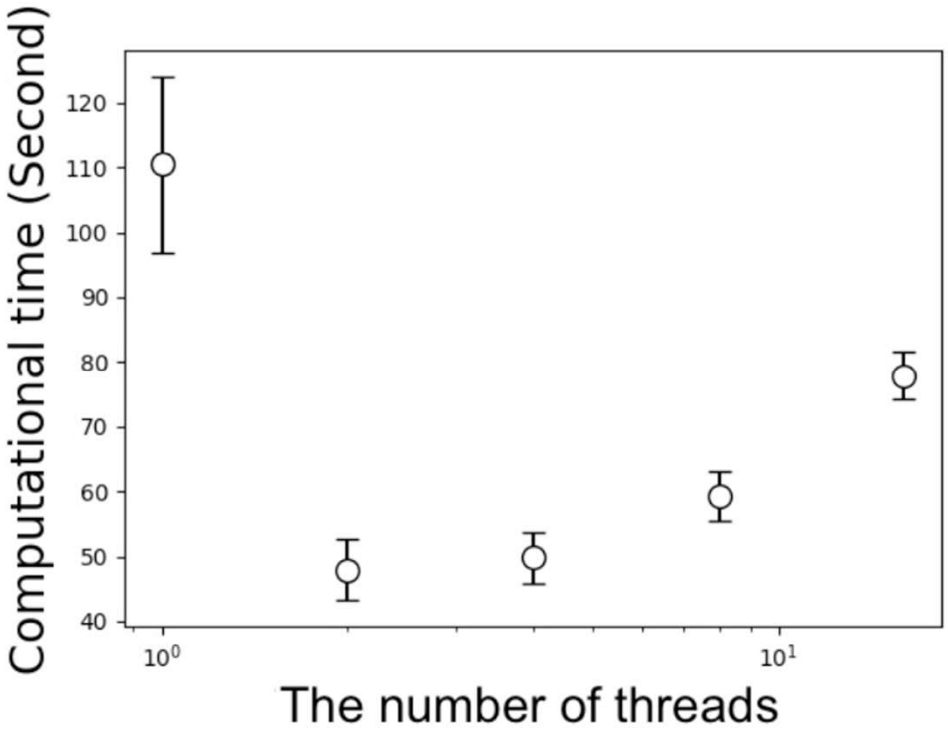

Parallelization efficiency depends on the number of mesh elements. The most efficient number cannot be known until you do the actual calculations.

Parallelization

The

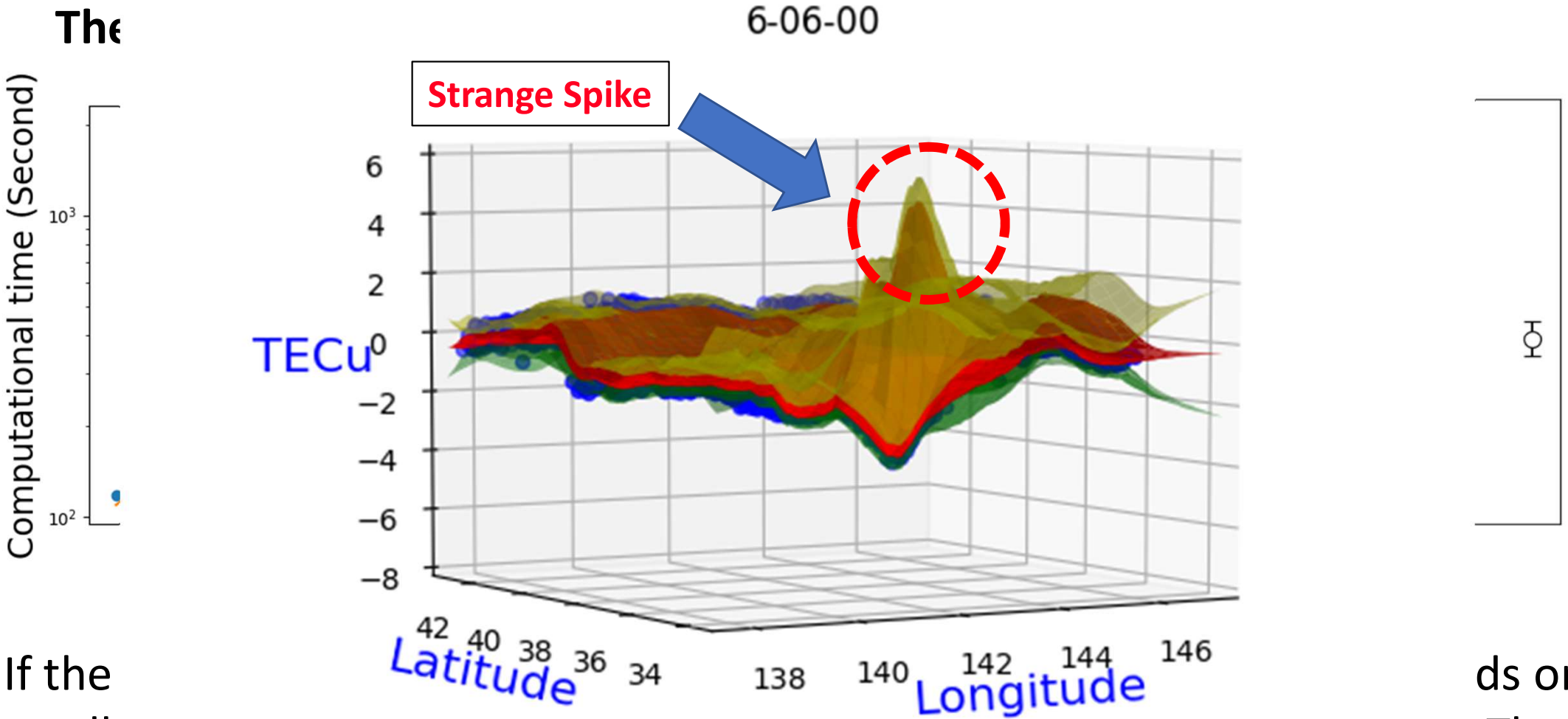

If the ds on

small The

surfac be

comp

calculations.

Accelerated computation

6:00:00

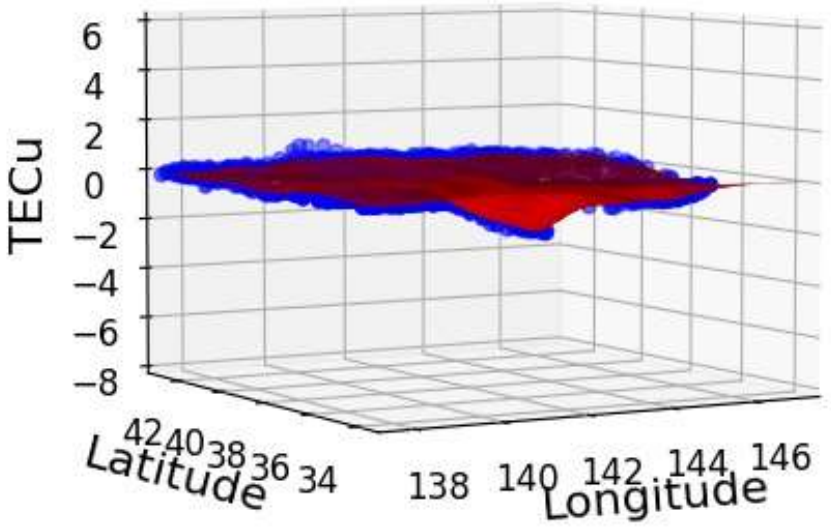

6:08:00

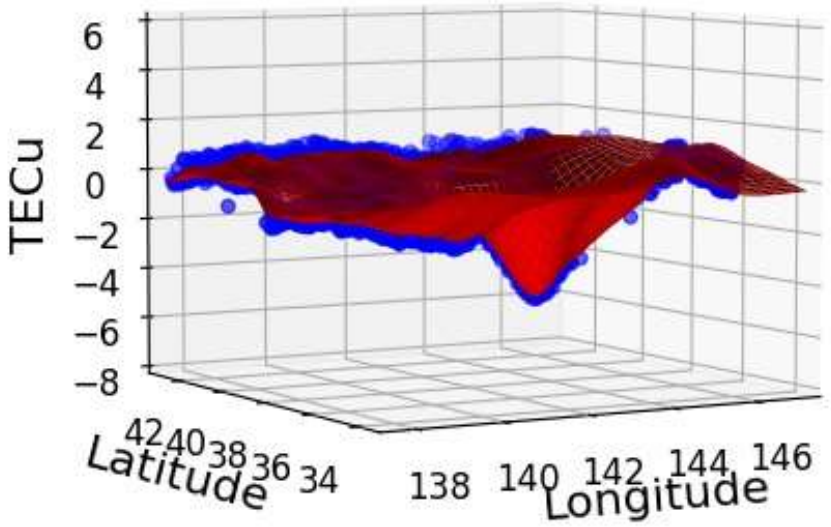

(sec)

Time	5:46:30	6:00:00	6:08:00	6:16:00
Ordinary Gaussian Process	411.5	627.6	653.6	736.7
INLA-SPDE	51.9	50.0	48.2	49.9

Computation time is less than 1 minute

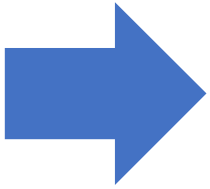

Real-time analysis

Contents

Anisotropic property

Our new method

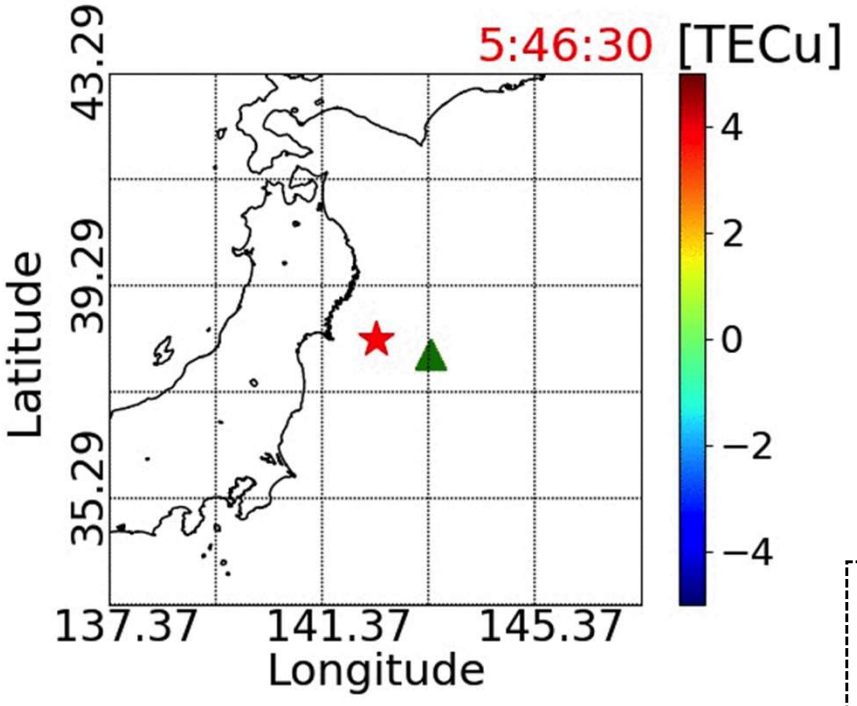

Anisotropy

Observation/our method

Symmetry

Simulation output

Previous study 1

H. Shinagawa, et. al., "Two-dimensional simulation of ionospheric variations in the vicinity of the epicenter of the Tohoku-oki earthquake on 11 March 2011", Geophysical Research Letters, 40, (2013)

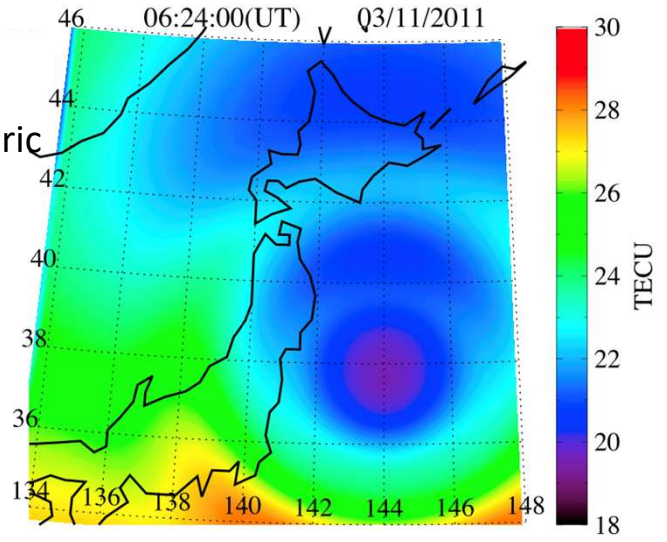

Previous study 2

M. D. Zettergren, et. al., "Latitude and Longitude Dependence of Ionospheric TEC and Magnetic Perturbations From Infrasonic-Acoustic Waves Generated by Strong Seismic Events", Geophysical Research Letters, 46, (2019)

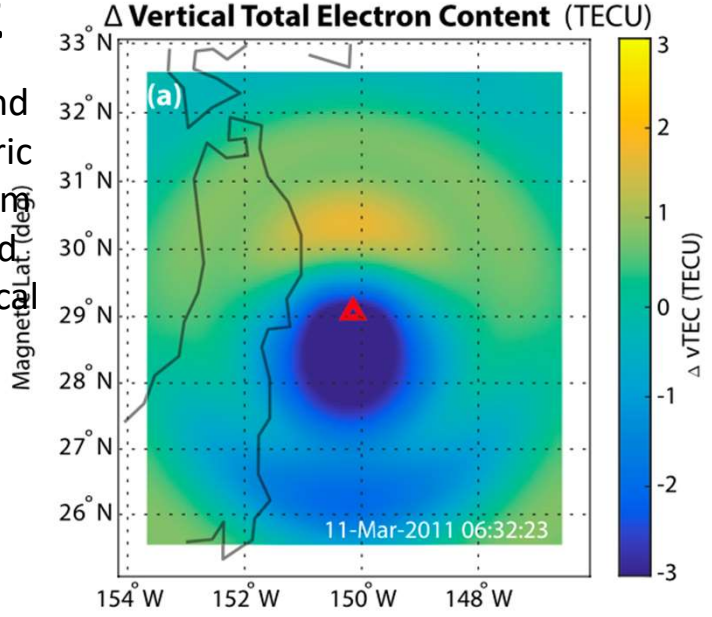

Expansion in each direction

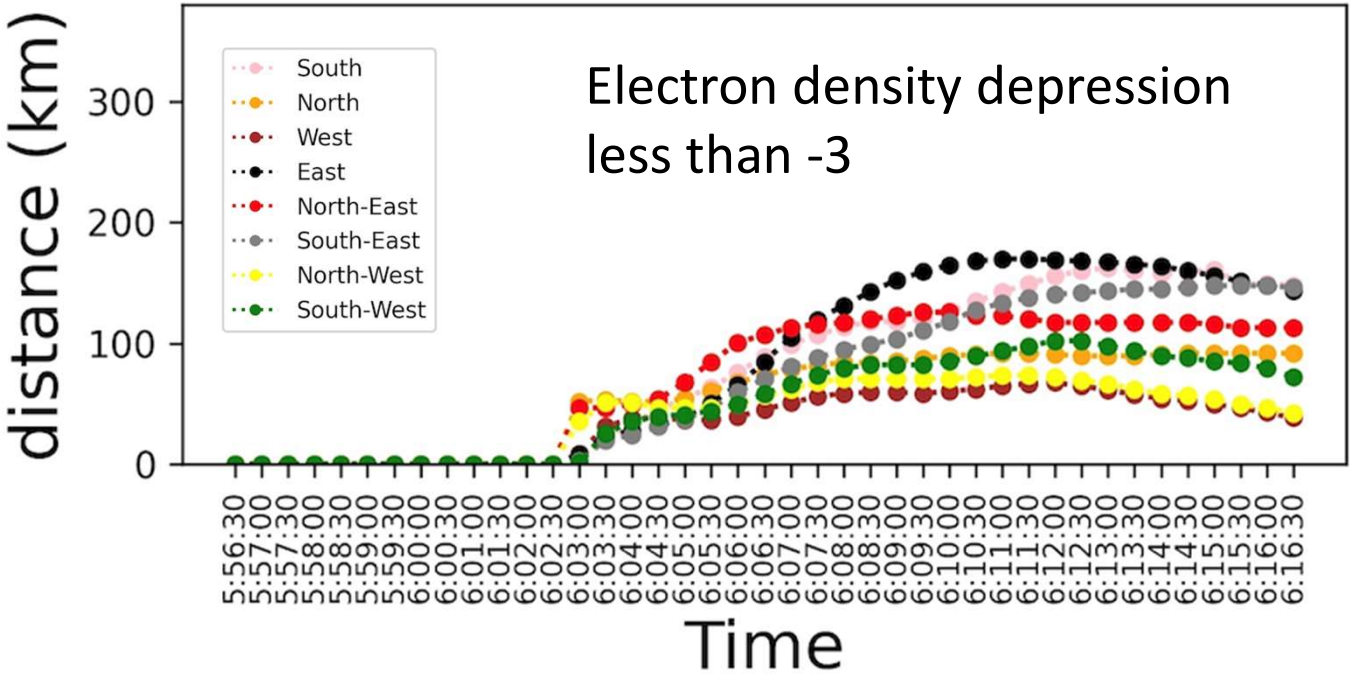

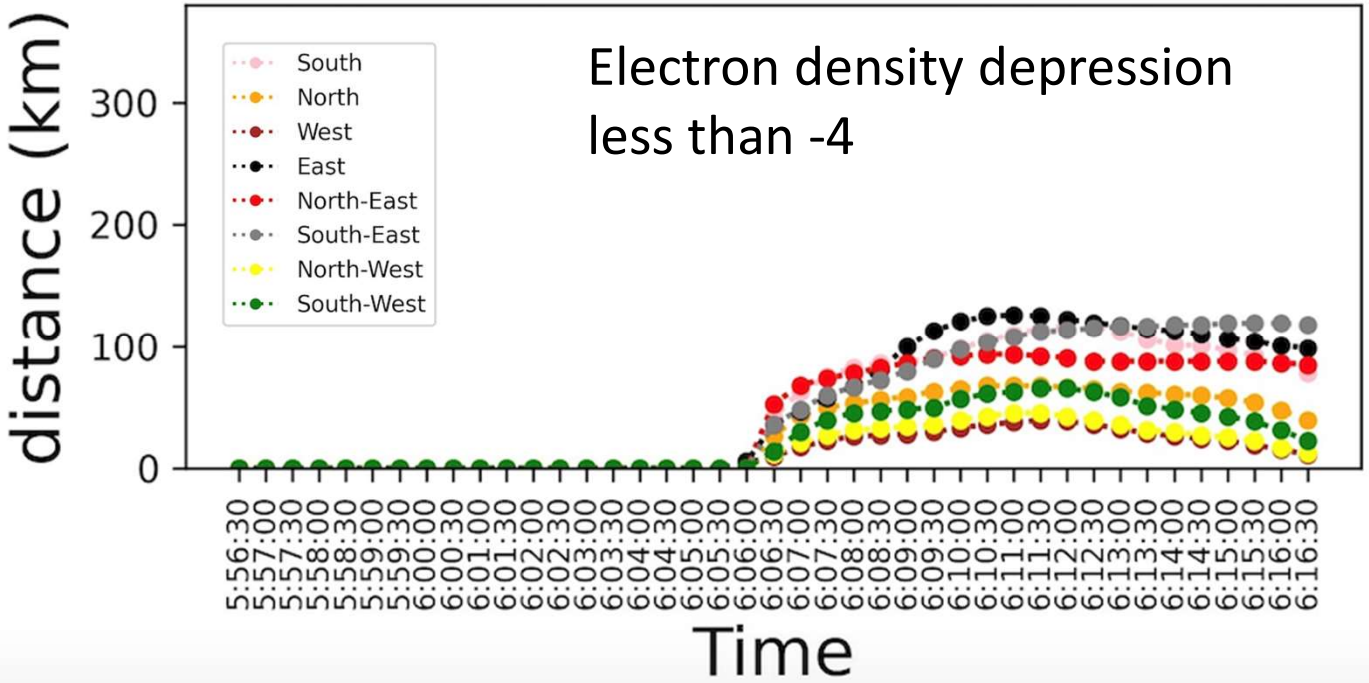

Original data **can't** show the expansion speed in each direction because of the data limitation.

Our method **succeeds** in estimating expansion speed in 8 direction for the first time.

Initial tsunami information

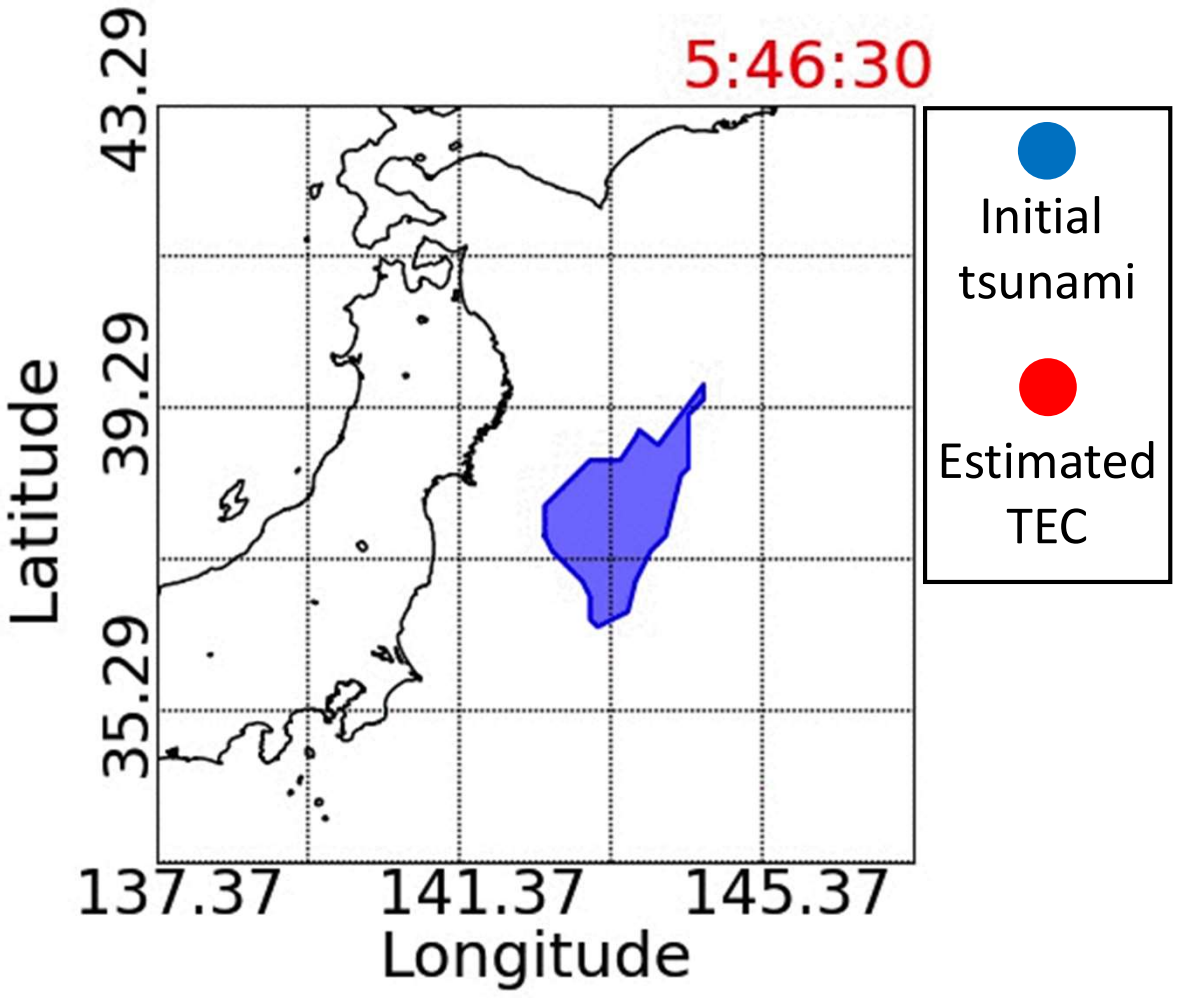

Saito, T. et al.,Tsunami source of the 2011 Tohoku-Oki earthquake, Japan: Inversion analysis based on dispersive tsunami simulations, Geophysical Research Letters, 38, (2011)

Initial tsunami area estimated by another research group **overlaps** the **electron density depression area**.

It indicates that the information obtained from the electron density depression contains the information about the initial tsunami.

Initial tsunami information

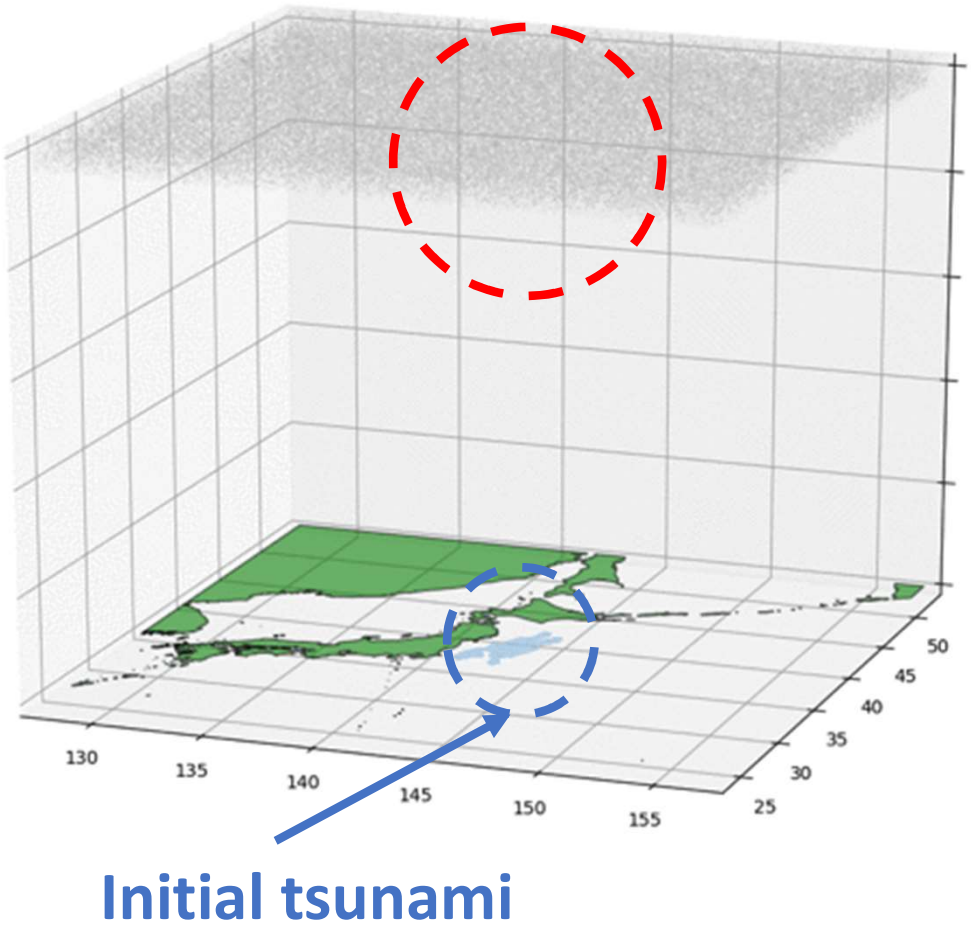

- ✓ Initial tsunami regeion
- ➢ Initial tsunami height?

Input data for tsunami propagation model.
E.g. Jugrus, VOLNA….

Initial tsunami information

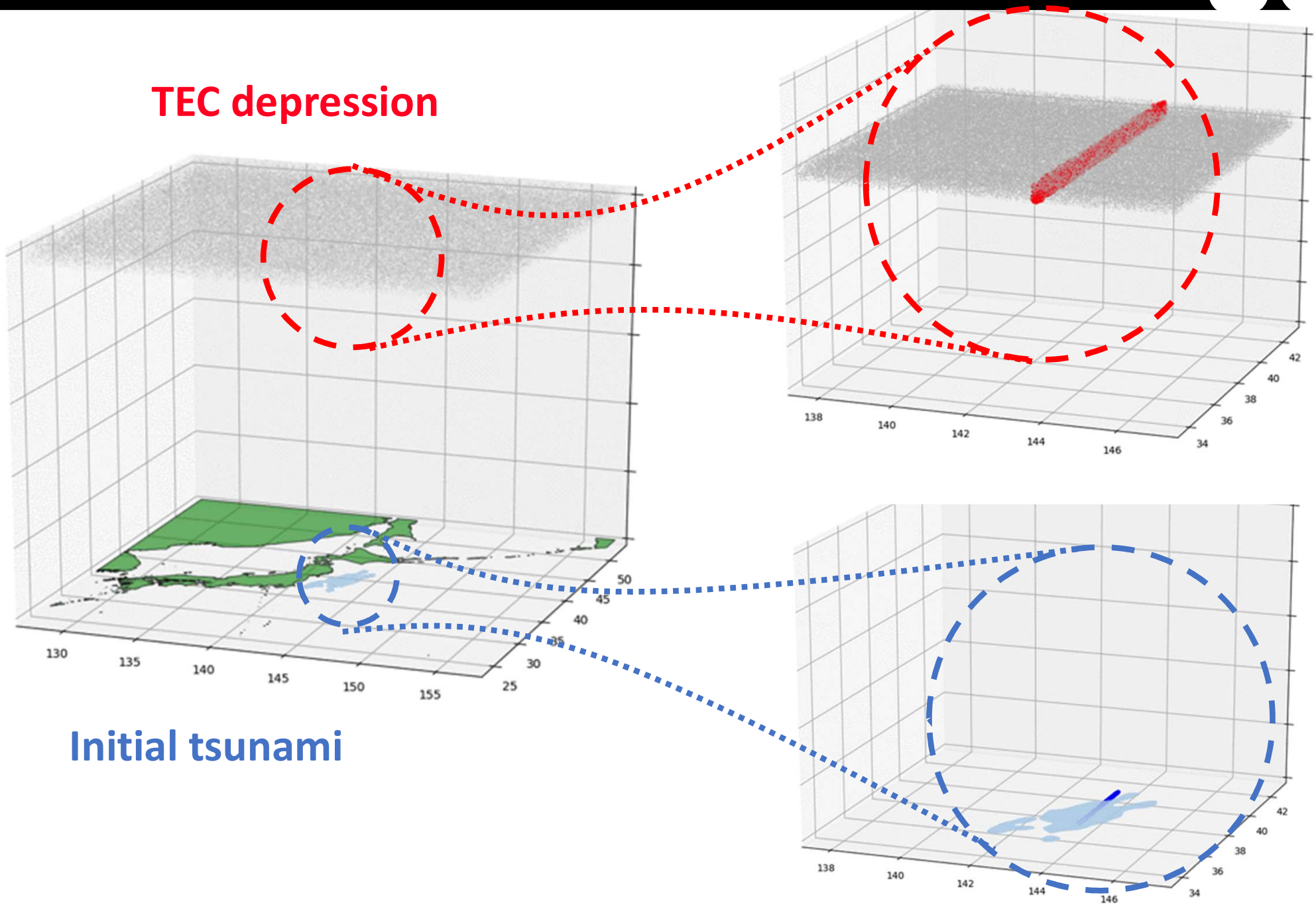

Initial tsunami information

TEC depression

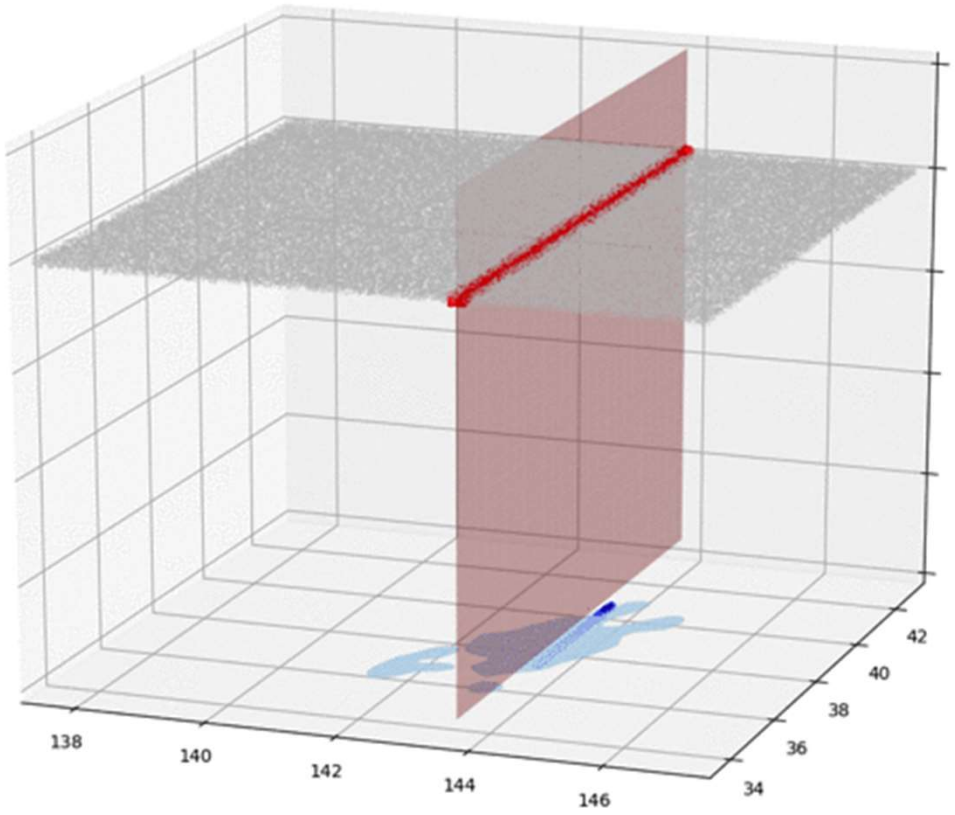

Initial tsunami

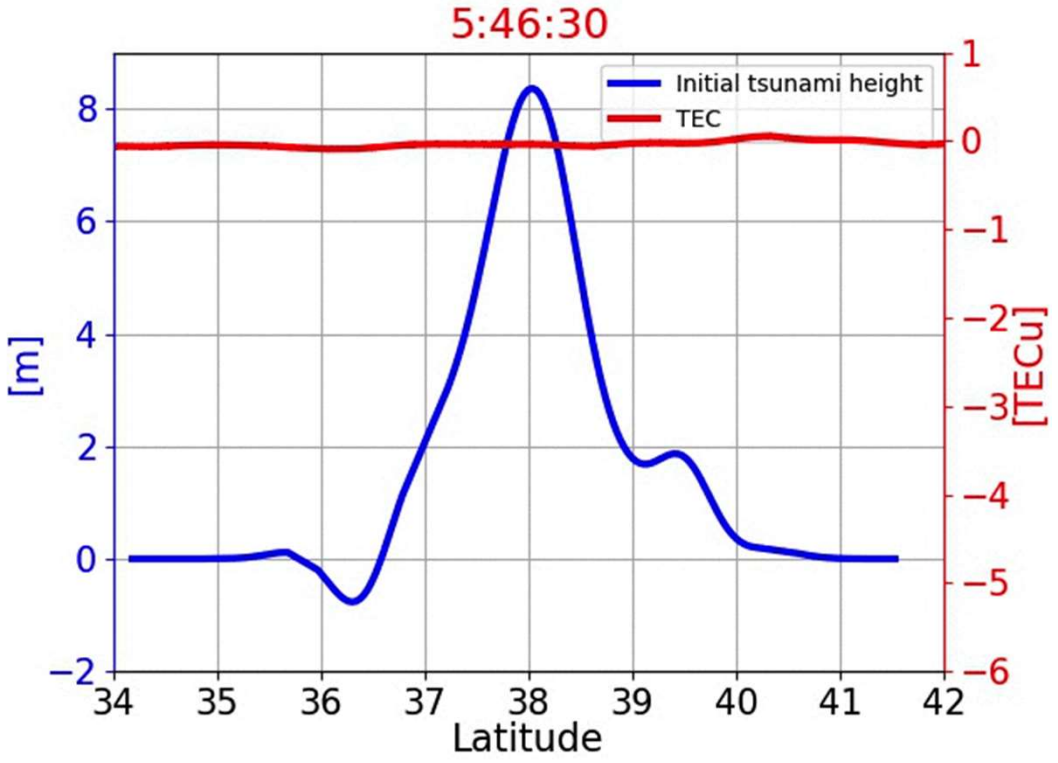

Initital tsunami shape and TEC depression shape are correlated.

Initial tsunami information

TEC depression

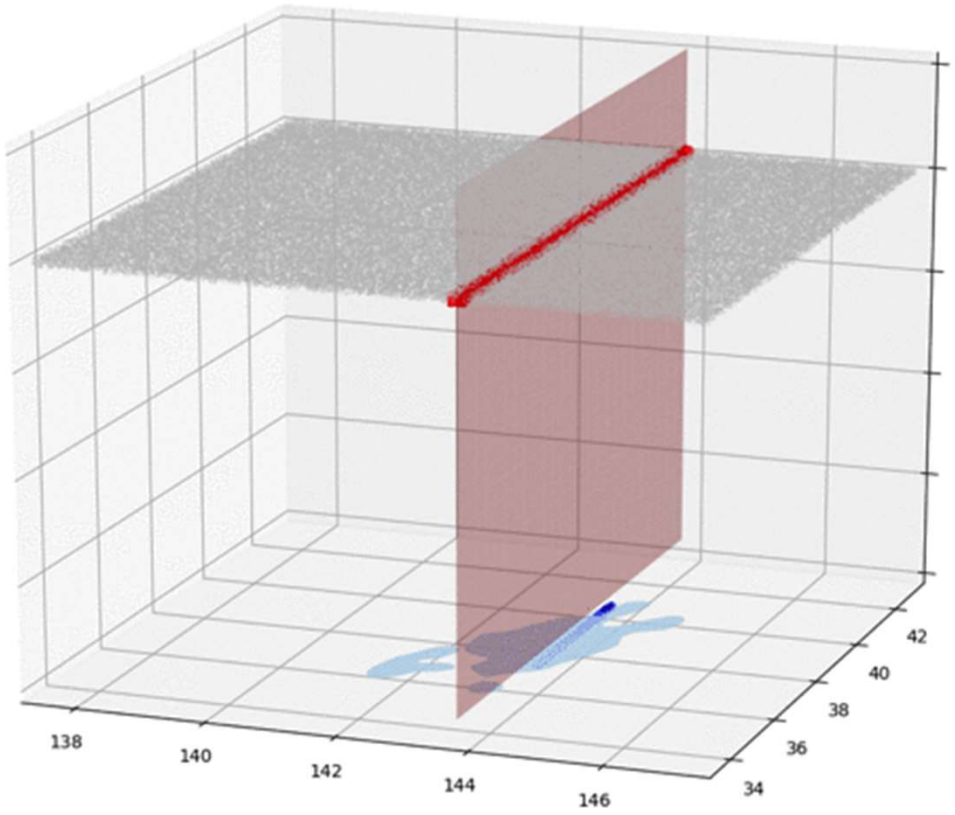

Initial tsunami

Turn it upside down

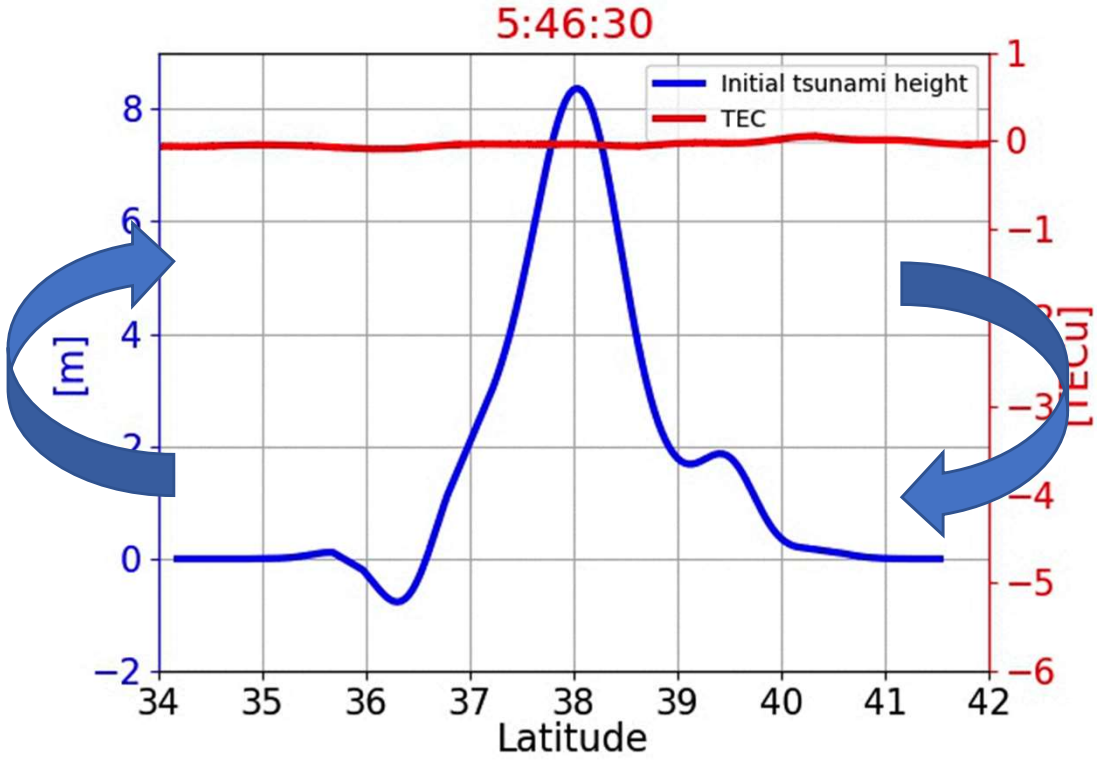

Initital tsunami shape and TEC depression shape are correlated.

Initial tsunami information

TEC depression

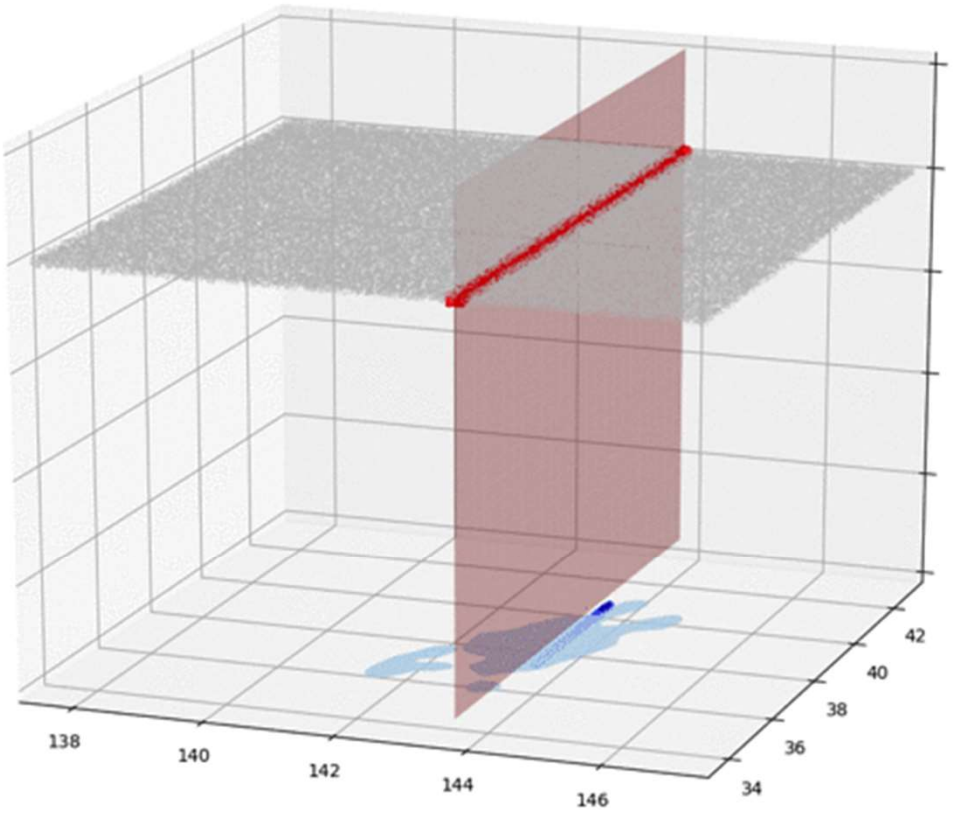

Initial tsunami

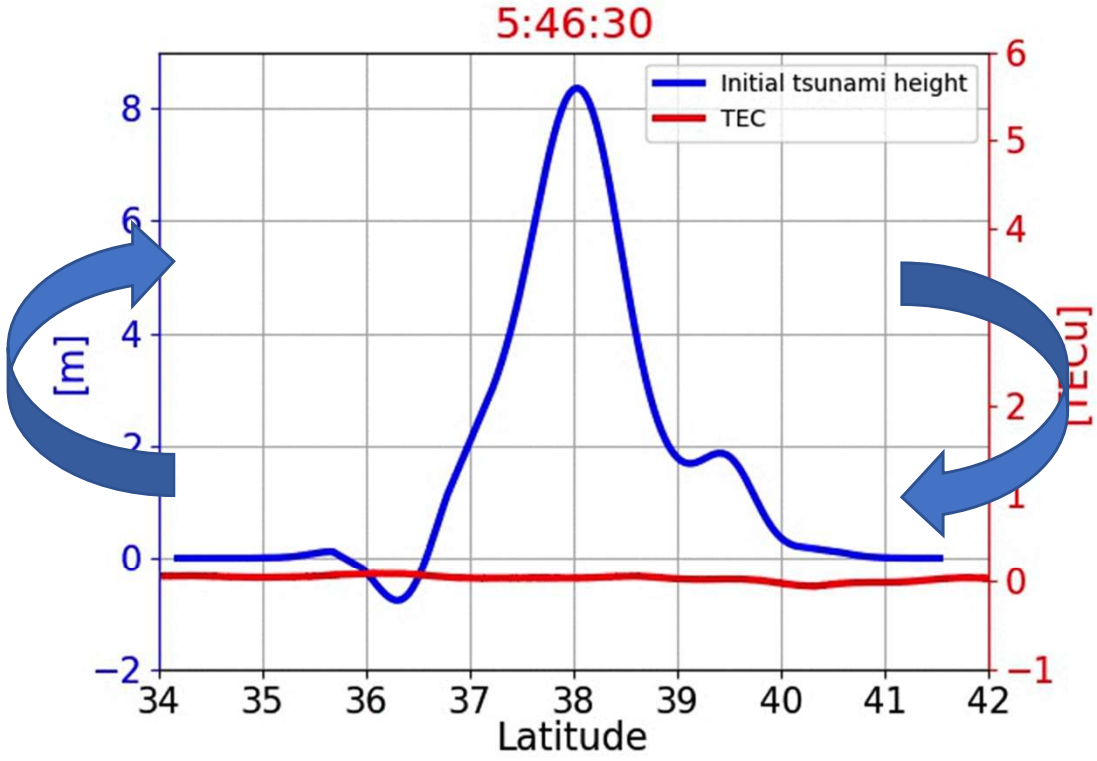

Explicitly TEC depression data has information about initial tsunami shape

Volume computation and warning system

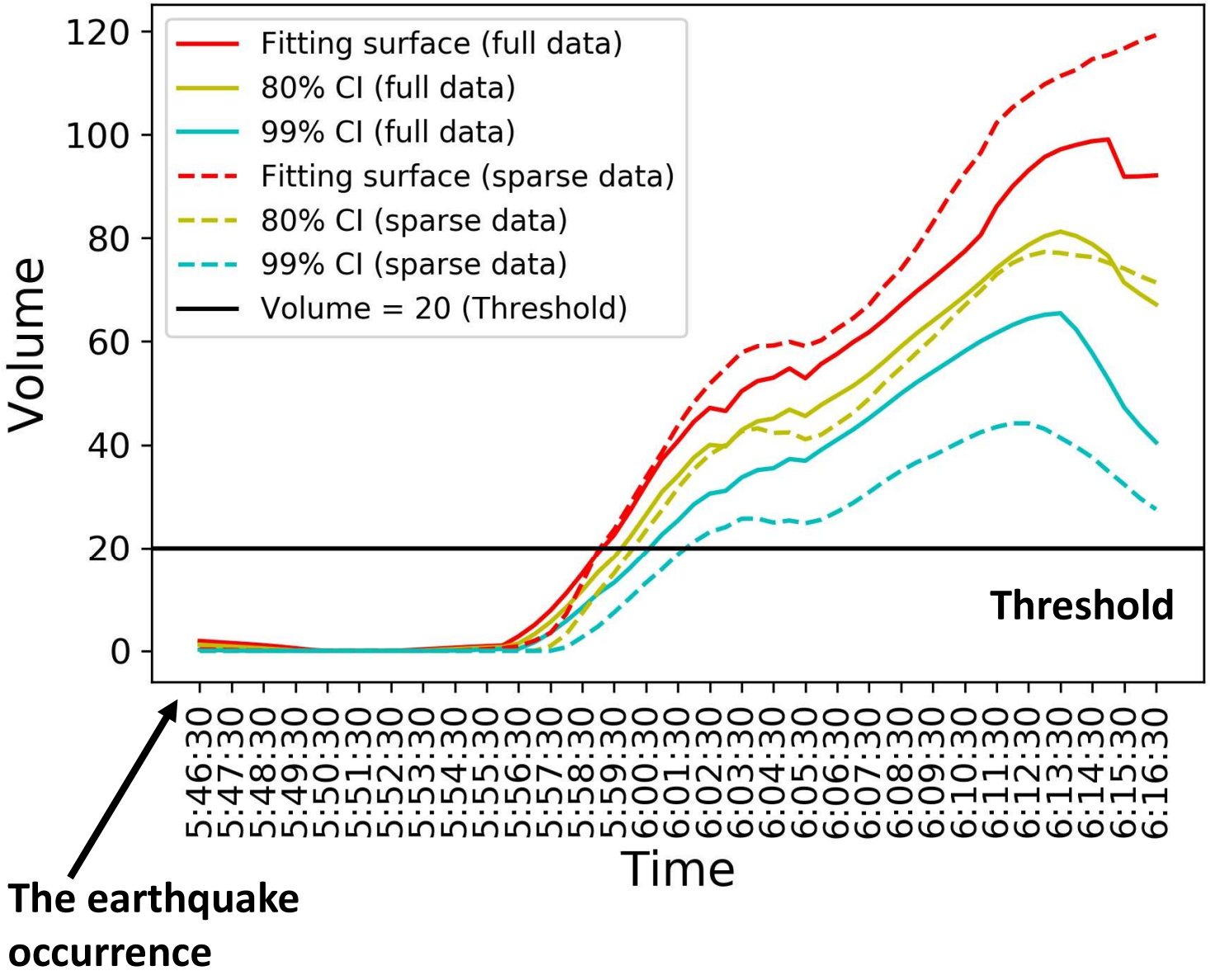

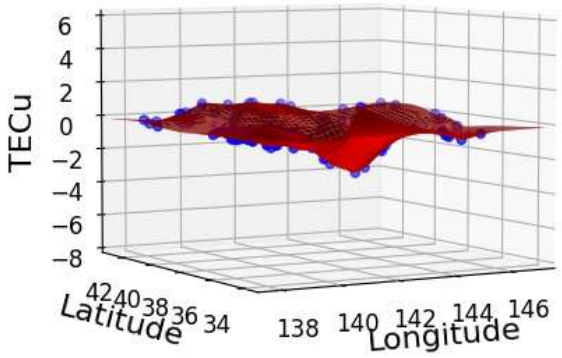

6:03:00

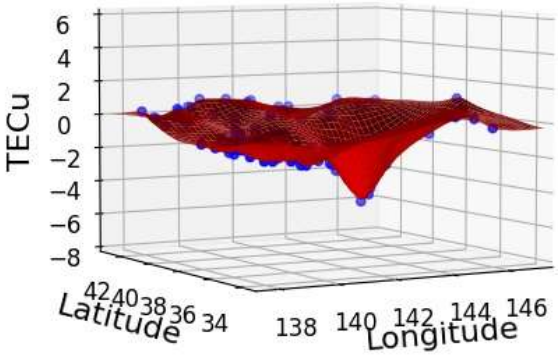

6:08:00

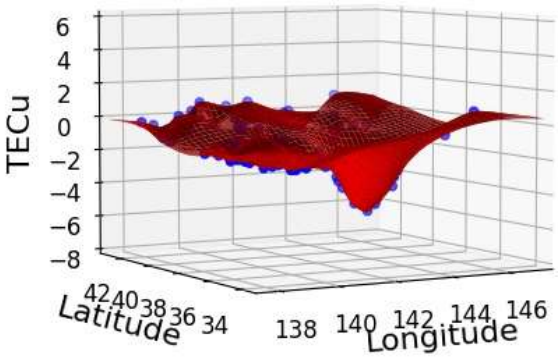

6:13:00

The depression time series

Our New Method

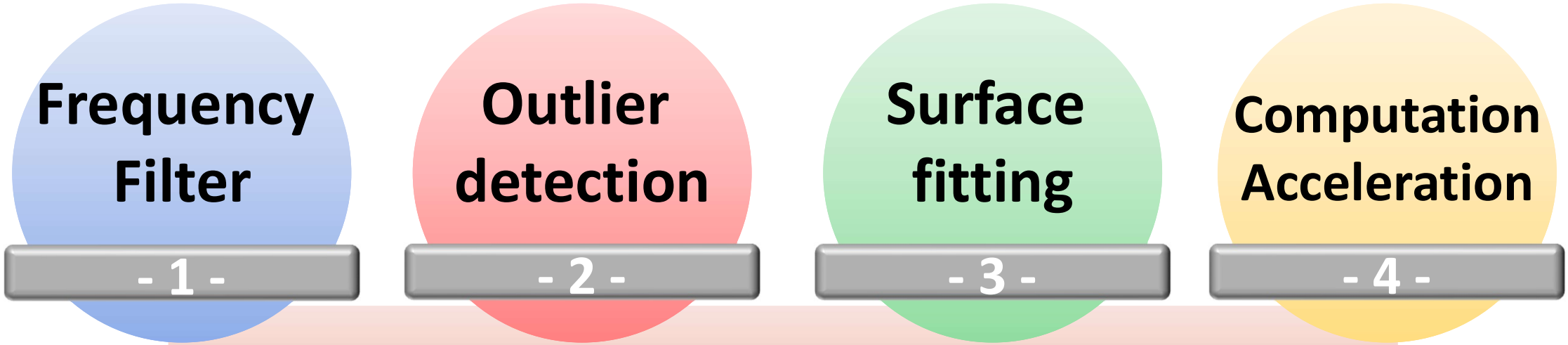

- ✔ Dense estimation with uncertainty
- ✔ Propagation speed estimation
- ✔ Tsunami early warning system
- ✔ Initial tsunami information possibility

R. Kanai, M. Kamogawa, T. Nagao, A. Smith, and S. Guillas "Robust uncertainty quantification of the volume of tsunami ionospheric holes for the 2011 Tohoku-Oki Earthquake: towards low-cost satellite-based tsunami warning systems" preprint. https://nhess.copernicus.org/articles/22/849/2022/nhess-22-849-2022.html

Contents

Ultimate goal

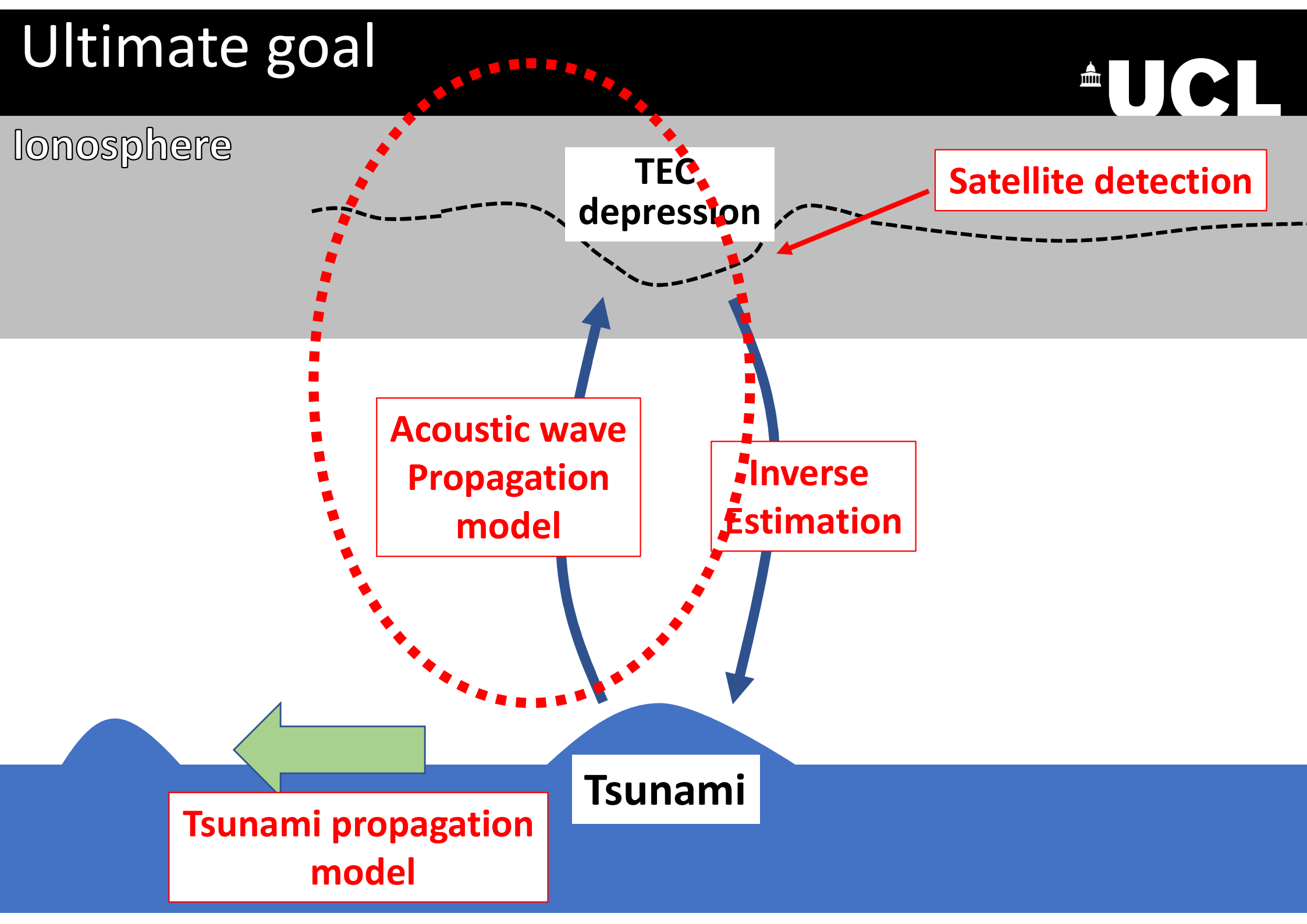

Initial tsunami

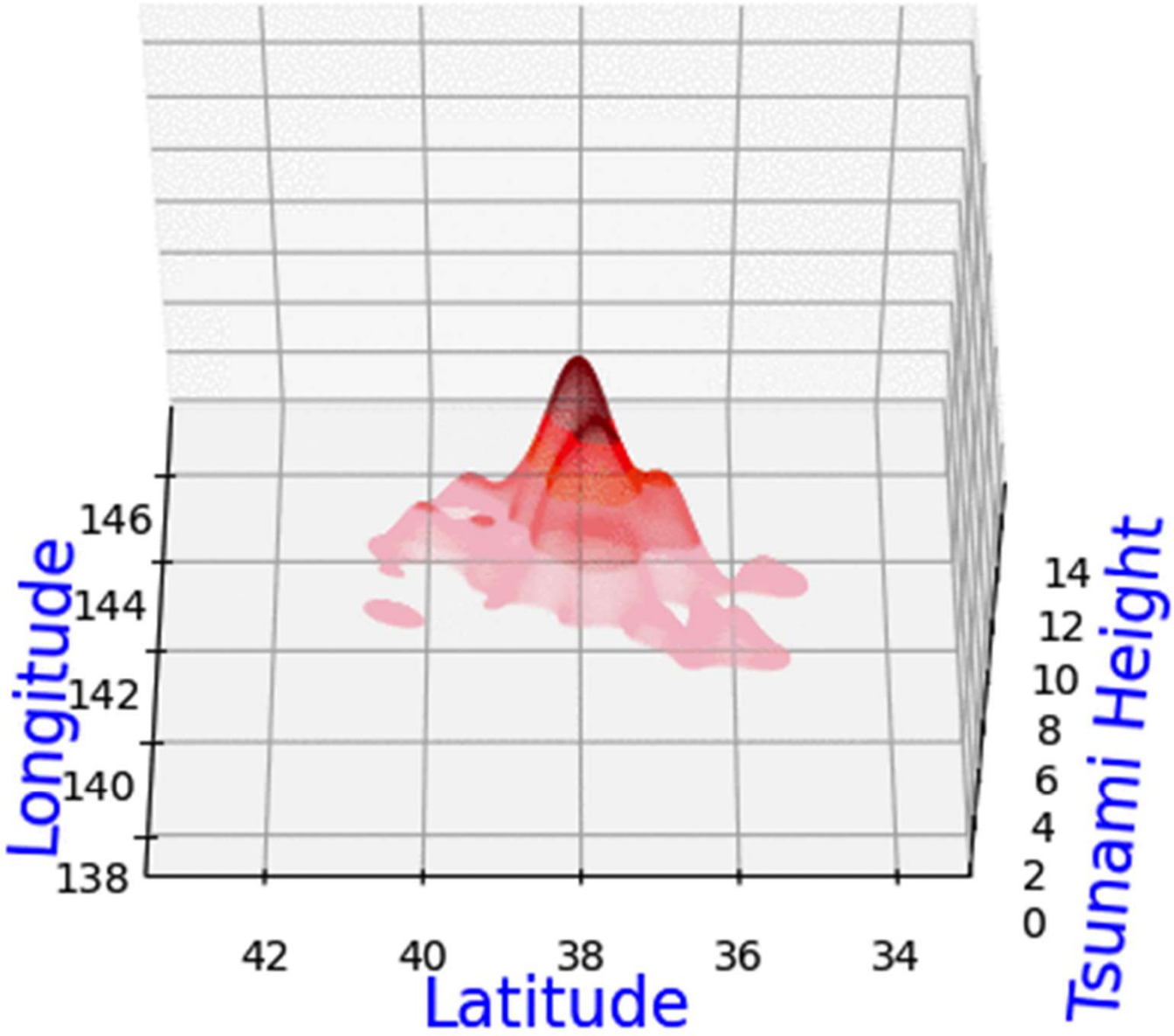

Initial Tsunami

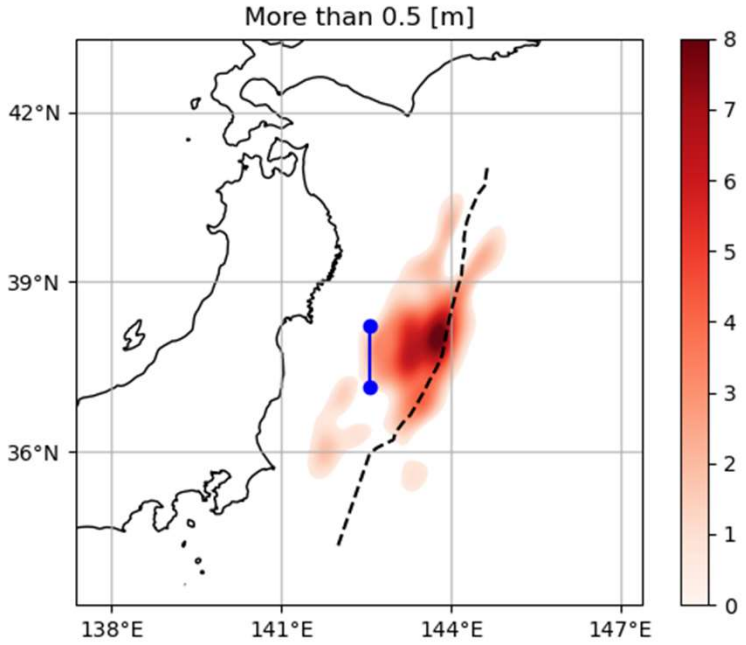

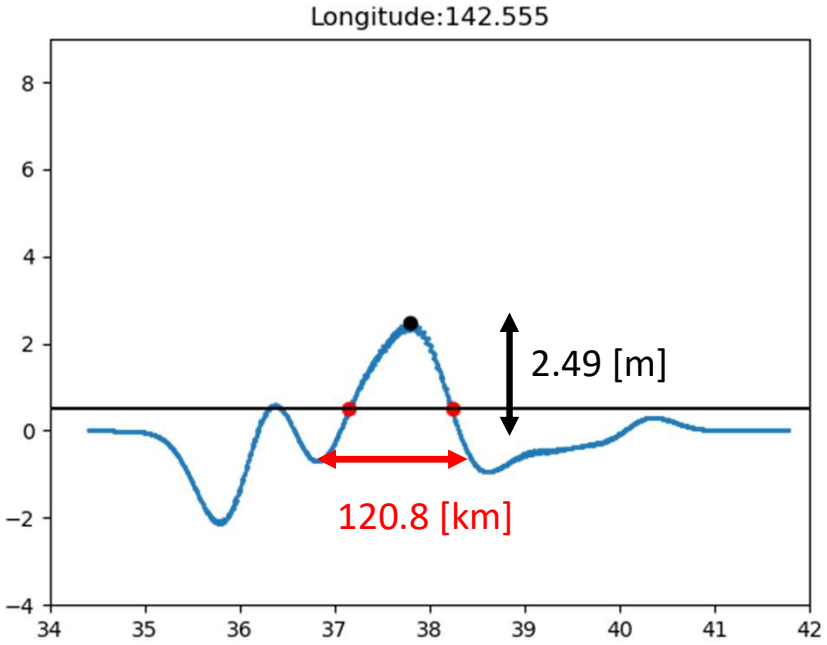

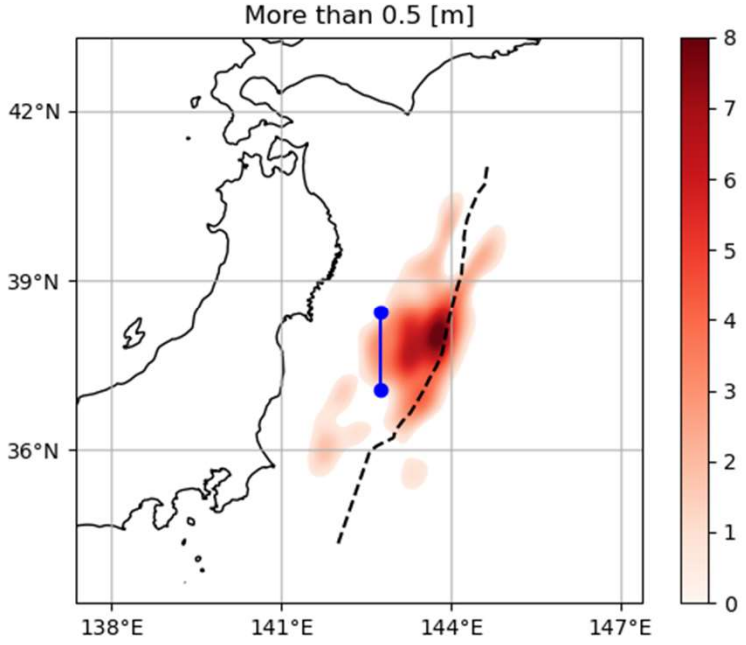

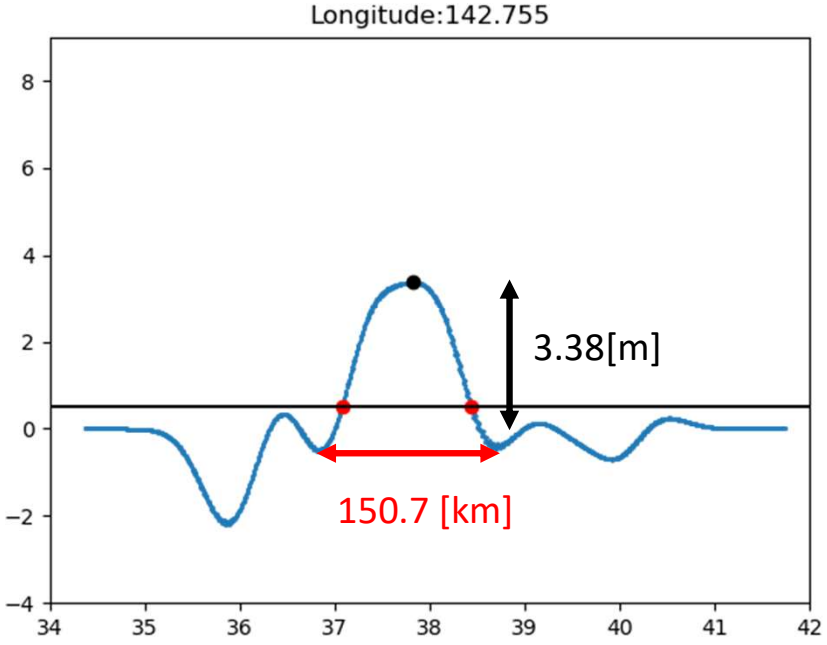

Initial Tsunami

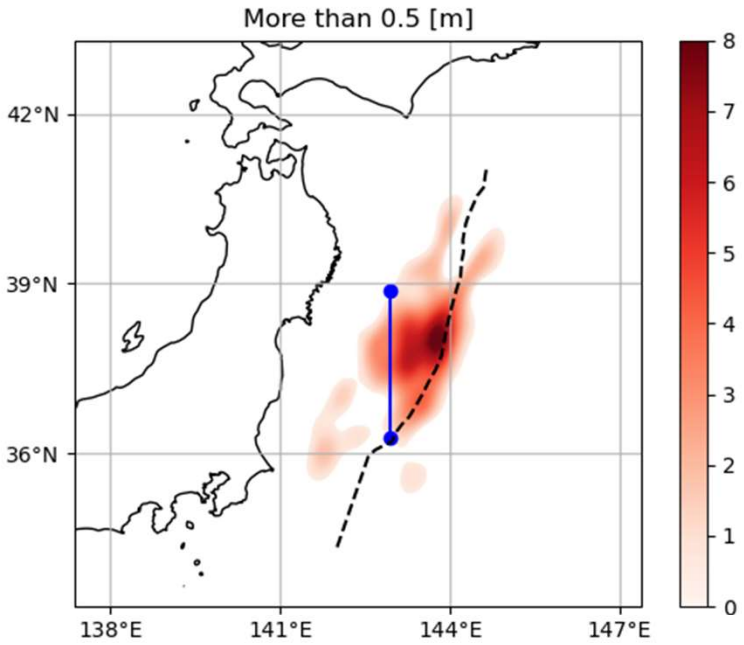

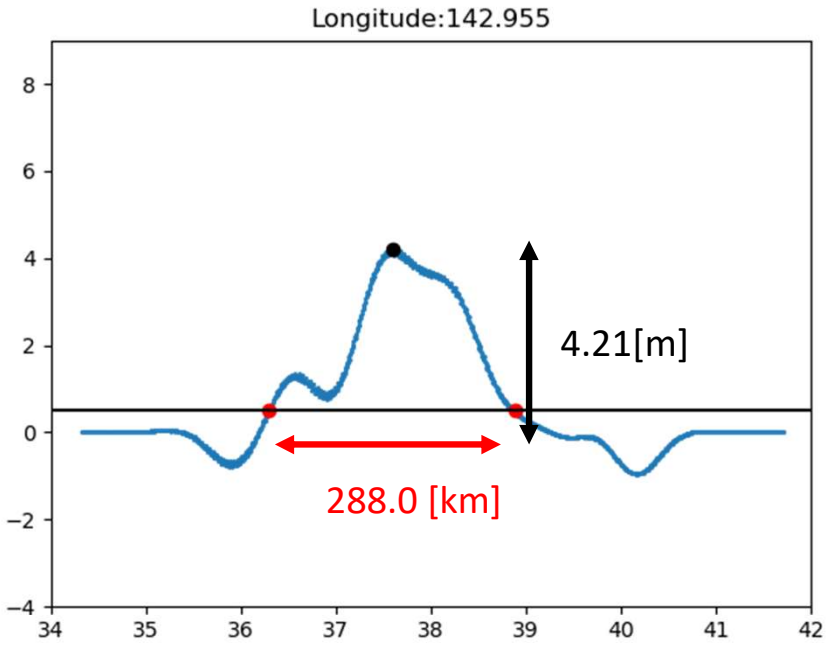

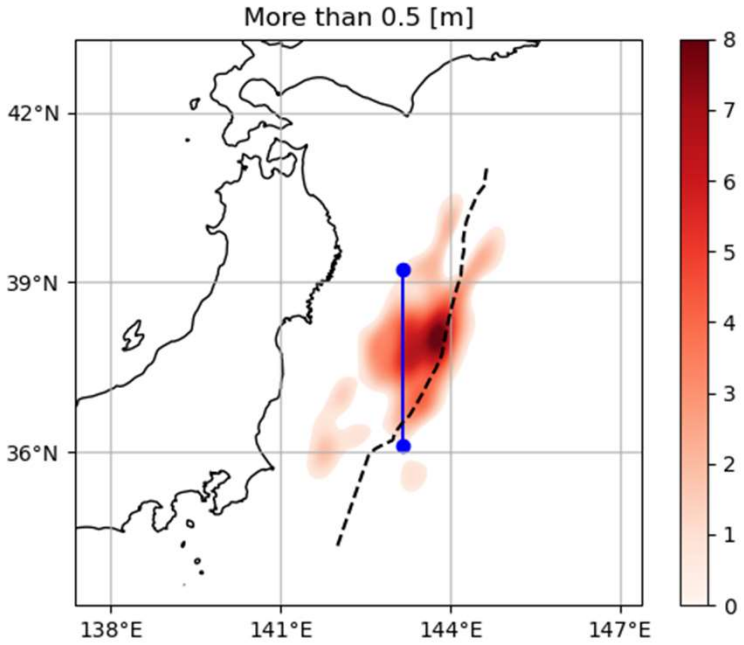

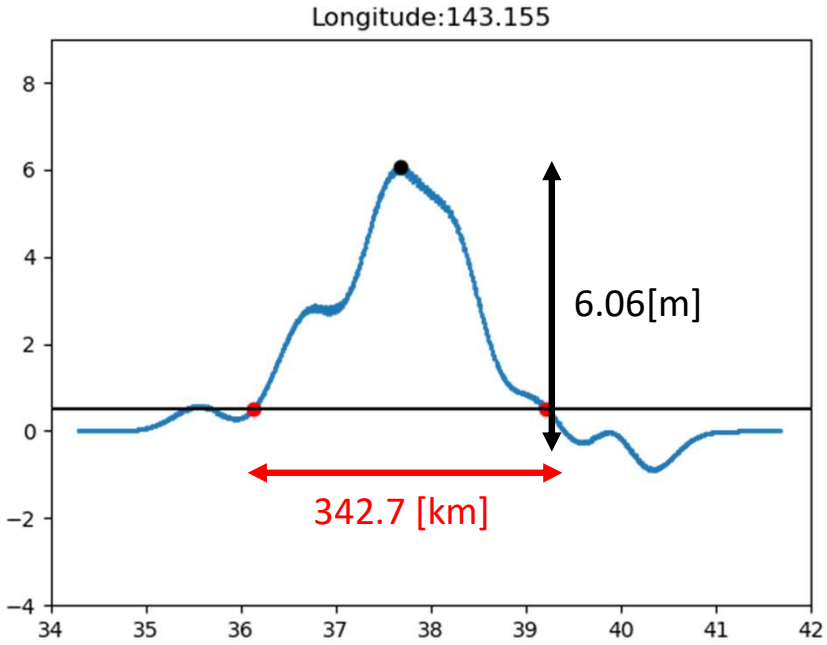

Initial Tsunami

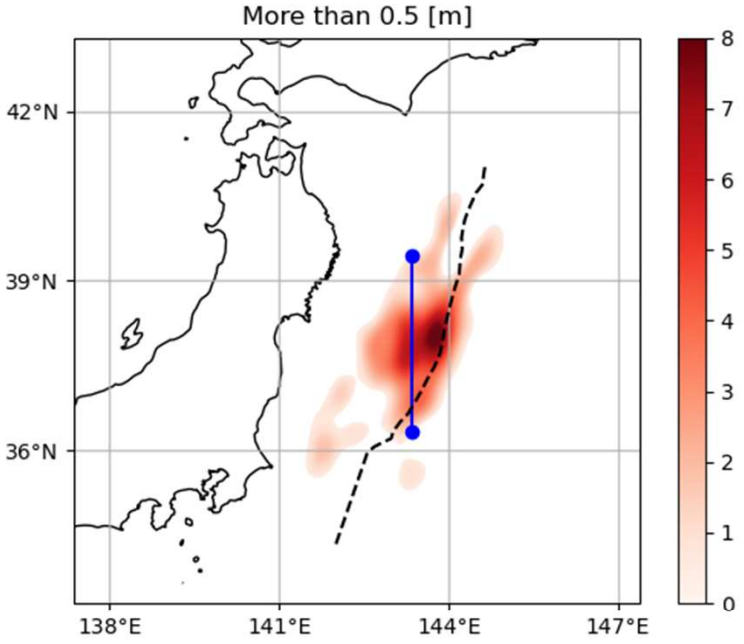

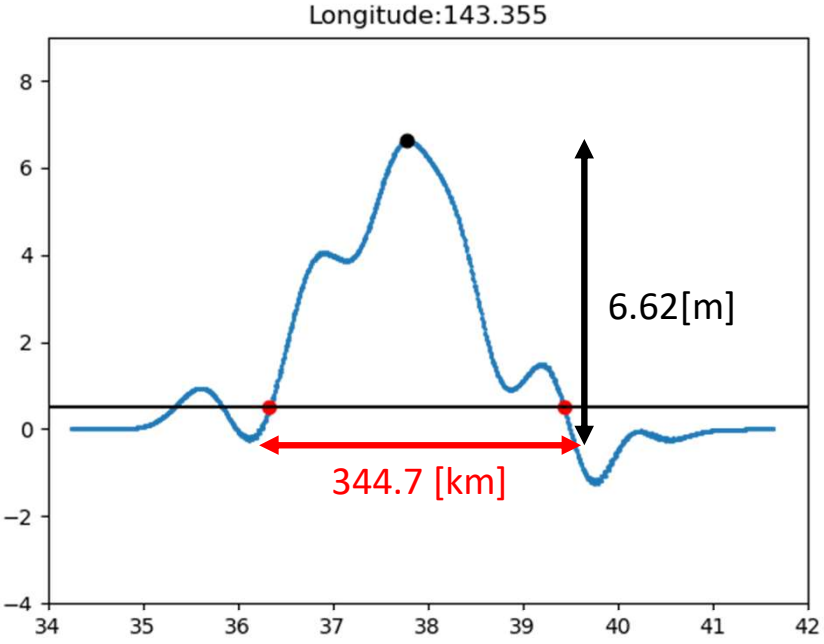

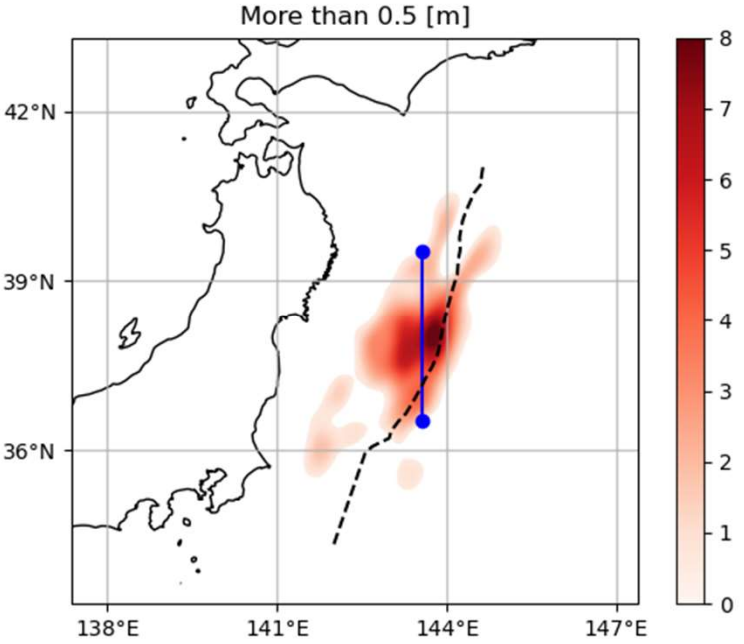

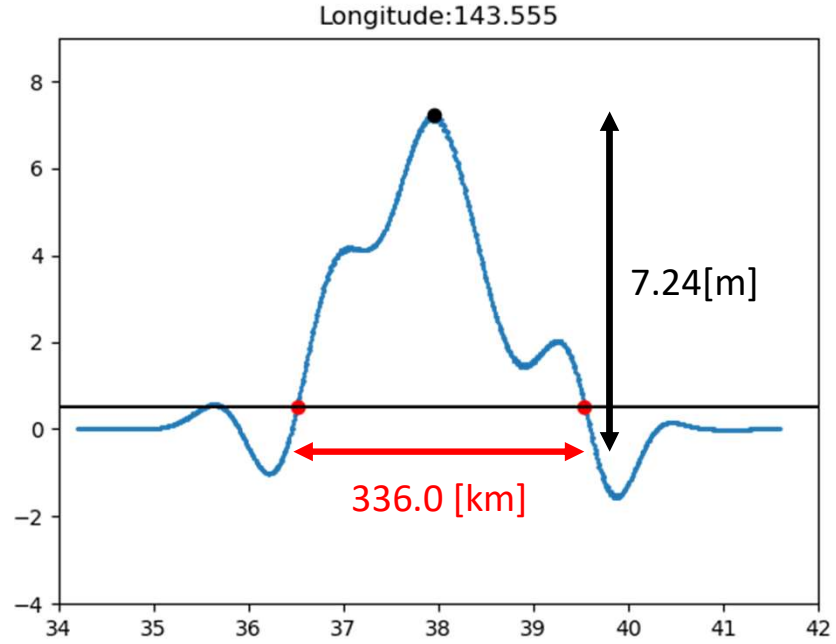

Initial Tsunami

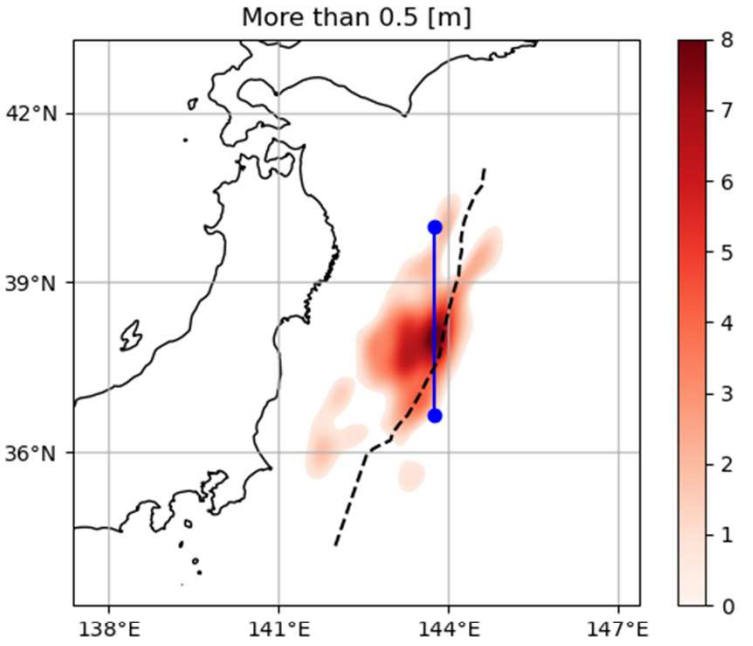

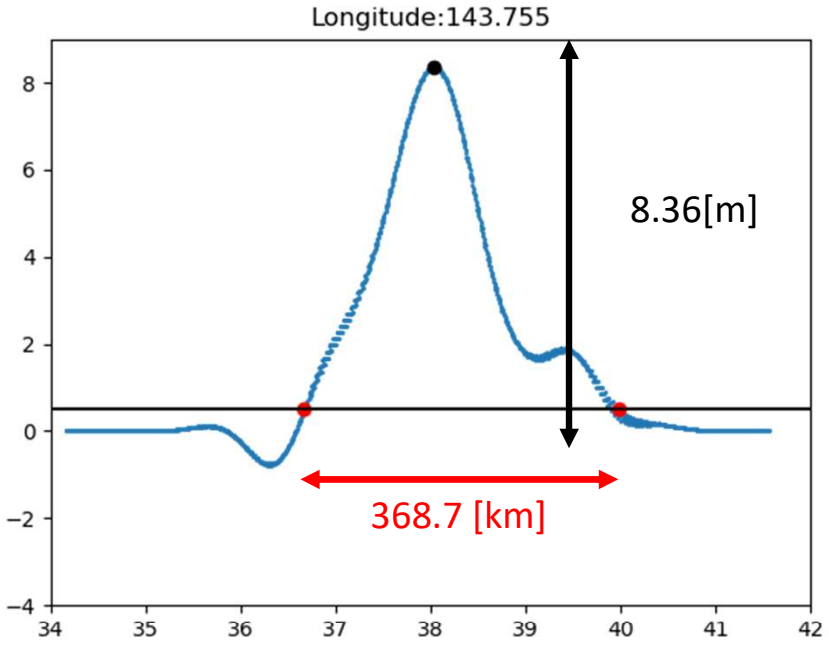

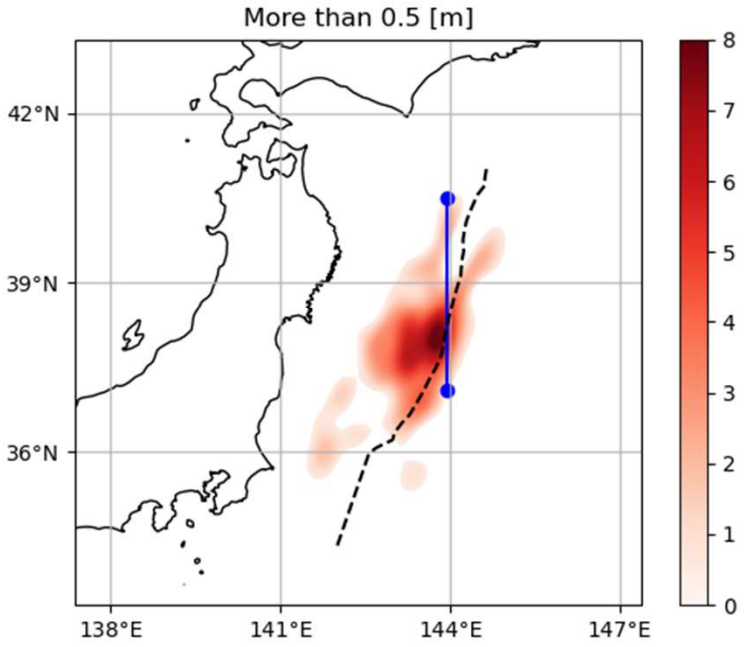

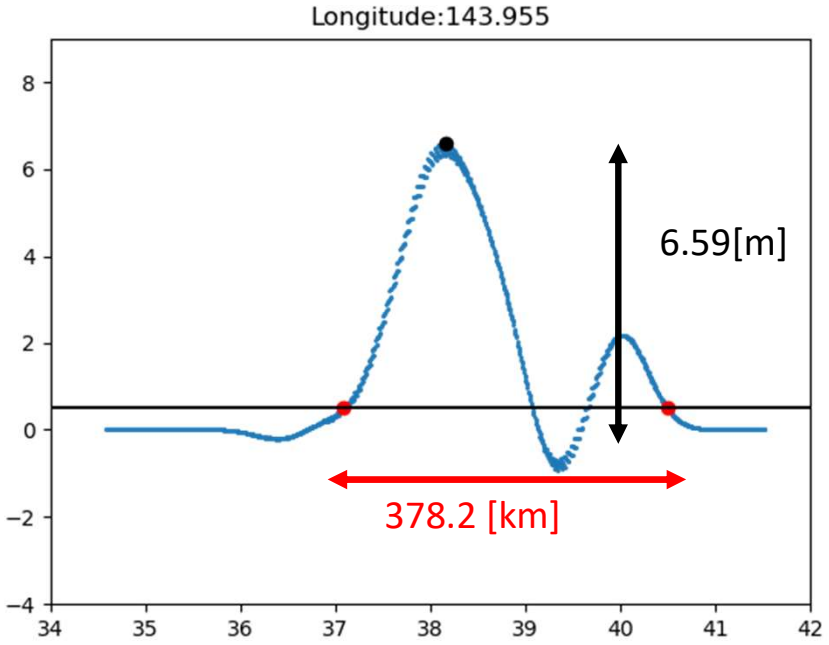

Initial Tsunami

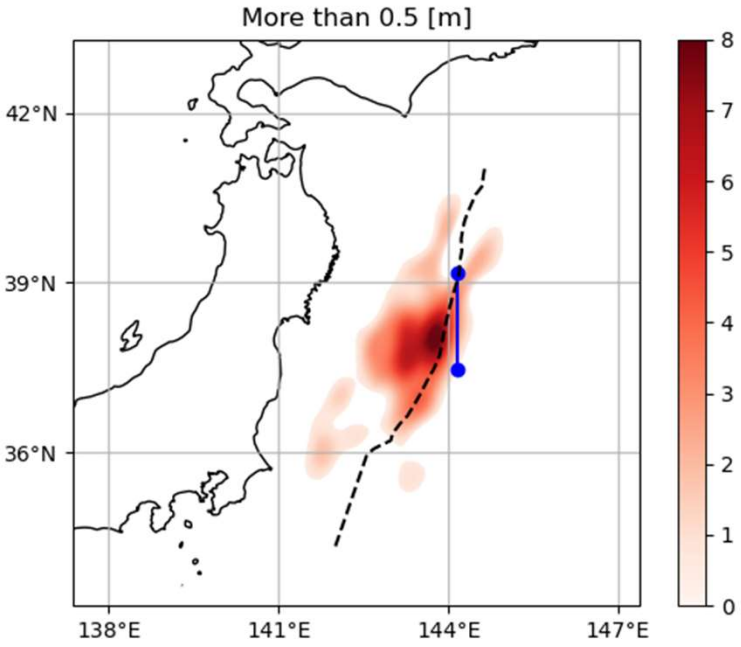

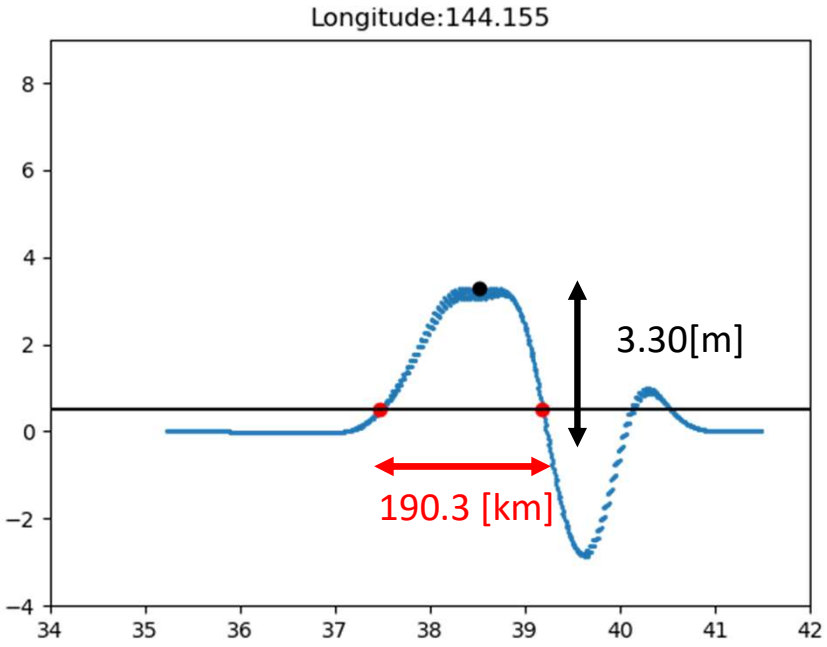

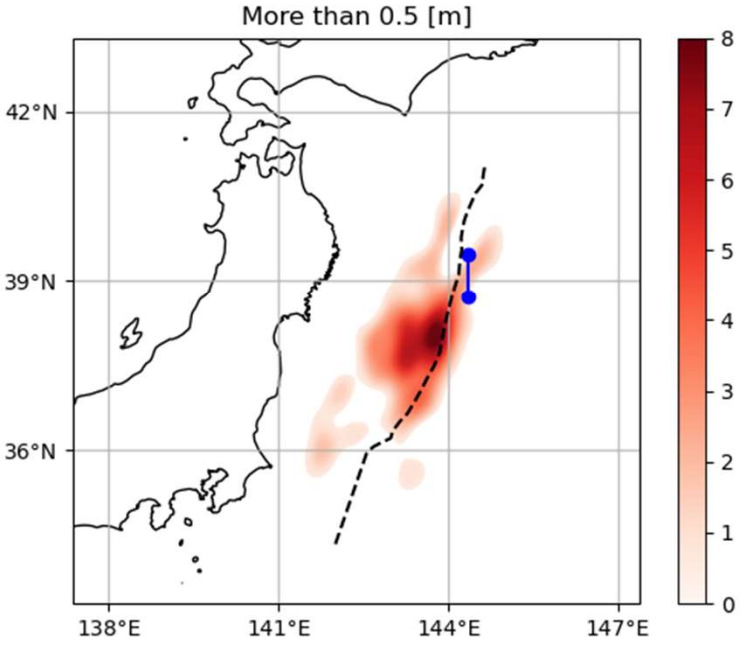

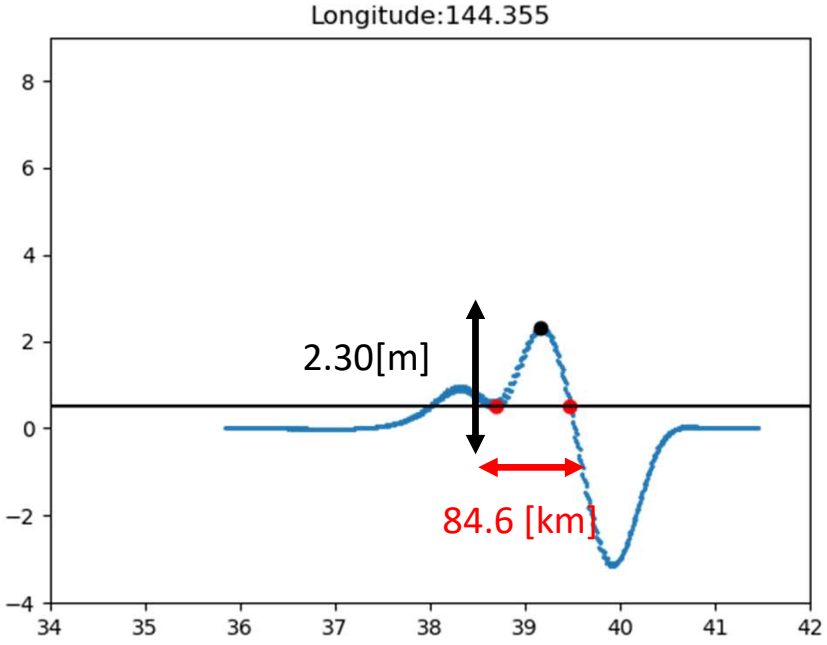

Ultimate goal

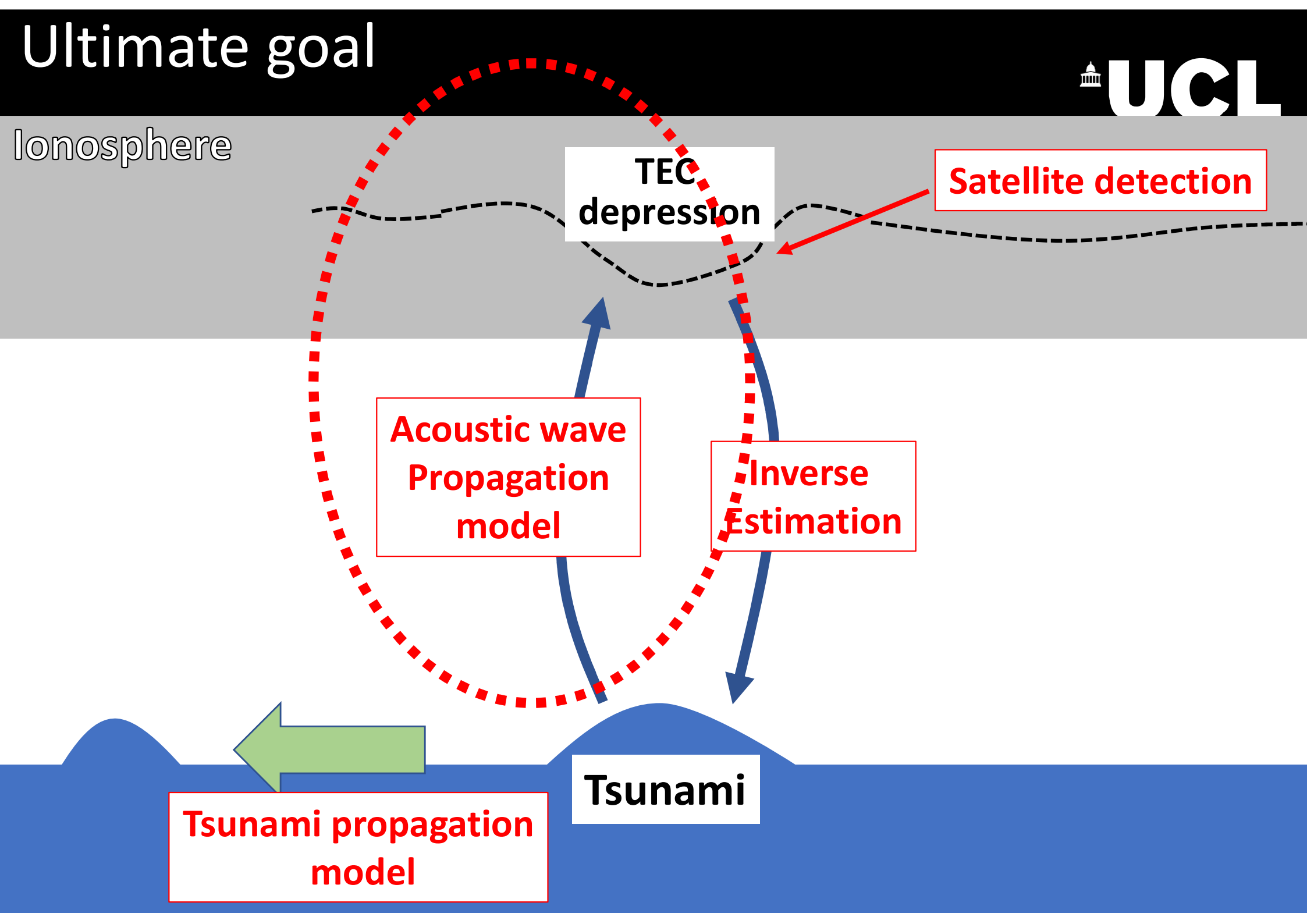

Ultimate goal

UCL

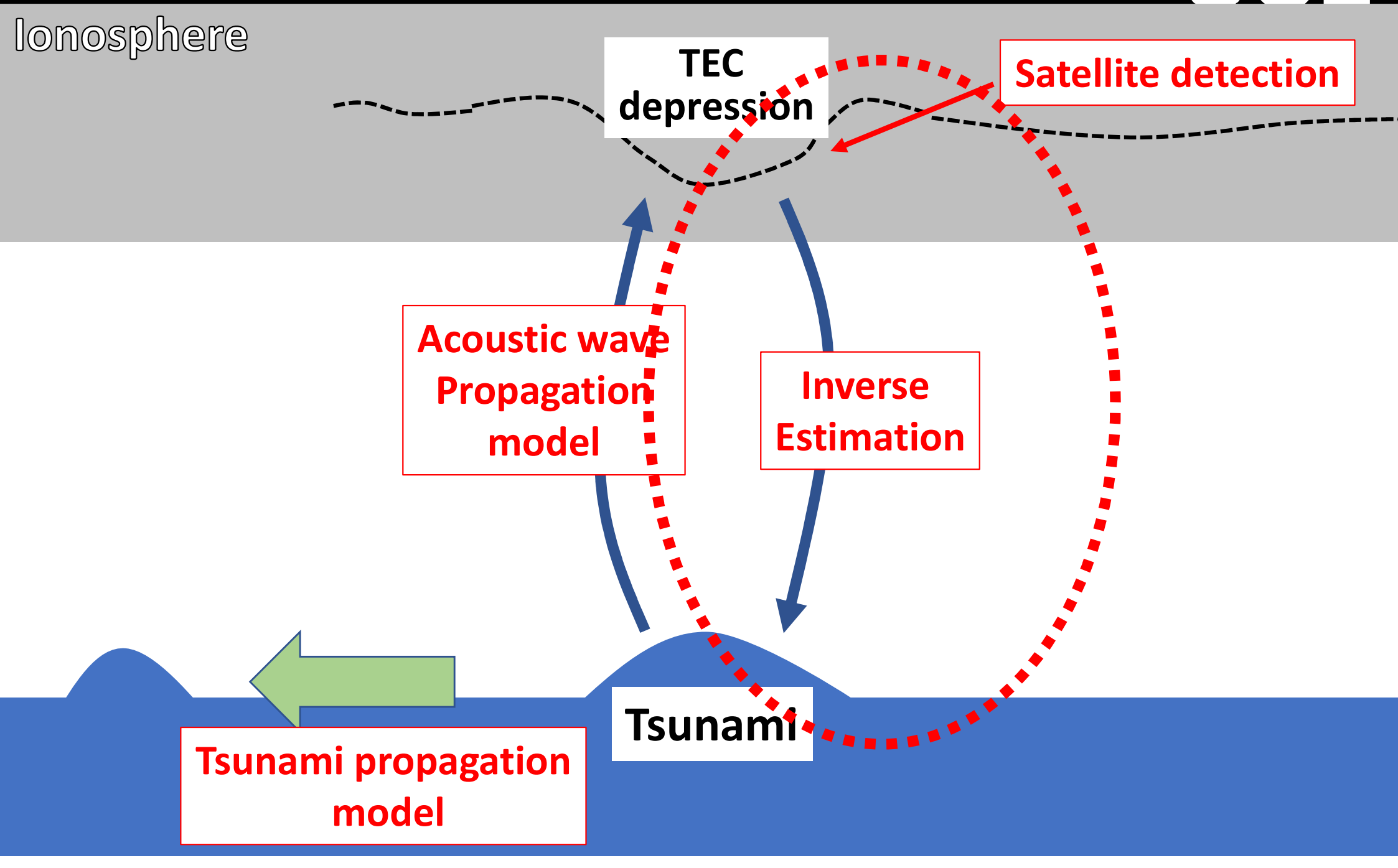

Ultimate goal

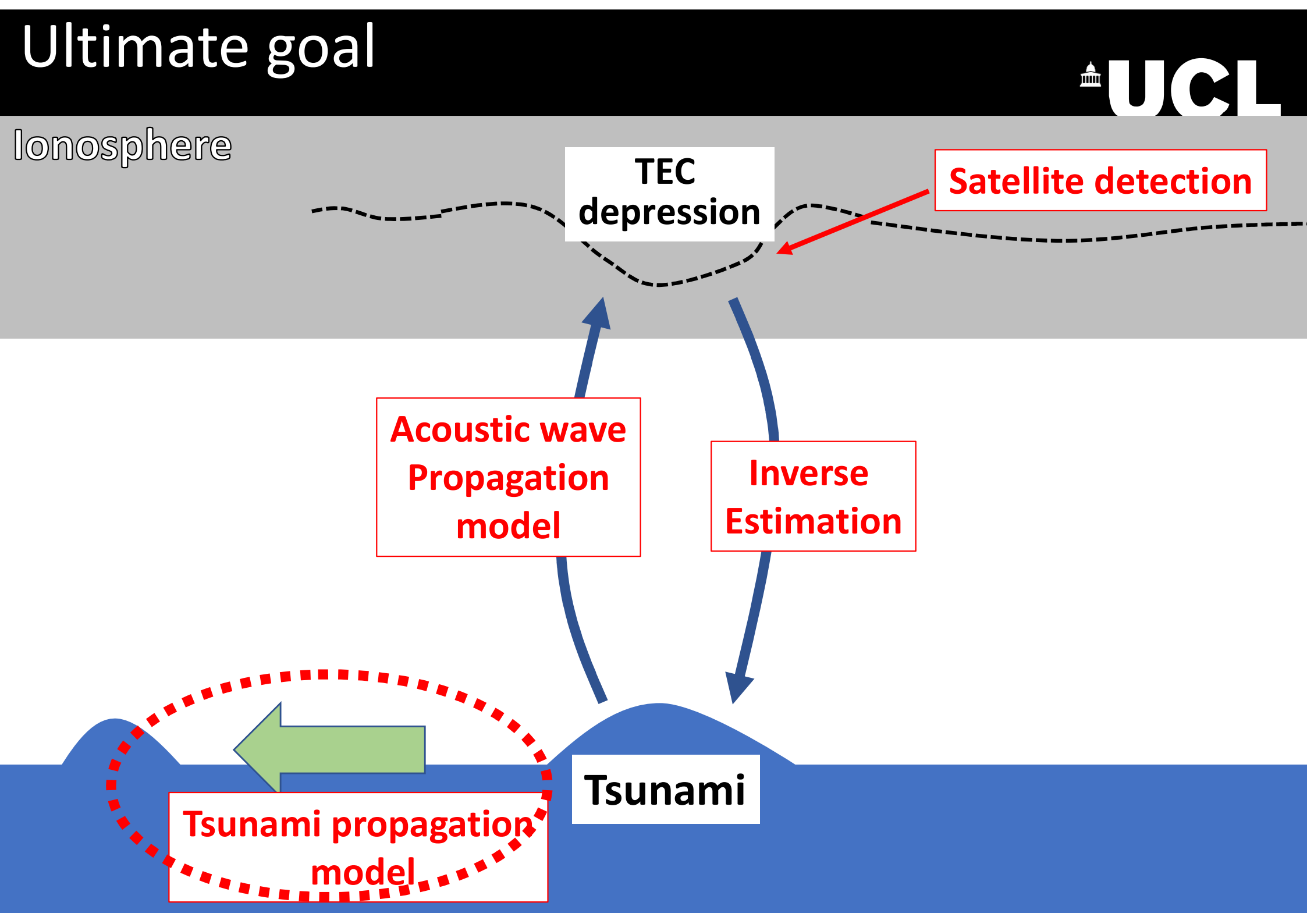

Concept of History Matching

Parameter space

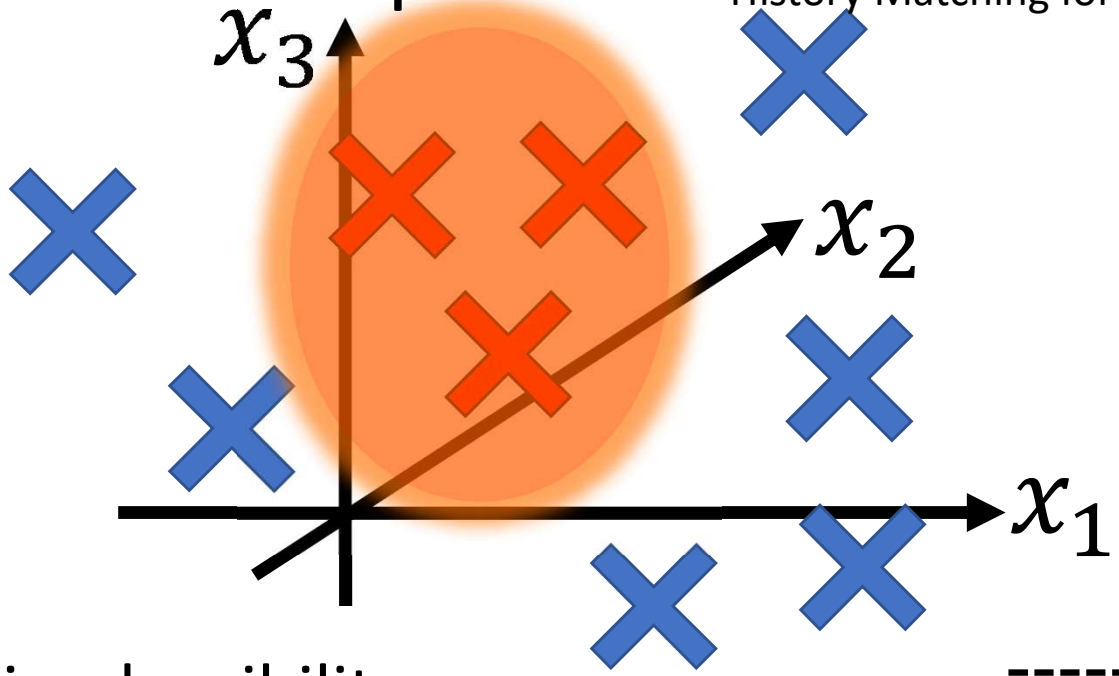

I. Vernon, Michael Goldstein, et. al., , *et al*. : "Galaxy Formation: Bayesian History Matching for the Observable Universe." *statistical science, 29.* (2014).

: implausible
: plausible
: plausible parameter subspace

$\boldsymbol{I}$:implausibility

$$\mathbf{I}(\boldsymbol{\theta}) = \frac{\|\boldsymbol{z} - \mathbf{E}(\boldsymbol{\eta}(\boldsymbol{\theta}))\|}{\sqrt{\mathbf{Var}\left(\boldsymbol{z} - \boldsymbol{E}(\boldsymbol{\eta}(\boldsymbol{\theta}))\right)}}$$

$\boldsymbol{z}$:Observation

$\mathbf{E}(\boldsymbol{\eta}(\boldsymbol{\theta}))$: Expectation of the model output

If the implausibility exceeds a certain threshold

The input parameter θ must be implausible

Toy Example (1 dimension)

1 dimensional example

Observation = -0.8

Observation error = 0.0004

Simulation model

$f_{sim}(\theta)$

This simulation model has high computational cost.

Only 6 points are computed.

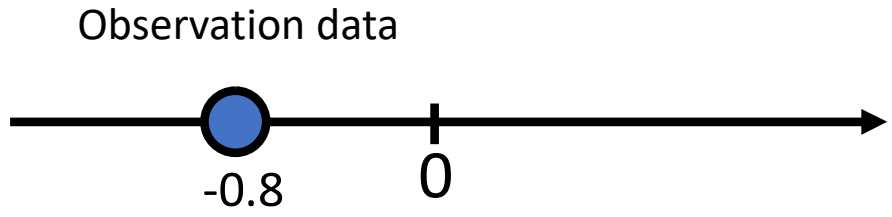

Toy Example (run a simulation model)

1 dimensional example

Observation = -0.8

Observation error = 0.0004

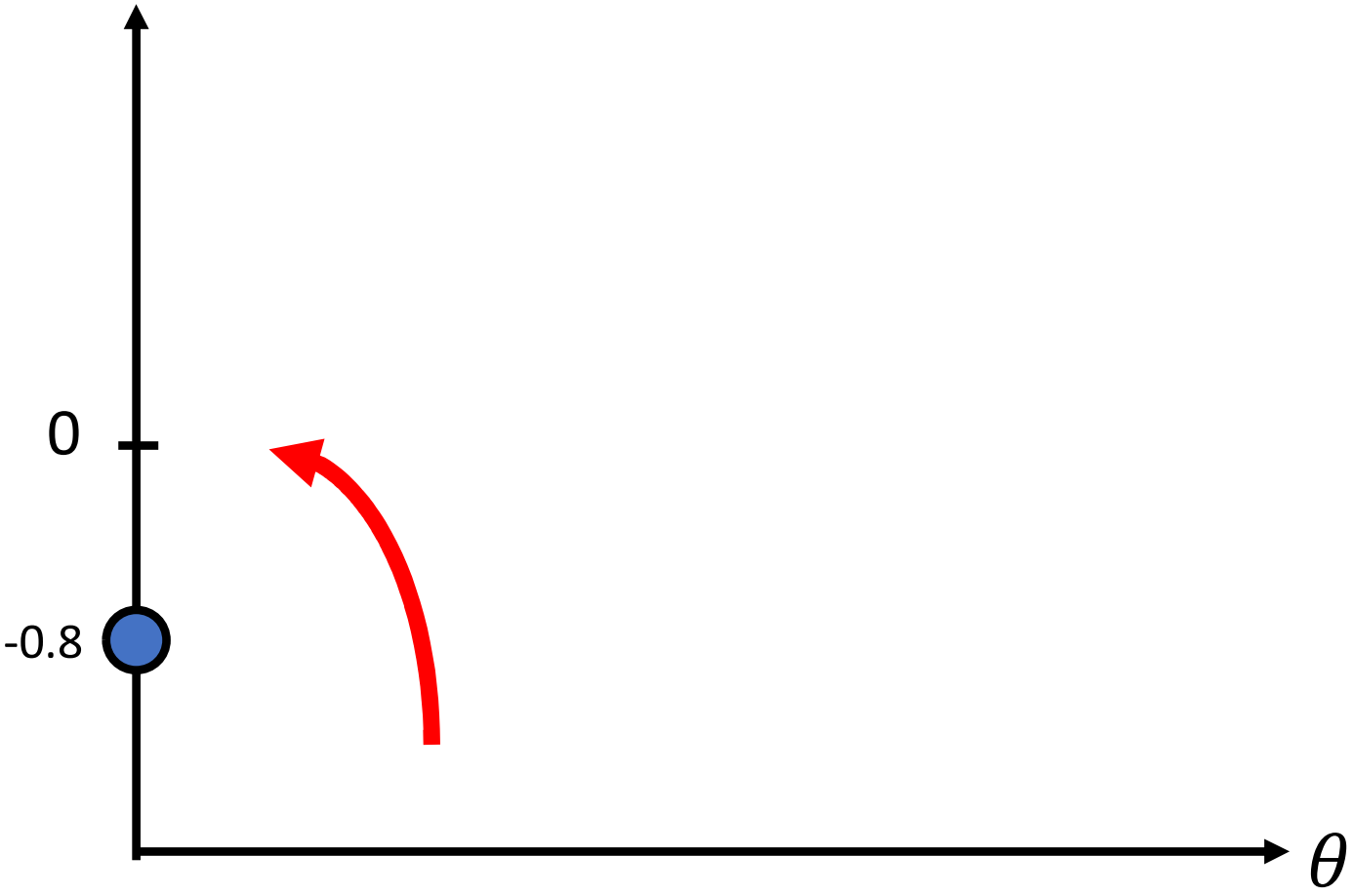

Toy Example (run a simulation model)

1 dimensional example

Observation = -0.8

Observation error = 0.0004

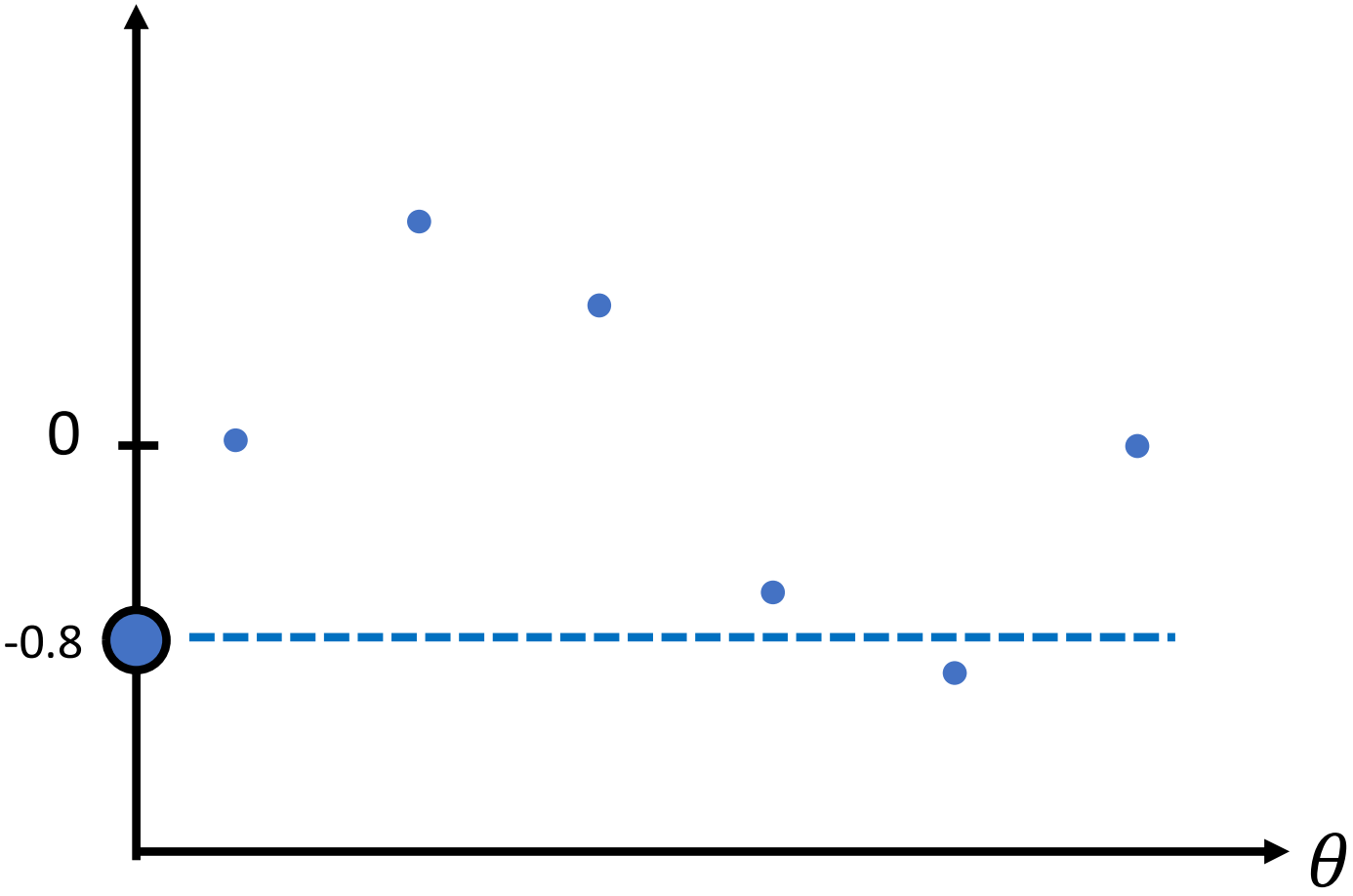

Toy Example (run an emulator)

1 dimensional example

Observation = -0.8

Observation error = 0.0004

Emulator

Gaussian process

Matern Kernel

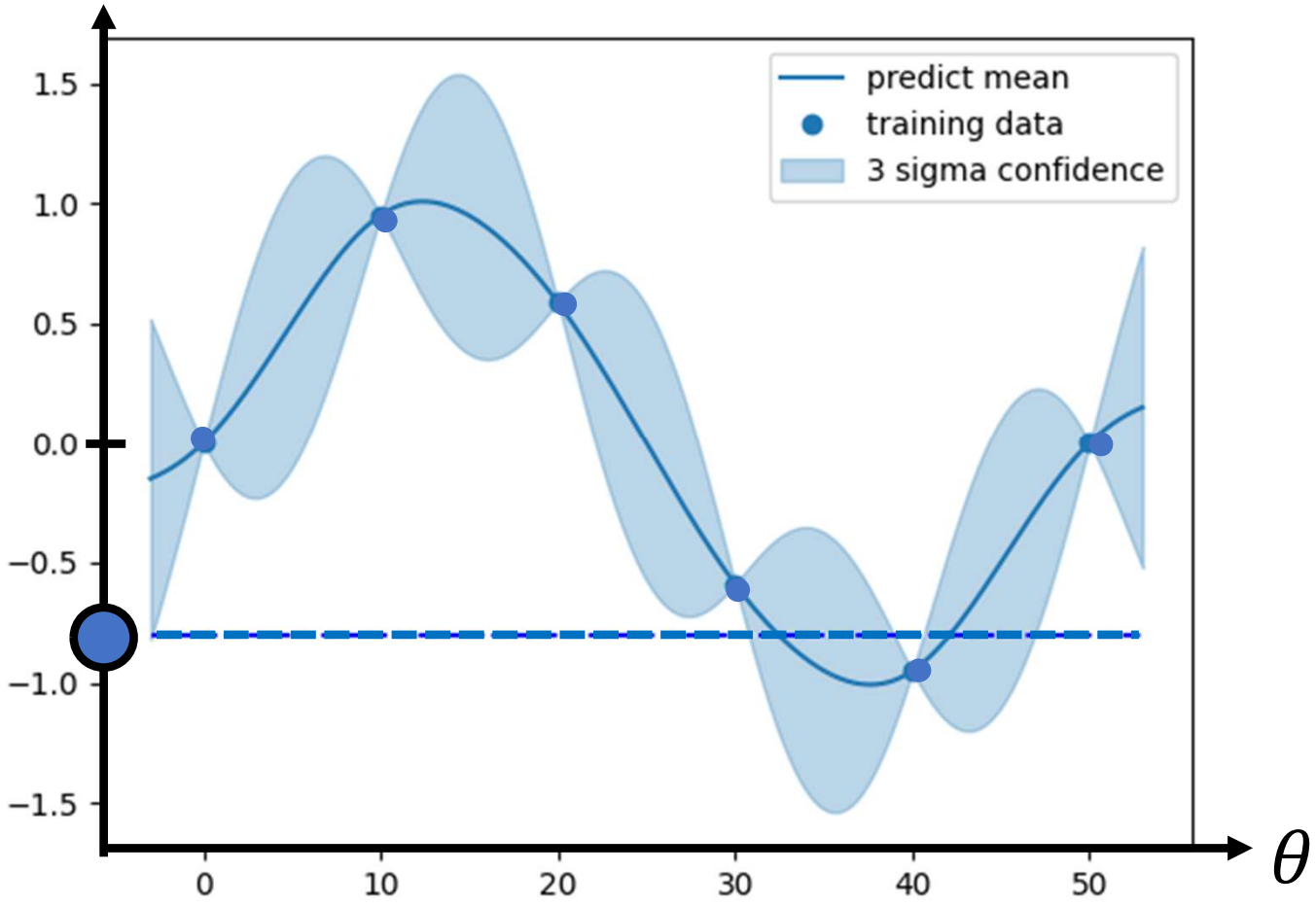

Implausibility

$$\mathbf{I}(\boldsymbol{\theta}) = \frac{\|\boldsymbol{z} - \mathbf{E}(\boldsymbol{\eta}(\boldsymbol{\theta}))\|}{\sqrt{\mathbf{Var}\left(\boldsymbol{z} - \boldsymbol{E}(\boldsymbol{\eta}(\boldsymbol{\theta}))\right)}}$$

Toy Example (compute the implausibility)

1 dimensional example

Observation = -0.8

Observation error = 0.0004

Emulator

Gaussian process

Matern Kernel

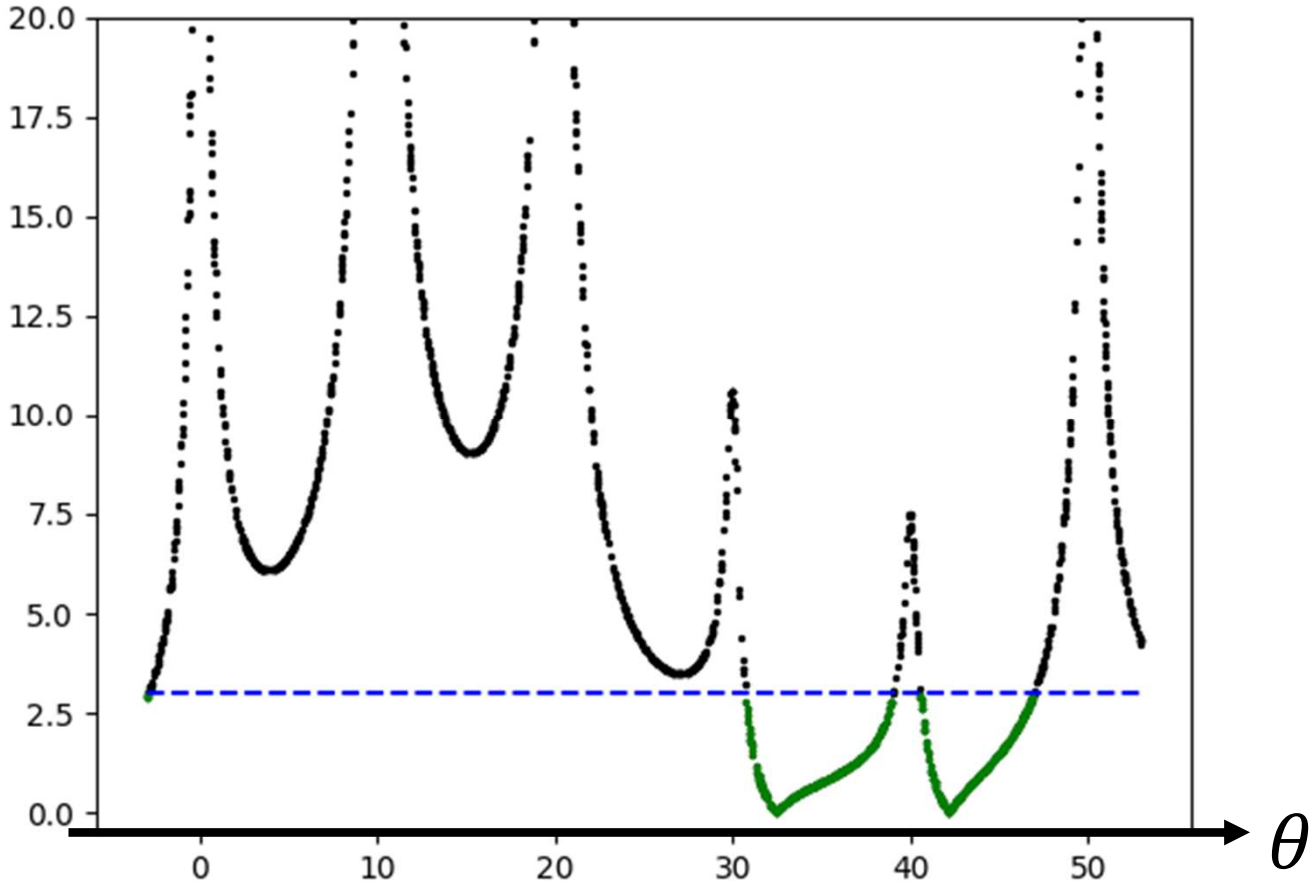

Implausibility

$$\mathbf{I}(\boldsymbol{\theta}) = \frac{\|\boldsymbol{z} - \mathbf{E}(\boldsymbol{\eta}(\boldsymbol{\theta}))\|}{\sqrt{\mathbf{Var}\left(\boldsymbol{z} - \boldsymbol{E}(\boldsymbol{\eta}(\boldsymbol{\theta}))\right)}}$$

Toy Example (compute the implausibility)

1 dimensional example

Observation = -0.8

Observation error = 0.0004

Emulator

Gaussian process

Matern Kernel

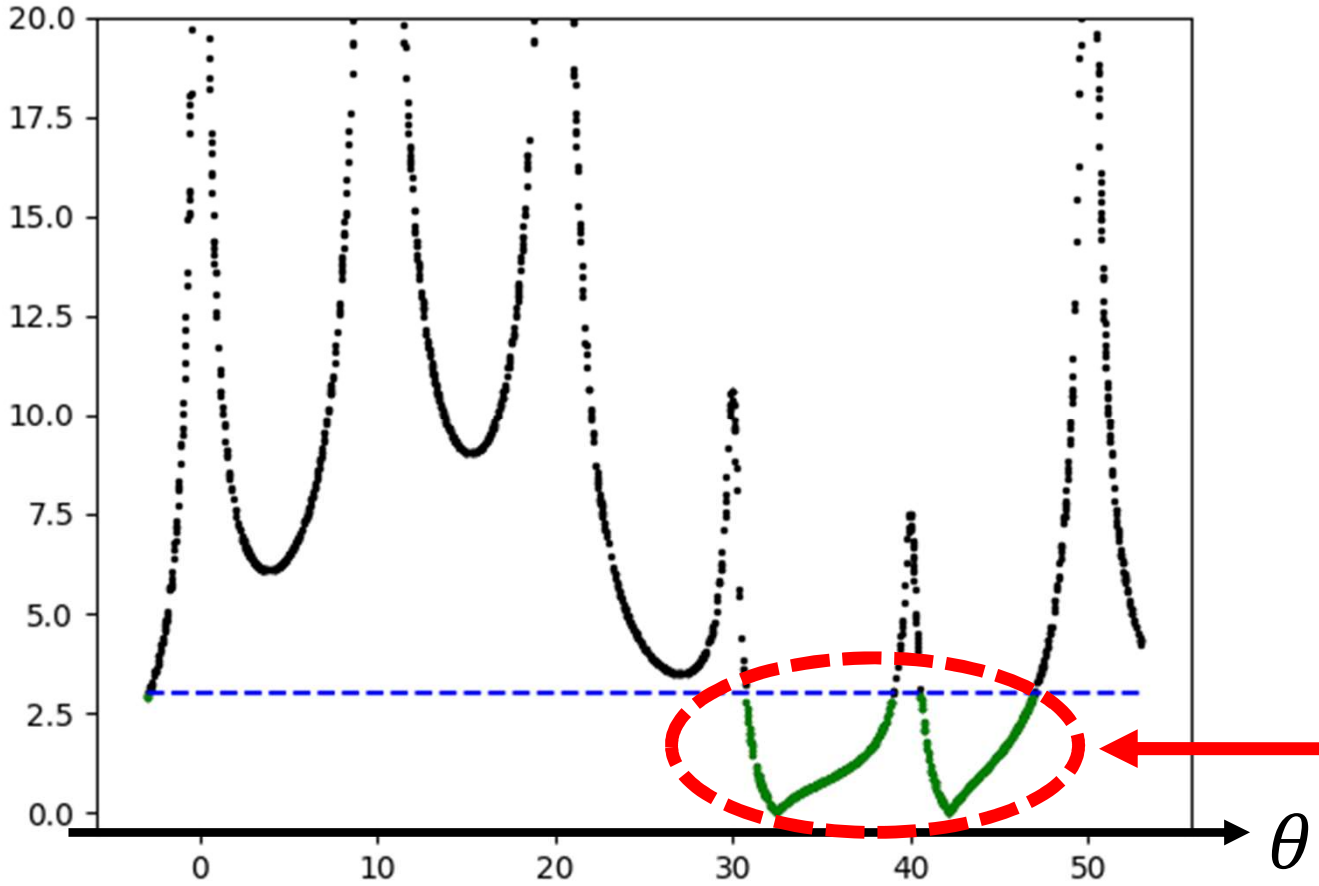

Implausibility

$$\mathbf{I}(\boldsymbol{\theta}) = \frac{\|\boldsymbol{z} - \mathbf{E}(\boldsymbol{\eta}(\boldsymbol{\theta}))\|}{\sqrt{\mathbf{Var}\left(\boldsymbol{z} - \boldsymbol{E}(\boldsymbol{\eta}(\boldsymbol{\theta}))\right)}}$$

Randomly choose an additional point to simulate

Toy Example (an additional point)

1 dimensional example

Observation = -0.8

Observation error = 0.0004

Emulator

Gaussian process

Matern Kernel

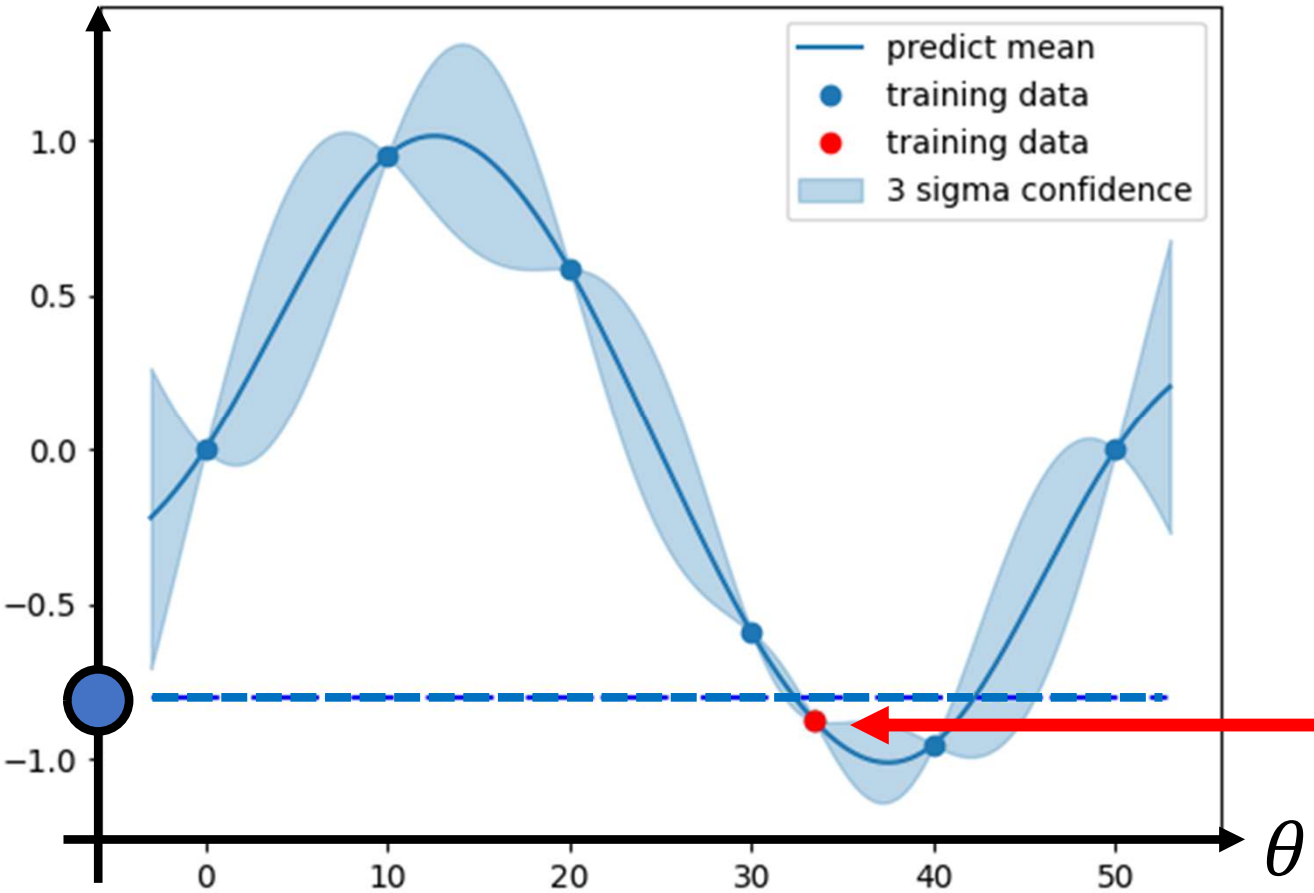

Implausibility

$$\mathbf{I}(\boldsymbol{\theta}) = \frac{\|\boldsymbol{z} - \mathbf{E}(\boldsymbol{\eta}(\boldsymbol{\theta}))\|}{\sqrt{\mathbf{Var}\left(\boldsymbol{z} - \boldsymbol{E}(\boldsymbol{\eta}(\boldsymbol{\theta}))\right)}}$$

Randomly choose an additional point to simulate

Toy Example (compute the implausibility)

1 dimensional example

Observation = -0.8

Observation error = 0.0004

Emulator

Gaussian process

Matern Kernel

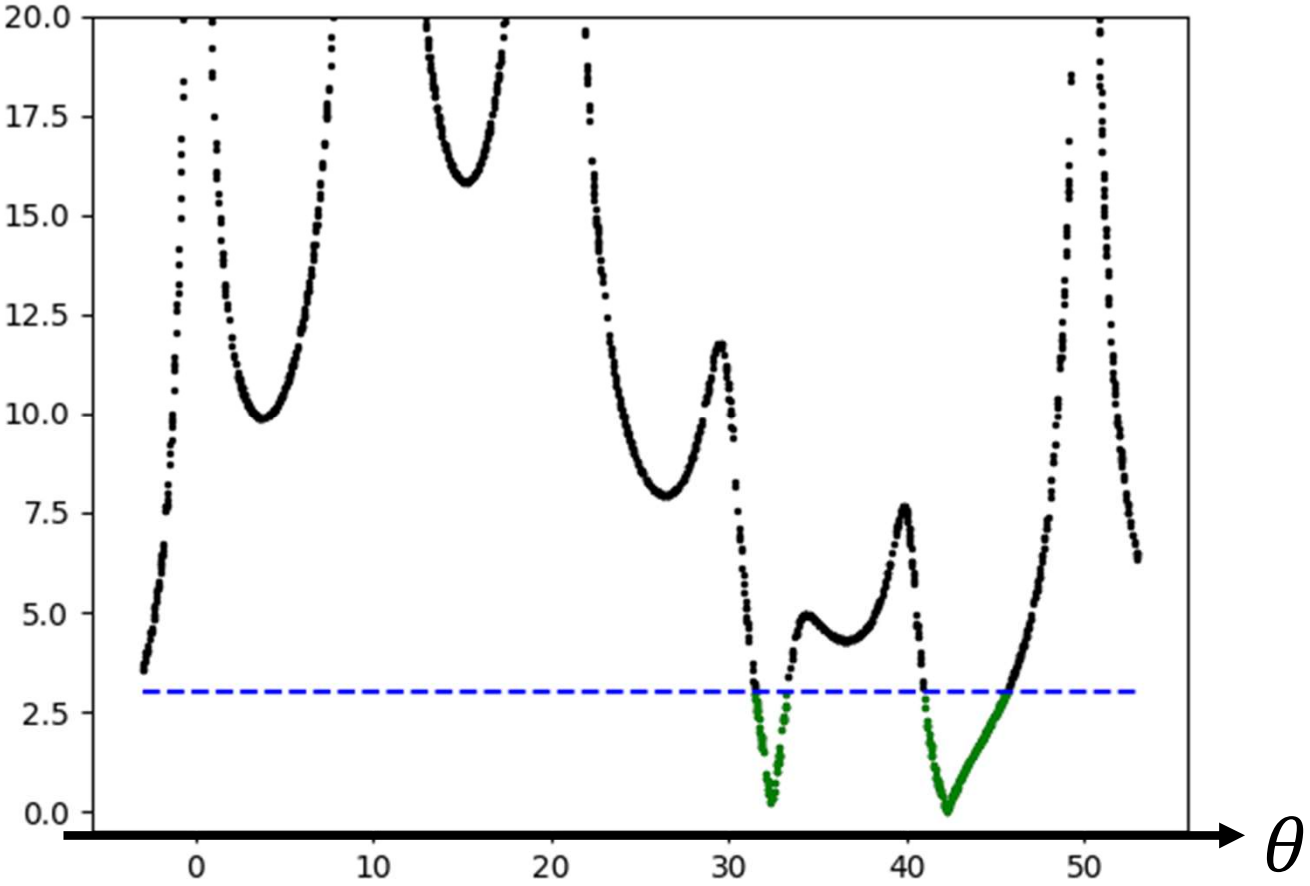

Implausibility

$$\mathbf{I}(\boldsymbol{\theta}) = \frac{\|\boldsymbol{z} - \mathbf{E}(\boldsymbol{\eta}(\boldsymbol{\theta}))\|}{\sqrt{\mathbf{Var}\left(\boldsymbol{z} - \boldsymbol{E}(\boldsymbol{\eta}(\boldsymbol{\theta}))\right)}}$$

Thank you for your listening!

[Our result]

R. Kanai, M. Kamogawa, T. Nagao, A. Smith, and S. Guillas "Robust uncertainty quantification of the volume of tsunami ionospheric holes for the 2011 Tohoku-Oki Earthquake: towards low-cost satellite-based tsunami warning systems" (preprint)
https://nhess.copernicus.org/articles/22/849/2022/nhess-22-849-2022.html

[Acoustic wave propagation]

- H. Shinagawa, et. al., “Two-dimensional simulation of ionospheric variations in the vicinity of the epicenter of the Tohoku-oki earthquake on 11 March 2011”, Geophysical Research Letters, 40, (2013)
- M. D. Zettergren, et. al., “Latitude and Longitude Dependence of Ionospheric TEC and Magnetic Perturbations From Infrasonic-Acoustic Waves Generated by Strong Seismic Events”, Geophysical Research Letters, 46, (2019)

[SPDE approach]

- P. Whittle "On stationary processes in the plane." Biometrika, 41, 434–449 (1954).
- F. Lindgren and H. Rue "An explicit link between Gaussian fields and Gaussian Markov random fields: the stochastic partial differential equation approach."J. R. Statist. Soc. B 73, Part4, 423–498 (2011).
- H. Rue and S. Martino "Approximate Bayesian inference for latent Gaussian models by using integrated nested Laplace approximations” J. R. Statist. Soc. B 71, Part2, 319–392 (2009)
- M. Cameletti, F. Lindgren, D. Simpson, H. Rue "Spatio-temporal modeling of particulate matter concentration through the SPDE approach." AStA Adv Stat Anal 97:109–131 (2013)
- D. Simpson, F. Lindgren, H. and Rue, "In order to make spatial statistics computationally feasible, we need to forget about the covariance function." Environmetrics 23.1 65-74 (2012)